

UNIVERSIDADE FEDERAL DO PARANÁ

MARIELI MACHADO ZAGO

PROSPECÇÃO CUPRÍFERA NO ESCUDO SUL-RIO-GRANDENSE: ANÁLISE  
GEOFÍSICA, INTERPRETAÇÃO GEOLÓGICA E ESTRATÉGIAS PARA REDUÇÃO  
DE CUSTOS E AUMENTO DA EFICIÊNCIA NA SELEÇÃO DE ALVOS

CURITIBA

2025

MARIELI MACHADO ZAGO

**PROSPECÇÃO CUPRÍFERA NO ESCUDO SUL-RIO-GRANDENSE: ANÁLISE  
GEOFÍSICA, INTERPRETAÇÃO GEOLÓGICA E ESTRATÉGIAS PARA REDUÇÃO  
DE CUSTOS E AUMENTO DA EFICIÊNCIA NA SELEÇÃO DE ALVOS**

Tese apresentada ao Programa de Pós-Graduação  
em Geologia, Setor de Ciências da Terra,  
Universidade Federal do Paraná, como requisito  
parcial à obtenção do título de Doutora em  
Geologia.

Orientador: Prof. Dr. Maximilian Fries

CURITIBA

2025

**DADOS INTERNACIONAIS DE CATALOGAÇÃO NA PUBLICAÇÃO (CIP)**  
**UNIVERSIDADE FEDERAL DO PARANÁ**  
**SISTEMA DE BIBLIOTECAS – BIBLIOTECA CIÉNCIA E TECNOLOGIA**

Zago, Marieli Machado

Prospecção cuprífera no Escudo Sul-Rio-Grandense: análise geofísica, interpretação geológica e estratégias para redução de custos e aumento da eficiência na seleção de alvos. / Marieli Machado Zago. – Curitiba, 2025.

1 recurso on-line : PDF.

Tese (Doutorado) - Universidade Federal do Paraná, Setor de Ciências da Terra. Programa de Pós-graduação em Geologia.

Orientador: Prof. Dr. Maximilian Fries

1. Geofísica aplicada. 2. Prospecção mineral. 3. Minérios de cobre. I. Universidade Federal do Paraná. II. Programa de Pós-Graduação em Ciências da Terra. III. Fries, Maximilian. IV. Título.

Bibliotecária: Roseny Rivelini Morciani CRB-9/1585



MINISTÉRIO DA EDUCAÇÃO  
SETOR DE CIENCIAS DA TERRA  
UNIVERSIDADE FEDERAL DO PARANÁ  
PRÓ-REITORIA DE PÓS-GRADUAÇÃO  
PROGRAMA DE PÓS-GRADUAÇÃO GEOLOGIA -  
40001016028P5

## TERMO DE APROVAÇÃO

Os membros da Banca Examinadora designada pelo Colegiado do Programa de Pós-Graduação GEOLOGIA da Universidade Federal do Paraná foram convocados para realizar a arguição da tese de Doutorado de **MARIELI MACHADO ZAGO**, intitulada: **PROSPECÇÃO CUPRÍFERA NO ESCUDO SUL-RIO-GRANDENSE: ANÁLISE GEOFÍSICA, INTERPRETAÇÃO GEOLÓGICA E ESTRATÉGIAS PARA REDUÇÃO DE CUSTOS E AUMENTO DA EFICIÊNCIA NA SELEÇÃO DE ALVOS**, sob orientação do Prof. Dr. MAXIMILIAN FRIES, que após terem inquirido a aluna e realizada a avaliação do trabalho, são de parecer pela sua APROVAÇÃO no rito de defesa.

A outorga do título de doutora está sujeita à homologação pelo colegiado, ao atendimento de todas as indicações e correções solicitadas pela banca e ao pleno atendimento das demandas regimentais do Programa de Pós-Graduação.

CURITIBA, 13 de Maio de 2025.

Assinatura Eletrônica  
14/05/2025 12:49:58.0  
MAXIMILIAN FRIES  
Presidente da Banca Examinadora

Assinatura Eletrônica  
27/05/2025 17:16:32.0  
FELIPE GUADAGNIN  
Avaliador Externo (INVERSIDADE FEDERAL DO PAMPA- CAMPUS CAÇAPAVA DO SUL)

Assinatura Eletrônica  
14/05/2025 13:37:17.0  
FABIO BRAZ MACHADO  
Avaliador Interno (UNIVERSIDADE FEDERAL DO PARANÁ)

Assinatura Eletrônica  
14/05/2025 17:01:29.0  
GIUSEPPE BETINO DE TONI  
Avaliador Externo (INVERSIDADE FEDERAL DO PAMPA- CAMPUS CAÇAPAVA DO SUL)

Assinatura Eletrônica  
14/05/2025 12:06:50.0  
DIONISIO UENDRO CARLOS  
Avaliador Externo (UNIVERSIDADE ESTADUAL PAULISTA - CAMPUS DE RIO CLARO)

---

DEPARTAMENTO DE GEOLOGIA-CENTRO POLITÉCNICO-UFPR - CURITIBA - Paraná - Brasil

CEP 81531-990 - Tel: (41) 3361-3365 - E-mail: posgeol@ufpr.br

Documento assinado eletronicamente de acordo com o disposto na legislação federal Decreto 8539 de 08 de outubro de 2015.

Gerado e autenticado pelo SIGA-UFPR, com a seguinte identificação única: 451098

Para autenticar este documento/assinatura, acesse <https://sigae.ufpr.br/siga/visitante/autenticacaoassinaturas.jsp>  
e insira o código 451098

*“Only good fishermen are successful, first by selecting the good lakes and then the good spots”*

Witherly e Allard (2010)

## AGRADECIMENTOS

Desenvolver uma pesquisa de doutorado requer paciência, dedicação e foco. São quatro anos de mudanças intensas — ideias, sonhos, caminhos e destinos se transformam ao longo da jornada. Construir uma carreira no mundo das geociências é um misto de emoções: nunca foi fácil, mas sempre foi movido por muita força de vontade.

Nesse percurso, encontrei pessoas especiais que tornaram a caminhada mais leve, me ajudaram nos momentos em que pensei em mudar de rumo e me incentivaram a seguir firme, alimentando o desejo de continuar sonhando e construindo uma trajetória no fascinante mundo da exploração mineral.

Agradeço, em primeiro lugar, ao meu pai, à minha mãe e ao meu irmão, que sempre estiveram ao meu lado, apoiando e incentivando em todas as etapas, vibrando comigo a cada pequena conquista. E peço desculpas por todas as ausências ao longo desse processo, nunca foi fácil achar tempo para tudo.

Agradeço também aos colegas da exploração mineral. Ao longo desses quatro anos, muitos profissionais contribuíram direta e indiretamente para o meu desenvolvimento. Esta tese é fruto de tudo que aprendi até aqui e também da minha curiosidade incessante. Em especial, agradeço ao Divanir Júnior, um dos maiores geofísicos da atualidade, pela ajuda incansável em todas as fases desta pesquisa — desde os primeiros seminários, passando pela semana intensa de preparação para a qualificação, pelas discussões que resultaram no primeiro artigo, até o apoio fundamental na reta final da tese e na conclusão do segundo artigo. Minha eterna gratidão!

Aos gestores da exploração mineral da Ero Caraíba, meu sincero agradecimento pelo apoio constante, pela liberação para participação em seminários e aulas, pela autorização para o uso de softwares e recursos essenciais ao desenvolvimento deste trabalho.

Sou também muito grata ao Pablo Mejia, que, mesmo diante de minhas inúmeras responsabilidades e da pressão do dia a dia, nunca deixou de me lembrar da importância de priorizar a finalização do doutorado. Ainda não comprehendo totalmente o motivo, mas suas palavras e incentivos sempre abriram meus olhos para seguir em frente e concluir mais esta etapa acadêmica.

Ao meu orientador Maximilian Fries, minha profunda gratidão. Durante esses dez anos de parceria — que começaram nos projetos de iniciação científica, passaram por duas graduações, inúmeros artigos, um mestrado e agora culminam neste doutorado —, tive a liberdade para amadurecer meu conhecimento e protagonizar minha trajetória acadêmica. Essa construção foi marcada pela abertura a ideias, pela criatividade e pela gentileza nas orientações. Foram muitas idas e vindas de revisões, e hoje, graças a esse processo de aprendizado contínuo, já consigo revisar meus próprios textos com um olhar crítico que antes não tinha. Minha paixão pela vida acadêmica e pela pesquisa tem, sem dúvida, raízes sólidas nessa longa e preciosa parceria.

Por fim, agradeço ao Programa de Pós-Graduação em Geologia da UFPR pela oportunidade de realizar mais essa etapa, sempre com seriedade, compreensão e suporte contínuo.

## **RESUMO**

O Escudo Sul-Rio-Grandense é reconhecido pela presença de importantes depósitos minerais metálicos, destacando-se as ocorrências cupríferas. Para a identificação de novos prospectos, a utilização de dados geofísicos, especialmente magnetometria e gamaespectrometria, é essencial no reconhecimento das assinaturas magnéticas e de radioelementos dos litotipos associados às mineralizações. Entretanto, há uma lacuna significativa em pesquisas que abordem metodologias sistemáticas e integradas para análise de dados geofísicos e geológicos pré-existentes no Escudo Sul-Rio-Grandense, especialmente no que diz respeito à integração e processamento de informações multidisciplinares para a caracterização de assinaturas geofísicas associadas a mineralizações. Este estudo propõe uma abordagem integrada para a interpretação dessas assinaturas na metade sul do estado do Rio Grande do Sul, correlacionando dados geofísicos com informações geológicas, estruturais e geoquímicas. A investigação concentra-se na identificação e caracterização dos principais litotipos associados às mineralizações de cobre, permitindo o entendimento das assinaturas geofísicas em escala regional e local a partir de levantamentos aerogeofísicos. Foram delimitadas áreas representativas para avaliação da qualidade dos sinais aeromagnetométricos e aerogamaespectrométricos, integrando-os a mapeamentos geológicos e estruturais, além de dados geoquímicos disponíveis. Os resultados incluem mapas 2D, inversões 3D e perfis litogeofísicos, que contribuem para a compreensão dos contrastes de propriedades físicas entre as principais rochas hospedeiras de mineralizações e encaixantes. Esses produtos oferecem uma abordagem metodológica que poderá ser aplicada a diferentes contextos geológicos e tipos de depósitos minerais, otimizando futuras investigações em escala de detalhe. Além de sua relevância acadêmica, o estudo pretende fornecer informações estratégicas para a indústria mineral, auxiliando na definição de novas áreas potenciais e na redução de custos exploratórios por meio do aproveitamento de dados preexistentes.

**Palavras-chave:** Geofísica aplicada; Prospecção mineral; Mineralizações cupríferas.

## ABSTRACT

The Sul-Rio-Grandense Shield is recognized for hosting important metallic mineral deposits, particularly copper occurrences. For the identification of new prospects, the use of geophysical data, especially magnetometry and gamma spectrometry, is essential for recognizing magnetic and radioelement signatures of lithotypes associated with mineralizations. However, there is a significant gap in research addressing systematic and integrated methodologies for the analysis of pre-existing geophysical and geological data in the Sul-Riograndense Shield, particularly regarding the integration and processing of multidisciplinary information for the characterization of geophysical signatures associated with mineralizations. This study proposes an integrated approach to interpret these signatures in the southern half of the state of Rio Grande do Sul, correlating geophysical data with geological, structural, and geochemical information. The investigation focuses on identifying and characterizing the main lithotypes associated with copper mineralizations, enabling the understanding of geophysical signatures on a regional scale based on airborne geophysical surveys. Representative areas were delineated to assess the quality of magnetic and gamma spectrometric signals, integrating them with geological and structural mappings, as well as geochemical data when available. The results include 2D maps, 3D inversions, and lithogeophysical profiles, which contribute to understanding the contrasts in physical properties of the main host rocks of mineralizations. These products provide a methodological approach that can be applied to different geological contexts and types of mineral deposits, optimizing future detailed investigations. In addition to its academic relevance, the study aims to provide strategic information for the mining industry, assisting in the definition of new potential areas and reducing exploration costs through the use of pre-existing data.

**Keywords:** Applied Geophysics; Mineral Exploration; Copper Mineralizations.

## **LISTA DE ILUSTRAÇÕES**

### **CAPÍTULO 1 e 2**

FIGURA 1 - Localização da área de estudo em a) Mapa geral com ênfase na localização da área de estudo no estado do Rio Grande do Sul (RS), em b) Mapa da área de estudo em detalhe com as rodovias de acesso e localização de cidades nas proximidades. Adaptado de Google (2025).....	20
FIGURA 2 - Contexto geológico da área de estudo em a) Unidades Geotectônicas do ESRG e em b) Principais litologias e lineamentos estruturais associados a ocorrências cupríferas. FONTE: Adaptado de Hartmann et al., (2007), Laux (2021) e Google (2025). .....	25

### **CAPÍTULO 4**

#### **ARTIGO 1**

FIGURE 1 - (a) Main access highways and location of copper occurrences in the study area (CPRM, 2021) and (b) map of the state of Rio Grande do Sul, the location of the leading regional geological features and the location of the study area. ....	37
FIGURE 2 - Flowchart of activities divided into four stages.....	42
FIGURE 3 - (a) Map of lithological units, (b) map of group separation. Adapted from CPRM (2021). .....	48
FIGURE 4 - (a) Potassium Channels, (b) Uranium, (c) Thorium, (d) Lithological Group Map, (e) RGB Ternary Map, and (f) Histograms showing the variation of the mean values of eTh, eU, and K concerning the rock groups in the area of interest (the colors represent: K, red; eTh, green; eU, blue), and (g) the table with the average radioelement values for each rock group. ....	50
FIGURE 5 - (a) Total Magnetic Anomaly Field Map and indication of the location of the cross-section A–A', (b) the Analytic Signal Map, (c) Lithological Group Map with structural context (CPRM, 2021), (d) First Vertical Derivative Map (1DVz), (e) 1DVz Map lighting structural lineaments and plutonic rocks, (f) Cross Section A–A' of the MVI Inversion Model, and (g) Rosette Diagram .....	52

FIGURE 6 - (a) Areas with mineral occurrences hosted in ultramafic bodies. (b) MVI inversion models for the four areas.....	53
FIGURE 7 - (a) Lithological map with records of Cu occurrences, stream sediment, and soil geochemistry, (b) detailed location of stream sediment samples, and (c) detailed profiles of the two soil sampling points; adapted from CPRM (2021) and Ribeiro (1978).....	55
FIGURE 8 - (a) Location map of litho-geophysical profiles and (b) detail of the location of Profile B–B” with information on stream sediment and soil samples. ....	57
FIGURE 9 - (a) Lithogeophysical Profile A–A”, (b) view of the MVI-generated inversion model. (c) A mosaic presenting the MVI-generated inversion model, graph with radioelement (K, eTh, eU) variations, and interpreted lithogeophysical profile.....	60
FIGURE 10 - (a) MVI Model of Profile B–B”, (b) separation of selected MVI higher anomalies, and (c) map of Profile B–B” location. ....	60

## ARTIGO 2

FIGURE 1 - a) Location of the study area near the municipality of Caçapava do Sul. b) Location within the state of Rio Grande do Sul and in the regional geological context. (Modified from Hartmann et al., 2007; Google, 2025).....	66
FIGURE 2 – Location of inactive mines in the study area and local geological context (Modified from Lopes et al., 2018; Ribeiro, 1978). ....	68
FIGURE 3 - (a) Scheme illustration showing the intersection of NE-NW oriented fault planes at the Barita Mine; (b) Diagram depicting the drill hole and associated clay mineral domains identified through XRD analysis (Modified from Lopes, 2011). ....	71
FIGURE 4 - Flowchart illustrating the adopted approach and the development stages defined for this study. ....	72
FIGURE 5 - (a) Conceptual model of a supergene profile in a porphyry copper deposit; (b) expected magnetic signature considering different lithologies and hydrothermal alterations (Modified from Sillitoe, 2005; Anderson et al., 2023). ....	74

FIGURE 6 - Maps displaying aerogeophysical anomaly values for the study area. a) Total Magnetic Intensity - TMI, b) Analytic Signal Amplitude - ASA, c) Tilt derivative, and d) RGB ternary gamma-ray spectrometry map. ....	83
FIGURE 7- (a) Euler Deconvolution map generated using a Structural Index of 2, overlaid with the lithological context; (b) same results overlaid with the digital elevation model (Adapted from Lopes et al., 2018). .....	85
FIGURE 8 – MVI models and generated sections for the study area. a) MVI inversion model; the yellow polygon outlines the study area. b) Selected vertical profiles from the MVI model. c) Geophysical profile overlaid with the geological map and Euler Deconvolution results.....	86
FIGURE 9 - Lithological map of the study area, defined profiles, and Euler Deconvolution results (Modified from Lopes et al., 2018). .....	87
FIGURE 10 - Lithogeophysical profiles A-A' (a), B-B' (b), C-C' (c) with magnetic inversion and Euler deconvolution, overlaid by the local geology map.	
.....	89
FIGURE 11 - Lithogeophysical profiles D–D' (a), E–E' (b), and F–F' (c) with magnetic inversion and Euler deconvolution, overlaid on the local geological map.	
.....	91

## SUMÁRIO

<b>1 INTRODUÇÃO .....</b>	<b>16</b>
1.1 ESTRUTURA DA TESE .....	18
1.2 LOCALIZAÇÃO DA ÁREA DE ESTUDO .....	19
1.3 JUSTIFICATIVA E HIPÓTESE DE TRABALHO.....	20
1.4 OBJETIVOS .....	21
1.4.1 Objetivo Geral .....	21
1.4.2 Objetivos Específicos .....	22
<b>2 CONTEXTO GEOLÓGICO .....</b>	<b>23</b>
<b>3 METODOLOGIA .....</b>	<b>27</b>
<b>4 RESULTADOS E DISCUSSÕES.....</b>	<b>29</b>
4.1 SELEÇÃO DE ÁREAS PARA O DETALHAMENTO GEOFÍSICO/GEOLÓGICO	29
4.2 ARTIGO 1 – <i>EXPLORING COPPER RESOURCES: A GEOPHYSICAL AND GEOLOGICAL APPROACH IN THE SOUTH RIOGRANDE SHIELD, RS, BRAZIL</i> ..	34
4.2.1 Introduction and Objectives .....	34
4.2.2 Study Area and Geological Settings .....	36
4.2.3 Magnetometry and Gamma-Ray Spectrometry: An Overview of Their Applications in Mineral Exploration.....	39
4.2.3.1 Gamma-Ray Spectrometry.....	39
4.2.3.2 Magnetometry .....	40
4.2.4 Material and Methods .....	42
4.2.4.1Geophysical Data Processing for Copper Occurrence: Theoretical Insights, Evolution, and Effectiveness .....	44
4.2.5 Results and Discussions .....	48
4.2.5.1 Separation of Lithological Units into Groups.....	48
4.2.5.2 Airborne Gamma-Ray Spectrometry, Airborne Magnetometry, and Structural Analysis .....	49
4.2.5.3 Mineral Occurrences, Soil Geochemistry, and Stream Sediment Analysis....	52
4.2.5.4 Palma Region—Occurrences and Geochemistry Information .....	54
4.2.5.5 Data Integration Litho-Geophysical Profiles Analysis .....	57
4.2.6 Concluding Remarks .....	60

<b>4.3 ARTIGO 2 - GEOPHYSICAL INSIGHTS INTO COPPER DEPOSITS AT MINA SEIVAL, CAÇAPAVA DO SUL, BRAZIL: 3D MAGNETIC INVERSIONS AND EULER DECONVOLUTION .....</b>	<b>62</b>
4.3.1 Introduction and Objectives .....	62
4.3.2 Study Area and Regional Geological Setting.....	65
4.3.2.1 Local Geological, Structural Context and Hydrothermal Alteration of the Seival Mine Region .....	67
4.3.3 Materials and Methods .....	71
4.3.3.1 The Importance of Rock Physical Properties in Analysis and Interpretation..	73
4.3.3.2 The Use of Filters and Enhancement Techniques in Magnetometric and Gamma-Ray Spectrometric Data for Mineral Exploration.....	75
4.3.3.3 Euler Deconvolution .....	77
4.3.3.4 Magnetic data inversion.....	80
4.3.4 Results and Discussion .....	81
4.3.4.1 Analysis of 2D Maps – Airborne Geophysical Maps .....	82
4.3.4.2 Semiquantitative Analysis – Euler Deconvolution, Integrations, and MVI Models.....	83
4.3.5 Conclusions .....	92
<b>5 CONSIDERAÇÕES FINAIS .....</b>	<b>94</b>
<b>REFERÊNCIAS.....</b>	<b>96</b>

## 1 INTRODUÇÃO

A exploração mineral enfrenta desafios cada vez maiores, especialmente na identificação de novos alvos potenciais. Como destacado por Witherly e Allard (2010) em seus estudos sobre a evolução da geofísica na busca por depósitos de sulfetos maciços vulcanogênicos (VHMS) no *Greenstone Belt* de Abitibi, Québec, a taxa de descoberta de novos depósitos tem diminuído significativamente nas últimas décadas, mesmo com os avanços tecnológicos e o aprimoramento das metodologias geofísicas. A realidade atual é que as regiões mais acessíveis e superficiais já foram amplamente investigadas, e os novos alvos tendem a estar em profundidade ou em condições geológicas mais complexas.

Neste contexto, a exploração mineral se assemelha à pesca: "*Only good fishermen are successful, first by selecting the good lakes and then the good spots*" (WITHERLY e ALLARD, 2010). A escolha das áreas mais promissoras é fundamental para o sucesso exploratório, uma vez que os alvos mais superficiais e evidentes já foram identificados. Assim, a abordagem atual exige a integração de dados geofísicos de alta resolução, modelagem geológica tridimensional e refinamento de métodos interpretativos para delimitar as áreas de maior potencial mineral.

Hronsky e Groves (2008) reconhecem que as descobertas minerais costumam ocorrer após o surgimento de novos conceitos ou tecnologias. O avanço tecnológico tem sido proposto como uma solução para o declínio na taxa de sucesso da exploração (MCCUAIG e SHERLOCK, 2017), tornando a mineração cada vez mais dependente de grandes volumes de dados, mas sem necessariamente aumentar a qualidade do conhecimento gerado. A utilização de algoritmos avançados e maior capacidade computacional tem o potencial de reconhecer padrões em conjuntos de dados complexos (MCCUAIG e SHERLOCK, 2017); contudo, a dependência excessiva da tecnologia pode não resolver questões contextuais fundamentais na busca por novos alvos (KLEIN, 2015). Por exemplo, o desenvolvimento de novos métodos geofísicos pode aprimorar o mapeamento de processos geológicos (DENTITH e MUDGE, 2014), mas não necessariamente indicar a localização ideal para levantamentos antes da aquisição de dados, nem oferecer a melhor forma de integrar os dados gerados ao processo de tomada de decisão exploratória.

A exploração em áreas denominadas de *greenfield*, caracteriza-se por ambientes com poucos dados geocientíficos, exige criatividade e inovação humana

para preencher lacunas nos conjuntos de dados existentes e integrar os resultados ao processo exploratório em andamento (AITKEN *et al.*, 2018; DAVIES *et al.*, 2020). Embora a inteligência artificial (IA) tenha avançado significativamente na análise de padrões e na otimização de alvos, sua criatividade é frequentemente criticada por apenas replicar dados existentes, sem gerar soluções verdadeiramente inovadoras (SCHMIDHUBER, 2015; MARCUS, 2018).

Sendo assim pode-se afirmar que o pensamento criativo é essencial na exploração mineral, permitindo a formulação de hipóteses inovadoras para a definição de alvos (DAVIES *et al.*, 2021) e todo o conhecimento acerca do conceito de Sistemas Minerais fornece um arcabouço científico robusto para a resolução criativa de problemas. Através da revisão de informação empírica existente, é possível separar características que representam processos essenciais de formação de minérios daquelas que são apenas relevantes localmente (MCCUAIG *et al.*, 2010). Com esse conhecimento, um explorador pode gerar hipóteses inovadoras e baseadas na ciência para novos espaços de busca, reconhecendo padrões fundamentais em diferentes ambientes geológicos e estilos de mineralização.

Na metade Sul do estado do Rio Grande do Sul, onde esse estudo foi proposto, tem-se o registro de ocorrências cupríferas, minas inativas e diversas possibilidades de continuidades de corpos mineralizados principalmente em profundidade (RIBEIRO, 1978; REMUS *et al.*, 1999; TONILO, 2004; LOPES, 2013; LOPES *et al.*, 2018). Desta maneira, a aplicação de métodos geofísicos clássicos, como magnetometria e gamaespectrometria, são essenciais para diferenciar e caracterizar litotipos e estruturas favoráveis à mineralização em diversos tipos de depósitos (SANDRIN E ELMING, 2007; MOSTAFAEI E KIANPOUR, 2022; LEÃO-SANTOS *et al.*, 2022; ANDERSON *et al.*, 2023).

É importante salientar que cada depósito mineral possui uma assinatura geofísica distinta variando de acordo com as mudanças de propriedades físicas. Estas mudanças devem ser analisadas de forma detalhada a partir da integração com dados geológicos. Uma metodologia sistemática e básica associados a um pensamento criativo se torna importante na seleção de novas áreas e no aumento do conhecimento.

Neste estudo, a utilização de inversão de dados magnetométricos, Deconvolução de Euler, filtros de realce avançados e análise de radioelementos associados com o contexto geológico permitiram detectar e delinear corpos

mineralizados em superfície e em profundidade auxiliando no entendimento de padrões estruturais relevantes para as mineralizações.

Diante desse cenário, este trabalho busca demonstrar que a exploração mineral deve ser conduzida com estratégia e precisão, maximizando o uso de dados preexistentes e incorporando sistemáticas de análises de dados geofísicos, partindo de técnicas existentes e aplicadas de maneira consciente e embasada em informações diretas do contexto geológico. Ao selecionar "bons lagos" e os "melhores pontos", a mineração pode reduzir incertezas e custos operacionais, otimizando a descoberta de novos depósitos minerais de interesse econômico.

## 1.1 ESTRUTURA DA TESE

A presente tese está estruturada em cinco capítulos. O Capítulo 1 introduz o tema, contextualizando a área e o objeto de estudo, e apresenta a justificativa, a hipótese e os objetivos da pesquisa. O Capítulo 2 descreve o contexto geológico das unidades investigadas, enquanto o Capítulo 3 detalha os métodos adotados na pesquisa. O Capítulo 4 apresenta os resultados, divididos em dois artigos científicos, derivados de um estudo preliminar que selecionou áreas com maior quantidade de informações pré-existentes. A divisão em dois artigos se deu pela complexidade geológica e pelas diferenças nas análises e integrações dos resultados dos dados geofísicos processados. O Capítulo 5 consiste nas considerações finais.

O primeiro artigo, intitulado "*Exploring Copper Resources: A Geophysical and Geological Approach in the South Riogrande Shield, RS, Brazil*", foi publicado na revista *Geosciences* em janeiro de 2025 e pode ser acessado em <https://doi.org/10.3390/geosciences15020038>. Este estudo obteve resultados satisfatórios ao delimitar áreas potenciais para a ocorrência de cobre no Escudo Sul-Rio-Grandense com ênfase na caracterização da assinatura geofísica em rochas ultramáficas hospedeiras de cobre utilizando a integração de dados geológicos, geoquímicos, estruturais e geofísicos. A aplicação de filtros de realce em dados aéreos de magnetometria revelou lineamentos estruturais, enquanto a inversão MVI (Magnetic Vector Inversion) destacou a continuidade dos corpos em profundidade. Mapas de radioelementos identificaram contatos litológicos e forneceram parâmetros para futuras investigações. Perfis geoquímicos e geofísicos confirmaram a correlação entre anomalias magnéticas e ocorrências de cobre, apontando áreas promissoras

para exploração mineral. A versão apresentada nesta tese corresponde a uma versão formatada previamente à sua submissão para publicação em revista.

O segundo artigo, intitulado “*Geophysical Insights into Copper Deposits at Mina Seival, Caçapava do Sul, Brazil: 3D Magnetic Inversions and Euler Deconvolution*”, utilizou técnicas avançadas de realce dos dados magnetométricos para identificar descontinuidades estruturais e caracterizar corpos mineralizados com ênfase em rochas vulcânicas. A aplicação da Deconvolução de Euler associada à inversão magnética gerou resultados robustos, revelando feições estruturais e contatos litológicos mais precisos que os métodos convencionais. As análises permitiram correlacionar assinaturas magnéticas com estruturas geológicas subjacentes, identificando a continuidade dos corpos magnéticos e destacando direções estruturais preferenciais (NE e NW) como controladoras das mineralizações. Áreas potenciais para exploração mineral foram delineadas, evidenciando a importância da integração de técnicas geofísicas avançadas com dados geológicos para aprimorar o mapeamento e modelagem dos depósitos. Este artigo está estruturado e em fase de submissão.

Com a elaboração dos dois artigos, buscou-se caracterizar de forma detalhada as assinaturas geofísicas associadas a diferentes litotipos hospedeiros de cobre no Escudo Sul-Rio-Grandense, contribuindo para o avanço do conhecimento geológico da região e para o aprimoramento das metodologias de prospecção mineral.

## 1.2 LOCALIZAÇÃO DA ÁREA DE ESTUDO

A área de estudo está situada na metade sul do estado do Rio Grande do Sul (RS), Brasil (FIGURA 1a). Especificamente, abrange regiões próximas aos municípios de Caçapava do Sul, Lavras do Sul, Vila Nova do Sul e São Gabriel. O acesso às áreas de estudo ocorre principalmente pelas rodovias ERS-357 e BR-290 (FIGURA 1b).

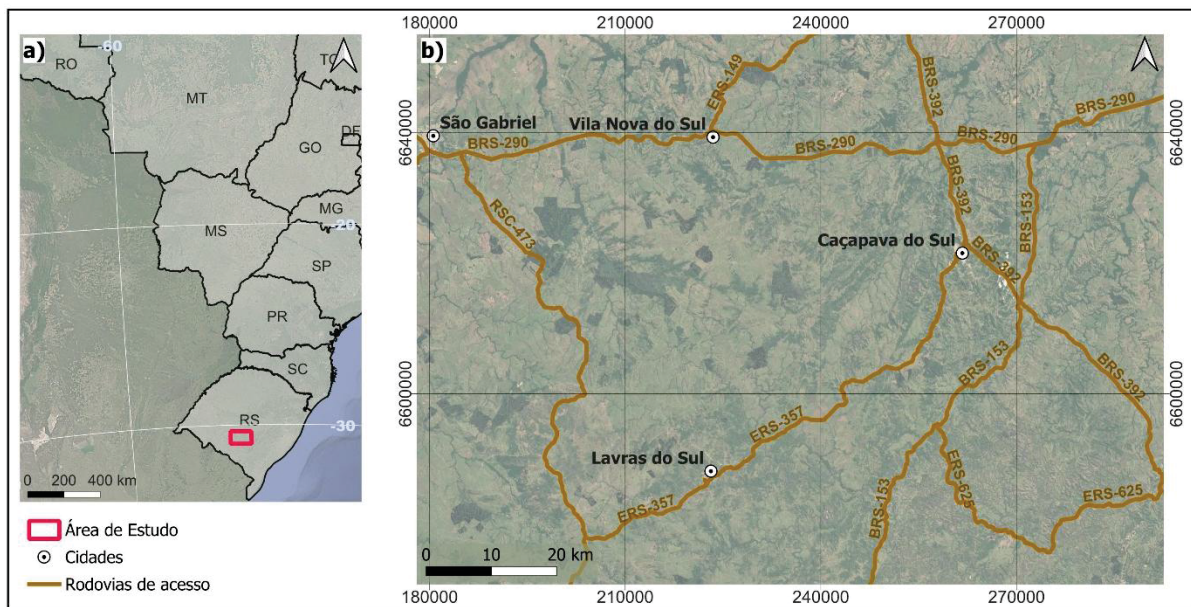


FIGURA 1 - Localização da área de estudo em a) Mapa geral com ênfase na localização da área de estudo no estado do Rio Grande do Sul (RS), em b) Mapa da área de estudo em detalhe com as rodovias de acesso e localização de cidades nas proximidades. Adaptado de Google (2025).

### 1.3 JUSTIFICATIVA E HIPÓTESE DE TRABALHO

A exploração mineral é um setor estratégico para o desenvolvimento econômico e tecnológico, demandando métodos cada vez mais eficientes para a identificação de depósitos minerais. Neste contexto, o presente estudo busca aprimorar as metodologias de pesquisa mineral existentes e apresentá-las de forma sistemática, propondo abordagens baseadas no processamento e na integração de dados geofísicos e geológicos. A utilização da deconvolução de Euler, inversões magnetométricas e análise de dados gamaespectrométricos, aliada a um minucioso levantamento bibliográfico sobre o contexto estrutural, mineralógico e litológico da área de estudo, ofereceu evidências que permitiram uma reinterpretação dos dados disponíveis e a proposição de novas áreas potenciais para mineralizações de cobre.

O impacto científico deste trabalho se destaca na contribuição para pesquisas na indústria mineral, ao demonstrar como o uso de dados existentes, públicos e previamente publicados pode ser maximizado para aumentar a assertividade na prospecção mineral. O estudo busca responder à questão fundamental: "Até onde pode-se chegar com os dados já disponíveis?" Ao enfatizar a importância da análise crítica e aprofundada de dados preexistentes, este trabalho visa reduzir custos

operacionais e otimizar a definição de áreas-alvo para novas investigações, promovendo uma abordagem mais eficiente na exploração mineral.

Ademais, os resultados desta pesquisa evidenciam a necessidade de um pensamento inovador no âmbito da indústria mineral. Constatase que a mera disponibilidade de recursos financeiros e a atuação de equipes altamente qualificadas não se mostram suficientes na ausência de uma abordagem estruturada, sistemática, crítica e criativa. Tal abordagem deve ser capaz de integrar informações pré-existentes e incorporar o conhecimento gerado por pesquisas acadêmicas consolidadas, as quais resultam de anos de estudos aprofundados dedicados à compreensão das questões petrológicas, dos processos de alteração hidrotermal e da caracterização petrográfica. O estudo propõe que, ao partir de uma base sólida de dados geofísicos e geológicos, tratados com excelência, é possível identificar novos alvos potenciais com maior precisão, agregando valor às campanhas exploratórias.

Este trabalho apresenta caráter inédito ao propor a caracterização e diferenciação das assinaturas geofísicas de rochas ultramáficas e vulcânicas associadas a ocorrências de cobre no Escudo Sul-Rio-Grandense, tema até então inexplorado na literatura científica.

A hipótese central deste estudo consiste na premissa de que uma análise integrada de assinaturas magnetométricas e gamaespectrométricas, associada a técnicas avançadas de processamento de dados, pode aprimorar significativamente a identificação e caracterização de ocorrências cupríferas no Escudo Sul-Rio-Grandense.

Dessa forma, as abordagens propostas nesta tese e consequente resultados têm como intuito reforçar que, por meio de uma abordagem sistemática e criteriosa, é possível maximizar o aproveitamento de dados preexistentes, proporcionando avanços significativos na exploração mineral e na definição de novas áreas potenciais de interesse econômico.

## 1.4 OBJETIVOS

### 1.4.1 Objetivo Geral

Desenvolver e aplicar uma metodologia sistemática para a análise de novas áreas potenciais para mineralizações cupríferas no Escudo Sul-Rio-Grandense,

utilizando dados geológicos e geofísicos preexistentes. A metodologia proposta visa gerar uma interpretação diferenciada das assinaturas geofísicas, a partir da aplicação de técnicas de realce de dados e integração com o contexto estrutural, de modo a definir áreas-alvo com maior assertividade e custos operacionais reduzidos.

#### 1.4.2 Objetivos Específicos

Especificamente, são propostos os seguintes objetivos:

- I. Propor uma abordagem sistemática para a pesquisa mineral, combinando técnicas de processamento de dados geofísicos e integração com dados geológicos, baseada em metodologias avançadas de inversão e realce de anomalias.
- II. Caracterizar a distribuição e variação dos valores de radioelementos em rochas máfico-ultramáficas, intermediárias, ígneas plutônicas, vulcanoclásticas e sedimentares, e sua relação com características estruturais, mineralógicas e litológicas.
- III. Aplicar técnicas qualitativas e semi-quantitativas de processamento geofísico, como filtragens e Deconvolução de Euler para a identificação e caracterização de lineamentos estruturais associados à mineralização.
- IV. Desenvolver modelos de inversão de aeromagnetometria para avaliar a continuidade, geometria e profundidade dos corpos mineralizados, fornecendo subsídios para inferências sobre a distribuição da mineralização em subsuperfície.
- V. Elaborar perfis litogeofísicos detalhados para correlacionar as variações de propriedades físicas com unidades litológicas, auxiliando na caracterização dos depósitos minerais.
- VI. Integrar modelos de inversão magnetométrica com dados geoquímicos de solo e sedimento de corrente, buscando aprimorar a definição de áreas-alvo para exploração mineral e aumentar a eficiência na identificação de novos depósitos.

## 2 CONTEXTO GEOLÓGICO

O estado do Rio Grande do Sul é composto por três províncias geológicas distintas — Mantiqueira, Paraná e Costeira —, cada uma com características litoestruturais, geocronológicas, geomorfológicas e evolutivas próprias (ALMEIDA, 1977). A área de estudo situa-se na porção meridional da Província Mantiqueira, correspondente a um sistema orogênico formado predominantemente por rochas do Proterozoico. Esta província se estende ao longo da região costeira, do sul da Bahia até o Rio Grande do Sul, prolongando-se até o Uruguai. No Rio Grande do Sul, a Província Mantiqueira está localizada na região central do estado e é referida como Escudo Sul-Rio-Grandense (ESRG) (HASUI et al., 1975).

O ESRG apresenta associações de rochas metamórficas, ígneas e sedimentares, organizadas em um complexo arranjo tectono-estratigráfico, segmentadas por lineamentos regionais orientados a NE-SW e NW-SE (LAUX, 2017). O ESRG registra processos de geração e deformação da crosta continental durante os ciclos Transamazônico (2,26–2,00 Ga) e Brasiliano (900–535 Ma), sendo composto por unidades do Cinturão Dom Feliciano formadas no Neoproterozoico, como o Bloco São Gabriel e o Batólito Pelotas, unidades paleoproterozoicas como o Bloco Taquarembó, além do Bloco Tijucas com domínios neoproterozoicos e paleoproterozoicos (HARTMANN et al., 2007) (FIGURA 2a). A área de estudo compreende os Blocos São Gabriel, Taquarembó e a Bacia do Camaquã, que serão descritos em detalhe abaixo:

O Bloco Taquarembó é representado pelo Complexo Granulítico Santa Maria Chico, composto principalmente por granulitos félsicos (trondhjemíticos) e máficos, piroxenitos, lentes de harzburgitos, gnaisses com sillimanita, mármore e gnaisses cálcio-silicáticos (HARTMANN et al., 2007). As idades de acreção dos magmas, determinadas por análises de zircão (SHRIMP), variam de 2,5 a 2,1 Ga, enquanto o evento colisional responsável pela formação dos granulitos ocorreu por volta de 2,02 Ga (HARTMANN et al., 1999, 2000).

O Bloco Tijucas apresenta dois domínios distintos. O primeiro, de idade paleoproterozoica, é representado pelo Complexo Encantadas, composto por gnaisses dioríticos e tonalítico-trondhjemíticos, com magmatismo entre 2,26 Ga e 2,1 Ga e metamorfismo anfibolítico em torno de 2,03 Ga (HARTMANN et al., 2007). O segundo domínio, neoproterozoico a eopaleozóico, é formado pela Faixa Porongos,

caracterizada por rochas metavulcânicas datadas entre 780 e 770 Ma (CHEMALE Jr., 2000) e metassedimentos que contêm zircões detriticos de até 1,998 Ga (HARTMANN et al., 2004). Evidências isotópicas e geocronológicas indicam que essa faixa se formou em uma bacia de rifte sobre crosta continental adelgaçada, sem apporte significativo de material juvenil neoproterozoico, contrariando hipóteses de formação em ambiente de retroarco coevo ao arco São Gabriel (CHEMALE, 2000; SAALMANN et al., 2006b). Assim, o Bloco Encantadas representa um segmento crustal paleoarqueano a paleoproterozoico que foi retrabalhado no Neoproterozoico, podendo ter afinidades com terrenos africanos, como o Complexo Epupa na Namíbia (LEITE et al., 2000; KRÖNER et al., 2004; KONOPÁSEK et al., 2008; SAALMANN et al., 2011).

O Bloco São Gabriel configura-se como um prisma acrescionário composto por associações petrotectônicas características de arcos magmáticos juvenis desenvolvidos entre aproximadamente 930 e 680 milhões de anos, conforme estudos recentes de Philipp et al. (2018). Esses arcos correspondem ao arco intraoceânico Passinho (890–860 Ma) e ao arco de margem continental São Gabriel (770–720 Ma), formados durante a abertura do Oceano Charrua e posterior subducção, com intensa isotopia juvenil e mínima influência de material mais antigo, com exceção dos granitos tardios como o Santa Zélia. Os corpos plutônicos cálcio-alcalinos, representados principalmente pelo Complexo Cambaí, possuem idades entre 735 e 680 Ma (BABINSKI et al., 1996; HARTMANN et al., 2000, 2011). Além disso, o Bloco inclui sequências vulcano-sedimentares dos Complexos Palma e Bossoroca, compostas por rochas metavulcânicas maficas e metassedimentares (HARTMANN et al., 2007). A acreção do Bloco São Gabriel ao Terreno Nico Pérez ocorreu entre 710 e 700 Ma, seguida pelo estágio pós-colisional marcado pela intrusão de granitos tardi-orogênicos (700–680 Ma), que culminou no colapso da estrutura representado pela bacia Pontas do Salso (PHILLIP et al., 2018; VEDANA e PHILIPP, 2016; VEDANA et al., 2017). Estruturalmente, o bloco é controlado por zonas de cisalhamento orientadas NE–SW, rotacionadas pela Zona de Cisalhamento Ibaré, evidenciada por anomalias magnéticas e formas elípticas dos corpos plutônicos. A justaposição do Bloco São Gabriel com o Bloco Encantadas foi mediada por zonas de cisalhamento crustais de direção SW–NE, associadas a intenso magmatismo granítico, integrando os estágios finais da amalgamação do Gondwana Ocidental até cerca de 530 Ma (SAALMANN et al., 2011).

O final do Neoproterozoico e o início do Paleozoico registram ainda a formação de unidades sedimentares e vulcanogênicas em bacias tectônicas alongadas. Esses depósitos consistem em espessas sucessões de conglomerados, arenitos e pelitos de ambientes continentais, costeiros e marinhos, associados a rochas vulcanogênicas de afinidade alcalina. No centro-sul do Rio Grande do Sul, destaca-se a Bacia do Camaquã, que recobre rochas pré-cambrianas e reúne espessas sucessões siliciclásticas e vulcanogênicas (ALMEIDA, 1969; FAMBRINI e FRAGOSO-CESAR, 2006).

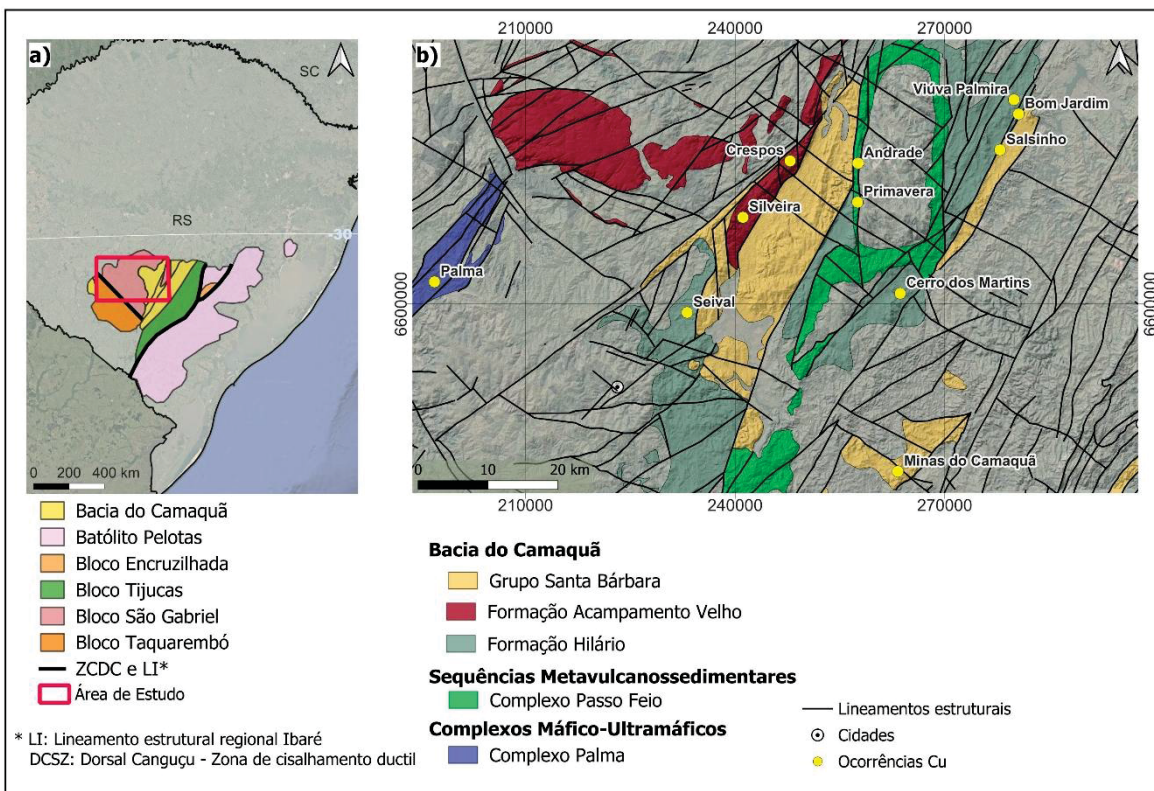


FIGURA 2 - Contexto geológico da área de estudo. Em a) Unidades Geotectônicas do ESRG e em b) Principais litologias e lineamentos estruturais associados a ocorrências cupríferas. FONTE: Adaptado de Hartmann et al., (2007), Laux (2021) e Google (2025).

A FIGURA 2b apresenta os principais litotipos associados a ocorrências minerais, prospectos previamente estudados e minas atualmente inativas, todos localizados na área de abrangência deste estudo. A seguir, serão detalhados apenas os litotipos relacionados aos casos mencionados. Informações mais completas sobre outros litotipos, incluindo rochas correlatas e contemporâneas, podem ser encontradas em referências como Laux (2021).

Ribeiro (1978) registrou ocorrências cupríferas denominadas de ocorrências Palma no Complexo Palma. Segundo Garcia (1980) e Laux (2021), esse complexo

integra o contexto do Bloco São Gabriel, sendo composto por associações de rochas máfico-ultramáficas que ocorrem como lascas tectônicas nos terrenos TTG e nas sequências vulcano-sedimentares. É composto por uma faixa constituída de rochas ultramáficas, xistos magnesianos, calcários e quartzitos. De acordo com Laux (2021), as idades de cristalização determinadas por U-Pb em zircão são de  $881 \pm 14$  Ma e  $780 \pm 5$  Ma, ambas correspondentes ao Neoproterozoico.

As ocorrências Andrades e Primavera (REMUS, 1999; CPRM, 2021) integram o Complexo Passo Feio, caracterizado por Bitencourt (1983) como uma sequência de rochas metavulcanossedimentares distribuídas ao redor do Granito Caçapava do Sul. Essa sequência é composta principalmente por metapelitos, anfibolitos xistosos, anfibolitos gnáissicos, metagabros e rochas metavulcanoclásticas, com presença subordinada de xistos magnesianos, gnaisses quartzo-feldspáticos, mármore, quartzitos e metavulcânicas (LAUX, 2021).

A Formação Hilário abriga diversas ocorrências minerais, entre elas Seival, Cerro dos Martins, Viúva Palmira e Bom Jardim (RIBEIRO, 1978; REMUS, 1999; TONILO, 2004; LOPES, 2013). Esta formação originou-se a partir do magmatismo pós-colisional associado à orogênese Dom Feliciano (660–550 Ma) e é contemporânea à sedimentação da Bacia do Camaquã (606–540 Ma). Esse magmatismo foi dividido em dois eventos principais, distintos em idade e geoquímica (GASTAL e LAFON, 1998).

O primeiro evento magmático (606–580 Ma) gerou as rochas vulcânicas efusivas e piroclásticas da Formação Hilário (NARDI e LIMA, 1985). Essa unidade é caracterizada por um vulcanismo andesítico expressivo, com ocorrência de derrames, tufos, brechas, conglomerados vulcânicos, fluxos de lama, diques, rochas maficas intrusivas e, localmente, rochas dacíticas e lamprofíricas (LAUX, 2021; RIBEIRO et al., 1966).

O segundo evento magmático é representado pela Formação Acampamento Velho, que abriga ocorrências como Crespos e Silveira (CPRM, 2021). Essa formação comprehende o vulcanismo relacionado à evolução da Bacia do Camaquã, caracterizado por derrames de lavas riolíticas, ignimbritos, tufos (de pó, cinza ou lápili) e brechas vulcânicas (WILDNER e LIMA, 1994; PORCHER et al., 1995; SOMMER, 1994, 2003). As idades atribuídas a esta unidade variam entre 540 e 570 Ma (CHEMALE Jr, 2000; ALMEIDA et al., 2002; SOMMER et al., 2005, 2006).

A mina inativa denominada de Minas do Camaquã e a ocorrência Salsinho fazem parte do Grupo Santa Bárbara, classificado por Laux (2021) como integrante das coberturas da Bacia do Camaquã. Este grupo é composto predominantemente por arenitos e arenitos conglomeráticos, com níveis cascalhosos e estratificação plano-paralela ou cruzada acanalada. Os fragmentos presentes são majoritariamente de rochas vulcânicas alcalinas, andesitos, traquitos e, em menor proporção, clastos de rochas sedimentares (BORBA e MIZUSAKI, 2003). Análises de zircões detriticos realizadas por Bicca et al. (2013) indicaram uma idade de  $566 \pm 9$  Ma, interpretada como a mínima para a deposição desses sedimentos.

As Minas do Camaquã, um dos exemplos de mina inativa na região, incluem os setores Uruguai e São Luiz, onde o minério foi explorado em rochas deformadas, que originaram zonas brechadas e, na porção central do corpo, uma zona de *stockwork* (TEIXEIRA e GONZALES, 1988). As mineralizações ocorrem em filões e como sulfetos de cobre disseminados, principalmente calcopirita, bornita e calcocita, com ouro e prata como subprodutos (REMUS et al., 1998). A Jazida Santa Maria, principal depósito das Minas do Camaquã, apresenta mineralização disseminada, estratiforme e zonada, ocorrendo em lentes controladas pela geometria e faciologia dos corpos sedimentares (BADI, 1983; BADI e GONZALEZ, 1988).

### 3 METODOLOGIA

A tese foi estruturada em um fluxo de atividades que abrange três etapas principais:

**1<sup>a</sup> Etapa** – Definição e seleção da área de estudo, com base em referências bibliográficas sobre ocorrências cupríferas e informações relacionadas à paragênese mineral e aos processos formadores de depósitos minerais no Escudo Sul-Rio-Grandense. Foram escolhidas duas áreas com o maior volume de dados geológicos disponíveis para permitir uma análise detalhada das assinaturas geofísicas, incluindo os contatos litológicos entre rochas hospedeiras e encaixantes, além do entendimento do contexto estrutural, a continuidade das principais estruturas e a correlação com os dados geoquímicos.

**2<sup>a</sup> Etapa** – Detalhamento dos dados geofísicos aerogamaespectrométricos e aeromagnetométricos, utilizando filtros de realce para identificar assinaturas geofísicas associadas à presença de corpos contínuos ou relacionados às ocorrências

cupríferas mencionadas em estudos anteriores. Foi dado ênfase nas ocorrências cupríferas hospedadas em rochas maficas-ultramáficas, e os resultados dessa etapa originaram o primeiro artigo.

**3<sup>a</sup> Etapa** – Detalhamento das características geofísicas e geológicas das ocorrências cupríferas em rochas vulcânicas que incluem tuhos, aglomerados vulcânicos e andesitos, culminando no desenvolvimento do segundo artigo.

Este fluxo metodológico proporcionou uma abordagem organizada e coerente para o desenvolvimento da tese e a produção dos dois artigos.

Os materiais utilizados neste estudo são descritos a seguir:

i) Dados geofísicos de aeromagnetometria e aerogamaespectrometria, na escala 1:250.000, pertencentes ao Projeto Escudo do Rio Grande do Sul, concluído em 2010 pelo Serviço Geológico do Brasil (CPRM). A aquisição e o processamento dos dados foram realizados pela LASA Prospecções S.A. O projeto abrangeu a porção do extremo sul do Brasil, com uma área de aproximadamente 75.600 km<sup>2</sup>. Segundo o CPRM (2010), os parâmetros de aquisição utilizados foram:

- Direção das linhas de voo: N-S;
- Espaçamento entre as linhas de voo: 500 metros;
- Altitude média de voo: 100 metros.

O aerolevantamento foi realizado com a aeronave Cessna C208 Caravan (prefixo PT-MEP), equipada com um aeromagnetômetro Scintrex modelo CS-2 (sensor de bombeamento ótico de vapor de césio), um gamaespectrômetro Exploranium modelo GR-820 e um sistema de GPS Trimble AgGPS 132 DGPS "Realtime" (CPRM, 2010). A resolução do aeromagnetômetro é de 0,001 nT, operando na faixa de 20.000 a 95.000 nT. As leituras do magnetômetro foram realizadas a cada 0,1 segundo, o que corresponde a aproximadamente 6,5 metros de intervalo de amostragem no terreno, considerando a velocidade de 235 km/h da aeronave. O processamento dos dados seguiu os procedimentos descritos pela IAEA (1991) e foi realizado pela LASA Prospecções S.A., conforme a CPRM (2010).

ii) Dados aeromagnetométricos e gamaespectrométricos adquiridos no Projeto Primavera, realizado no ano de 2010. A aquisição e o processamento dos dados foram conduzidos pela LASA Prospecções S.A. Os dados pertencem ao Laboratório de Geofísica Aplicada na Universidade Federal do Pampa e foram cedidos para a

realização desse estudo. A área de abrangência do projeto está localizada no extremo sul do Brasil, abrangendo os municípios de Caçapava do Sul e Lavras do Sul, com uma cobertura total de aproximadamente 12.681 km<sup>2</sup>.

Os parâmetros técnicos utilizados no levantamento aerogeofísico foram:

- Direção das linhas de voo: N14W;
- Espaçamento entre linhas de voo na área que abrange o estudo: 200 metros;
- Altitude média de voo: 100 metros.

iii) Geoprocessamento e integração de informações (SIG) foram realizados por meio de interpretações de fotos aéreas e imagens de satélite. Os modelos digitais de elevação, curvas de nível e mapa de declividade do terreno foram gerados com base nos dados do sensor *Alos Palsar*, fornecidos pelo ASF DAAC (2019), com resolução de 12,5 metros.

iv) Mapa de associações tectônicas e recursos minerais do Escudo Sul-Rio-Grandense, com escala 1:500.000, desenvolvido pelo CPRM em 2021, junto com o banco de dados vetorizados de mapeamento geológico, estrutural e de recursos minerais.

v) Mapas geológicos e estruturais de detalhe e banco de dados desenvolvidos e disponibilizados por RIBEIRO (1978), TONILOLO *et al.*, (2007); FONTANA *et al.*, (2017) e LOPES *et al.*, (2018).

vi) Planilhas de análise de elementos geoquímicos obtidos por coleta de solo e sedimento de corrente do Projeto Levantamento Geoquímico do Rio Grande do Sul, realizado em 1976 e revisado em 2020 para validação da consistência dos dados e atualização das coordenadas e sistema de projeção para SIRGAS 2000.

## **4 RESULTADOS E DISCUSSÕES**

Os resultados consistem no desenvolvimento da pesquisa de acordo com o que foi exposto nas etapas 1, 2 e 3.

### **4.1 SELEÇÃO DE ÁREAS PARA O DETALHAMENTO GEOFÍSICO/GEOLÓGICO**

A definição das áreas de estudo é etapa fundamental para o sucesso de projetos de prospecção mineral, pois direciona os esforços para regiões com maior potencial de ocorrência de depósitos econômicos. Neste trabalho, a escolha das áreas priorizadas baseou-se na integração de dados geológicos, geoquímicos e geofísicos disponíveis, associada à análise crítica de estudos anteriores, com destaque para os trabalhos de Ribeiro (1978) e Remus (1999). Foram utilizadas informações de geoquímica de amostras de solo, sedimentos de corrente, mapeamentos de afloramentos geológicos e a localização de ocorrências de cobre, prospectos e minas inativas de CPRM (2021) e Ribeiro (1978). E também, informações de levantamentos de dados como o projeto BANEO (TONILOLO *et al.*, 2007), que consiste na análise e caracterização da metalogenia das bacias neoproterozoicas-eopaleozoicas do Sul do Brasil, (FIGURA 3). A seguir, são apresentados os critérios de seleção e as áreas priorizadas para investigação.

As considerações de Ribeiro (1978) foram fundamentais para a escolha das áreas. O autor compilou informações sobre ocorrências cupríferas no Escudo Sul-Rio-Grandense e elaborou um mapa previsional do cobre, categorizando as áreas potenciais em sete grupos distintos com base em similaridades litológicas, mineralógicas e tectônicas. Entre os principais critérios utilizados, destacam-se:

- i) Presença de cobre em minas ou garimpos conhecidos e/ou indícios em campo, como a identificação de malaquita e outros minerais oxidados;
- ii) Presença de rochas mães e hospedeiras, como os andesitos da Formação Hilário, rochas básicas-ultrabásicas da Formação Cerro Mantiqueiras, granitos de Lavras do Sul, Caçapava do Sul e Jaguarari, andesitos Rodeio Velho e riolitos do Acampamento Velho;
- iii) Condicionamento tectônico favorável, como observado nas Minas do Camaquã, onde as mineralizações são controladas por falhas de direção NW. No estado do Rio Grande do Sul, são reconhecidos dois sistemas principais de falhas: (a) N20–30E, caracterizado por falhas inversas, e (b) N50–60W, formado por falhas de menor extensão;
- iv) Presença de anomalias magnéticas e potássicas.

Complementando esses critérios, Remus (1999) realizou estudos detalhados em prospectos e ocorrências de cobre. Na área das Minas do Camaquã, o autor destacou que fraturas regionais orientadas E–W e NW, bem como suas interseções, representam feições estruturais importantes, atuando como possíveis canalizadoras

de fluidos hidrotermais por volta de 594 Ma. As litologias predominantes — conglomerados e arenitos, caracterizados por alta porosidade, e metamargas e mármore, altamente reativos aos processos de substituição — são apontadas como encaixantes preferenciais para a mineralização.

De acordo com Remus (1999), os depósitos epigenéticos hidrotermais do Complexo Passo Feio (por exemplo, a ocorrência de Andraditas) apresentam potencial econômico relativamente menor, estando sua gênese associada à remobilização e/ou assimilação de sulfetos pré-existentes durante a intrusão sin-tectônica do Granito Caçapava. O autor também sugere que o plutonismo pós-colisional, relacionado ao final da Orogênese Dom Feliciano, foi uma provável fonte de calor, enxofre e metais-base, responsável pela geração das mineralizações. Dessa forma, o final da Orogênese é interpretado como o período mais favorável para a formação dos depósitos de metais-base no Escudo Sul-Rio-Grandense.

A partir dessas considerações, foram priorizadas áreas que reúnem a presença de cobre, seja em prospectos já conhecidos ou em ocorrências cupríferas pouco estudadas, associadas a contextos geológicos favoráveis, relacionados a rochas encaixantes e hospedeiras, além da presença de principais direções estruturais que controlam a mineralização. Também foram analisados mapas geofísicos, priorizando-se áreas com assinaturas magnéticas contrastantes.

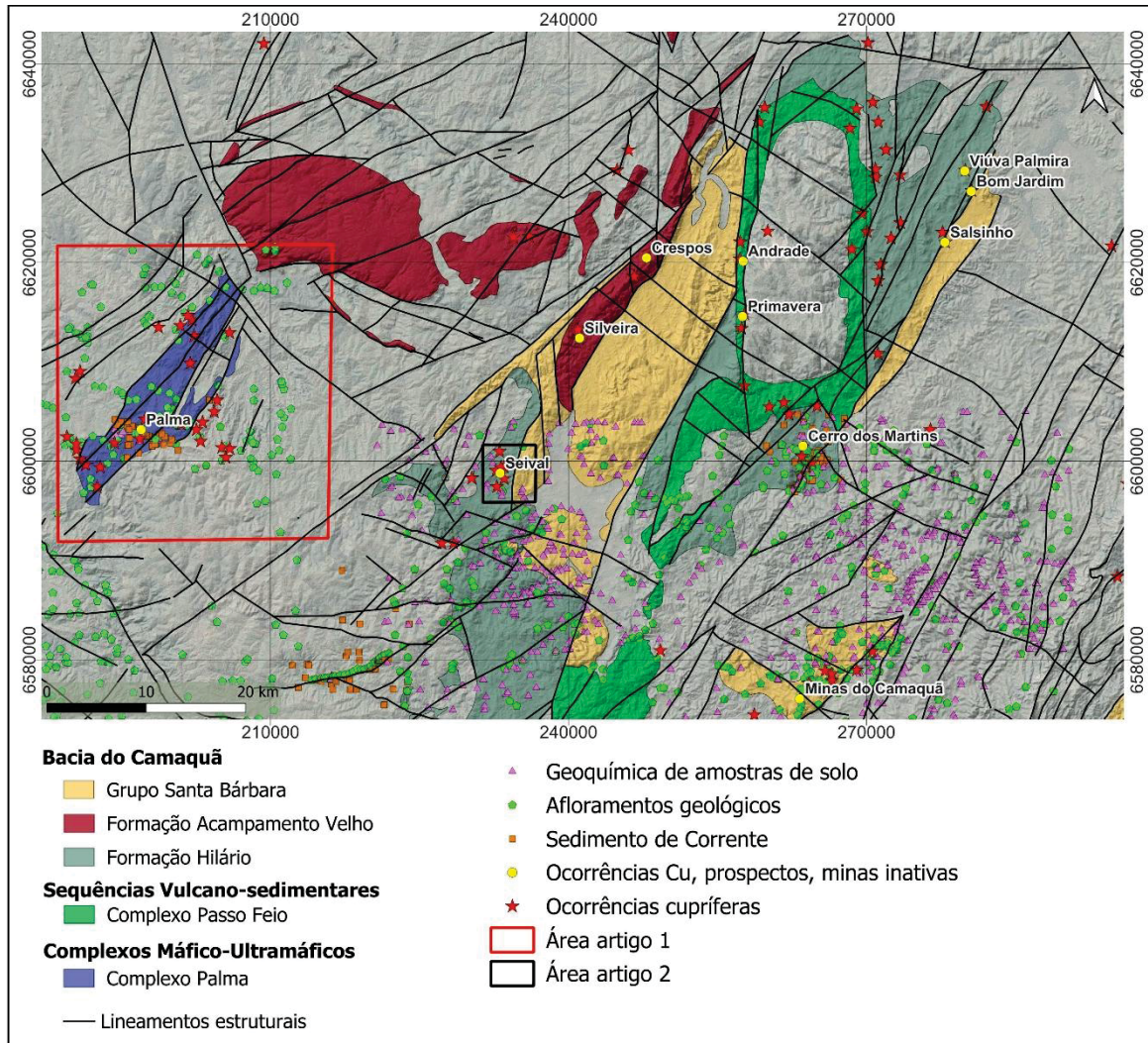


FIGURA 3 – Localização de dados geoquímicos, afloramentos geológicos e ocorrências de Cu. FONTE: Adaptado de CPRM (2021), Google (2025), Ribeiro (1978) e Toniolo et al. (2007).

A primeira área selecionada foi a ocorrência Palma, localizada no Complexo Palma, um corpo máfico-ultramáfico que abriga diversas ocorrências cupríferas já descritas por Ribeiro (1978). Esta região reúne um volume expressivo de dados, incluindo amostras de sedimentos de corrente, mapeamentos de afloramentos geológicos e análises geoquímicas de solo. Adicionalmente, estão disponíveis dados de geofísica aérea da CPRM, contemplando levantamentos aeromagnetométricos e gamaespectrométricos. Esses fatores possibilitaram uma análise detalhada das assinaturas geofísicas, dos contatos litológicos e do contexto estrutural. A área de Palma é o foco do Artigo 1 (retângulo vermelho, FIGURA 3).

A segunda área corresponde à ocorrência Seival, inserida nas unidades da Formação Hilário e do Grupo Santa Bárbara, pertencentes à Bacia do Camaquã. A Mina Seival compartilha de um contexto geológico de idades e processos de formação

correlatos a outros prospectos relevantes da região, como Cerro dos Martins, Bom Jardim, Viúva Palmira e as Minas do Camaquã. A seleção desta área foi favorecida pela presença de minas inativas e pela abundância de estudos anteriores, que forneceram informações detalhadas sobre petrografia, alteração hidrotermal e contexto estrutural. Assim como na área de Palma, a região também dispõe de dados de geofísica aérea, mapeamento de afloramentos e geoquímica de amostras de solo, permitindo uma abordagem integrada para a análise. Esta área é abordada no Artigo 2 (retângulo amarelo, FIGURA 3).

Dessa forma, a seleção das áreas de Palma e Seival baseou-se em uma abordagem integrada, que combinou a análise de dados geológicos, geoquímicos e geofísicos com o embasamento teórico proporcionado por estudos anteriores. Essa metodologia permitiu priorizar regiões com maiores chances de sucesso exploratório, alinhando os objetivos do presente trabalho às perspectivas geológicas promissoras do Escudo Sul-Rio-Grandense.

## 4.2 ARTIGO 1 – EXPLORING COPPER RESOURCES: A GEOPHYSICAL AND GEOLOGICAL APPROACH IN THE SOUTH RIOGRANDE SHIELD, RS, BRAZIL

### ABSTRACT

The search for mineral resources presents an enduring challenge as these demands consistently surge, and the utilization of geophysics is undeniably intertwined with the pursuit of novel prospects. Technological advancements over recent decades have facilitated access to 2D and 3D visualization software, enabling robust data integrations. Consequently, interpreters possess the latitude to harness their ingenuity and technical acumen in conducting multifarious analyses. Mineral exploration in greenfield areas, a particularly challenging endeavor, often commences with regional surveys and circumscribed information about the terrain. Notwithstanding limited preliminary data, the judicious deployment of filtering, modeling, and inversion techniques with geophysical data holds sway in catalyzing discoveries. This study, with its comprehensive amalgamation of diverse copper occurrence indicators and the novel procedural framework it establishes for processing and integrating airborne gamma-ray spectrometry and magnetometry geophysical and geological data, exemplifies the complexity and depth of our field. Elaborate litho-geophysical profiles, linked with data concerning mineral occurrences and geochemistry, pinpoint potential copper deposits in the area. This multidisciplinary approach and inversion mode provide detailed insights into probable mineralized body continuity and regional structural frameworks, offering valuable guidance for future regional mineral exploration efforts.

**Keywords:** mineral exploration; MVI; data integration techniques; copper occurrences; airborne magnetometry; airborne gamma-ray spectrometry

#### 4.2.1 Introduction and Objectives

A new mineral discovery holds immense value, particularly in the context of evergrowing market demands. Metallic minerals, including copper, are highly sought after due to their critical role in advancing modern technologies. Copper in particular is indispensable for sustaining contemporary life, with its applications spanning renewable energy systems, electronics, and infrastructure. However, experts warn of

a looming copper scarcity in the coming years, which could lead to significant economic disruptions (ATTWOOD, 2022). This looming crisis underscores the importance of efficient mineral exploration and the development of new mines. Yet, this journey is fraught with challenges, as evidenced by the recent volatility in copper prices, which signals potential constraints on mine development sooner than anticipated. The situation in Chile, one of the world's largest copper suppliers, exemplifies these projections, with major companies facing declining export revenues due to production issues stemming from diminishing ore quality and increased extraction costs.

In light of these challenges, the need for new copper discoveries is more urgent than ever to meet or sustain global demand until alternative energy solutions emerge. However, as Oliveira (2024) and Costa (2024) note, finding significant new deposits has become increasingly difficult. Most large, economically valuable mineral provinces have already been identified, leaving researchers to target deeper and more complex deposits. Modern mineral exploration now relies heavily on advanced equipment, robust software, and data processing techniques capable of creating detailed 3D models. However, success in exploration hinges on integrating these geophysical results with comprehensive geological data, including structural, geochemical, and petrological information.

The state of Rio Grande do Sul (RS) exemplifies the potential for polymetallic mineral exploitation, including copper. Metal exploration in RS began in the early 20th century, gained momentum in the 1960s, and continues today, primarily driven by private sector interest. The state has hosted notable mines such as Minas do Camaquã and Mina Seival, though both are currently inactive. Ribeiro (1978) classified numerous copper occurrences in RS based on their associated lithologies, providing a foundation for subsequent exploration. Building on decades of geological work by the Geological Survey of Brazil (CPRM), which includes mineral resource mapping, lithological studies, geochemical data, and aero-geophysical surveys, this study seeks to refine the understanding of copper occurrences in RS. Despite the regional scale of much of the existing data (1:500,000/1:250,000), the aim is to identify areas with higher potential for localized research.

Geophysical methods such as gamma spectrometry and magnetometry have proven invaluable in copper exploration and characterization. Gamma spectrometry measures the natural radioactivity of rocks and soils, revealing the distribution of elements like potassium, uranium, and thorium, which often indicate hydrothermal

alteration associated with copper mineralization (WILFORD *et al.*, 1997). Magnetometry detects variations in the Earth's magnetic field, providing insights into magnetite-rich mineralization and geological structures, such as faults and intrusions, often linked to porphyry copper systems (REEVES, 2005). These methods have been successfully applied in various studies, such as mapping copper-rich lithologies in Zambia's Copperbelt (BREUSTEDT *et al.*, 2011) and identifying mineralized zones in the Andes of South America (CLARK, 1997).

To advance copper exploration in RS, this study presents a workflow that integrates geological data with processed airborne magnetic and gamma-ray spectrometry geophysical datasets. This integrated approach enables a better understanding of lithological contacts, structural frameworks, and the depth and continuity of magnetic bodies associated with copper occurrences, thereby enhancing the precision and effectiveness of mineral research.

#### 4.2.2 Study Area and Geological Settings

The study area is located near the municipalities of Vila Nova do Sul, São Gabriel, and Lavras do Sul in Rio Grande do Sul, Brazil (Figure 1a). Geologically, it is situated in the southern portion of the Mantiqueira Province and is referred to as the South Riograndense Shield (SRGS) (Figure 1b). This region, recognized for its geological characteristics and mineral occurrences, is the result of a process of continental crust generation and deformation, with the most significant contributions occurring during the Transamazonian cycle (2.26–2.00 Ga) and the Brasiliano cycle (900–535 Ma) (HASUI *et al.*, 1975; ALMEIDA *et al.*, 1981).

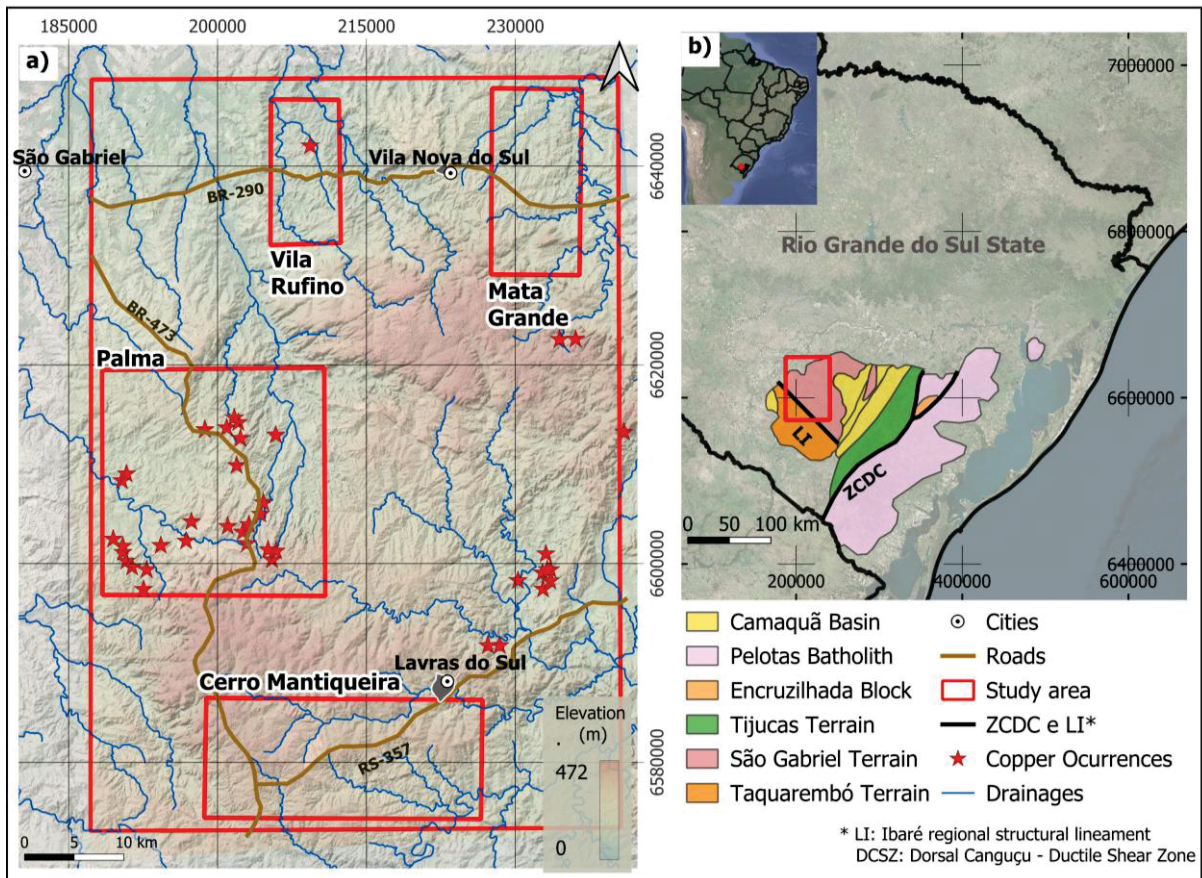


FIGURE 1 - (a) Main access highways and location of copper occurrences in the study area (CPRM, 2021) and (b) map of the state of Rio Grande do Sul, the location of the leading regional geological features and the location of the study area.

The SRGS comprises units of the Dom Feliciano Belt established in the Neoproterozoic, represented by the São Gabriel Tijucas and Pelotas Batholith terrains. Additionally, Paleoproterozoic units occur, such as the Taquarembó Terrain and the Tijucas terrain (HARTMANN *et al.*, 2007) (Figure 1a). Locally, the study area is located within the tectonostratigraphic units of the Taquarembó Terrain and São Gabriel Terrain.

The Taquarembó Terrain is represented by the Santa Maria Chico Granulite Complex, predominantly consisting of felsic granulites (trondhjemitic) and mafic rocks, pyroxenites, lenses of harzburgites, sillimanite gneisses, marbles, and calcium-silicate gneisses (HARTMANN *et al.*, 2007). Ages of magma accretion for the granulite complex (zircon, SHRIMP) were obtained between 2.5–2.1 Ga, with the collisional event that generated the granulites occurring at 2.02 Ga (HARTMANN *et al.*, 1999, 2000).

The São Gabriel Terrain consists of an accretionary prism with petrotectonic associations of passive margin and back-arc environments, ophiolites, volcano-

sedimentary magmatic arcs, and plutonic arcs. It is represented by juvenile rocks (meso to Neoproterozoic) including plutonic rocks and low to medium-K calc-alkaline arc rocks (represented by the Cambaí Complex). Zircon ages (TIMS and SHRIMP) range from around 735–680 Ma (BABINSKI *et al.*, 1996; HARTMANN *et al.*, 2000, 2011). According to Hartmann *et al.* (2007), there is also a volcano-sedimentary sequence called the Palma Complex (lower part of the sequence) and the Bossoroca Complex (upper part of the sequence), composed of mafic metavolcanic and associated metasedimentary rocks. The metasedimentary rocks are older than the igneous rocks, but studies suggest they were derived from a juvenile Neoproterozoic source, with little contribution from the older crust. They originated from andesitic sources and basic and felsic arc rock mixtures (HARTMANN *et al.*, 2007).

The detailed study area (Figure 1a) corresponds to the São Gabriel Terrain, where copper occurrences associated with mafic-ultramafic bodies have been documented. Ribeiro (1978) identified four key areas with mafic-ultramafic bodies for investigation: the Vila Rufino Massif, Mata Grande Massif, Palma Complex, and Cerro Mantiqueira. The Vila Rufino and Mata Grande massifs comprise serpentized dunites and schists, with notable chrysotile asbestos and minor pyrrhotite occurrences. The Palma Complex exhibits significant disseminated sulfide mineralization and geochemical anomalies, while Cerro Mantiqueira is characterized by magnesian silicate and carbonate sequences containing ultrabasic intrusions.

The Palma Complex is particularly notable for its mineral occurrences and historical geochemical data, with specific sites such as the Passo do Ivo massif, Jazida da Palma, and Cerro Verde offering detailed insights (RIBEIRO, 1978; CPRM, 2021). The Passo do Ivo massif hosts disseminated sulfides, including pyrite, chalcopyrite, and pyrrhotite, attributed to metamorphic remobilization and hydrothermal activity. At Jazida da Palma, copper, nickel, and cobalt are associated with ultrabasic masses and contact metasomatism in limestones, producing a mineral paragenesis of pyrite, chalcopyrite, and gold (ALMEIDA, 1970). Cerro Verde features quartz lenses mineralized with magnetite, molybdenite, chalcopyrite, and supergene minerals such as malachite and azurite, linked with quartz and fluorite (VILWOCK and JOST, 1967; CPRM, 2021). CPRM (2021) also identified additional copper occurrences in the study area, including disseminated and vein associated chalcopyrite, pyrite, and molybdenite in metamorphic and plutonic rocks, underscoring the region's potential for porphyritic Cu-Mo deposits and related resources.

#### 4.2.3 Magnetometry and Gamma-Ray Spectrometry: An Overview of Their Applications in Mineral Exploration

Airborne magnetometry and gamma-ray spectrometry are effective large scale methods for identifying potential copper mineralization areas. These geophysical techniques detect anomalies associated with copper deposits, aiding exploration efforts. Ford *et al.*, (2007) provided an early overview of geophysical signals characteristic of various deposit types, emphasizing their relevance in mineral exploration. Sampaio *et al.*, (2024) demonstrated the use of airborne gamma-ray spectrometry data in identifying radiometric anomalies correlated with known copper and iron occurrences. More recently, Ogah and Abubakar (2024) highlighted the application of filtering and enhancement techniques in processing geophysical data to delineate potential mineral targets.

##### 4.2.3.1 Gamma-Ray Spectrometry

The gamma-ray spectrometric method measures the relative abundance or concentration of potassium (K), uranium (eU), and thorium (eTh) in rocks and weathered materials up to 30 cm deep by detecting the gamma radiation emitted from the natural radioactive decay of these elements (DICKSON and SCOTT, 1997). According to Dickson and Scott (1997), the average content of radioelements in igneous rocks tends to increase with the silica content of the rock, with felsic rocks having higher concentrations of these radioelements than mafic or ultramafic rocks. The K, eU, and eTh channels generate primary images of these elements for processing gamma-ray spectrometric data. Various products can be derived from the primary images, including channel ratio maps and RGB ternary maps, which are among the most common and efficient techniques. These methods highlight contrasts between the elements, which may be less apparent in the primary maps.

Souza and Ferreira (2005) employed gamma-ray spectrometry to understand pedogenetic processes and the behavior of phosphatic fertilizers. Silva *et al.* (2007) applied the method to assist in identifying lithological units. Ferreira et al. (2009) utilized ground gamma-ray spectrometry for geological mapping and distinguishing facies in granitoids.

Gamma-ray spectrometry has also been effectively used to identify copper occurrences by detecting variations in the concentration of radioelements associated with mineralization processes. This method is particularly useful in mapping potassium (K), equivalent uranium (eU), and equivalent thorium (eTh) anomalies, as these elements can indicate hydrothermal alteration zones often linked to copper deposits. High potassium concentrations, for instance, may reflect the potassic alteration characteristic of porphyry copper systems. Additionally, K, eU, and eTh ratio maps have been employed to delineate alteration halos, highlighting contrasts between mineralized and unmineralized zones. This approach aids in narrowing down prospective areas for exploration and drilling, especially when integrated with geological and geochemical data (MERO, 1960).

In the Bathurst Mining Camp, northeastern New Brunswick, gamma-ray spectrometry has been applied to map various rock types and detect alterations associated with mineralizing hydrothermal systems, aiding in the exploration of massive sulfide deposits (SHIVES *et al.*, 2003). In the Gebel Monql area of Egypt, the coherence between copper mineralization and uranium enrichment has demonstrated the effectiveness of gamma-ray spectrometry in copper exploration (HEGAB *et al.*, 2021). More recently, Alhumimidi *et al.* (2021) described the effective use of gamma-ray spectrometry as an exploration tool in conjunction with geochemical analyses for identifying and quantifying potential targets.

By integrating gamma-ray spectrometry with other geophysical and geochemical methods, exploration efforts can more effectively target copper mineralization.

#### 4.2.3.2 Magnetometry

The magnetometry method is essential for understanding the continuity of bodies with magnetic signatures, such as mafic and ultramafic rocks, as well as bodies with sulfidation. It also plays a crucial role in understanding the structural framework, helping to map and identify key geological features. Magnetometry is particularly effective in identifying and mapping ore bodies associated with magnetic minerals, such as magnetite and pyrrhotite, and in delineating structures like faults, folds, and intrusive bodies, which are often related to mineralization (KEAREY *et al.*, 2009). Integrating magnetometric data with other geophysical methods, such as gamma-ray

spectrometry and electromagnetic surveys, enhances the accuracy of geological models, reduces exploration risks, and improves the identification of potential mineral targets. The ability to conduct surveys over large areas quickly and cost-effectively makes magnetometry indispensable in greenfield and brownfield exploration settings (KEAREY *et al.*, 2009).

Magnetometry has proven to be a powerful tool in copper exploration, especially in complex geological settings. Airborne methods such as electromagnetic (AEM), magnetic surveys, and Induced Polarization (IP) are employed to identify porphyry copper deposits. These techniques help detect subtle electromagnetic signatures of disseminated sulfides and structural features associated with mineralization. For instance, the Mt. Milligan Au-Cu deposit in Canada demonstrated how geophysical tools can map concealed ore bodies, enhancing the ability to target economically viable mineral deposits through advanced data processing and integrated exploration strategies (KWAN e MÜLLER, 2020).

Additionally, these methods aid in delineating geological structures like faults, folds, and intrusive contacts, which are key features controlling copper distribution. Uwiduhaye *et al.*, 2021 and Djolmo *et al.*, 2024 showcased the effectiveness of aeromagnetic data in structural and geological mapping, identifying new areas of potential mineralization for exploration. Integrating geophysical data, such as airborne magnetic surveys, electromagnetic methods (e.g., ZTEM), and helicopter TDEM, is essential for identifying porphyry and SEDEX copper deposits. Discrete magnetic anomalies often correlate with hydrothermal magnetite in potassic alteration zones of Cu-Au porphyry deposits.

Gravity and magnetic surveys play a crucial role in IOCG systems, as evidenced by the discovery of the Olympic Dam deposit through coincident anomalies. Structural complexity analysis enhances target selection by highlighting structurally controlled mineralizations. These geophysical methods and AIP (Apparent Induced Polarization) effects help delineate hydrothermal alteration zones critical for copper exploration (KWAN and REFORD, 2025).

Furthermore, magnetometric surveys have been successfully applied in various regions, including significant iron deposits in Victoria. These deposits, concentrated in the Buchan Rift, are primarily replacement deposits in Silurian sediments and the basal Snowy River Volcanics. Initially explored for iron ore and later for copper and gold, they exhibit intense magnetic responses. The Five Mile deposit, identified from 1950s

surveys, revealed about 6 Mt of magnetite-haematite mineralization. The Three Mile prospect, discovered in 1983, showed promising copper intersections, including 5.2 m at 4.8% copper. Induced polarization surveys helped define mineralized areas, although pyrite responses can overshadow subtle chalcopyrite signals. The complex geology suggests these may be sulfur-poor massive sulfide deposits, offering further exploration opportunities (WILLOCKS, 1999).

#### 4.2.4 Material and Methods

For the development of this study, four main stages were defined and are detailed in Figure 2.

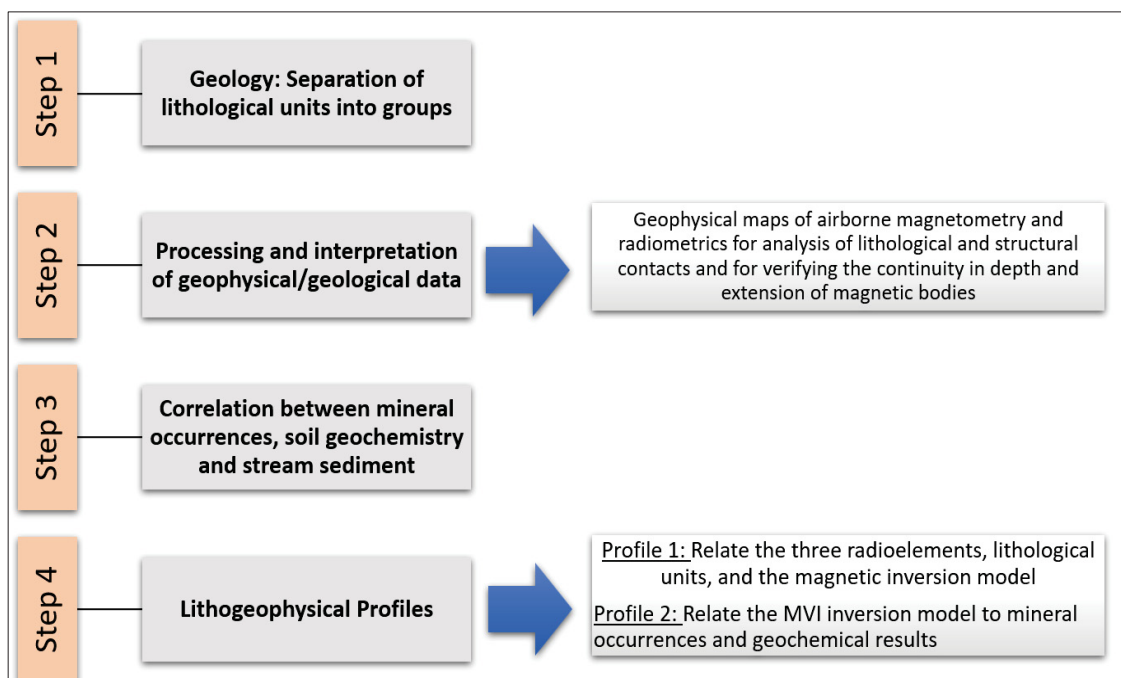


FIGURE 2 - Flowchart of activities divided into four stages.

The study began by grouping lithological units into five major representative rock categories based on similar petrographic characteristics and formation ages (Step 1). This initial step was crucial for organizing the data and creating a framework for interpreting the geological context. By compartmentalizing the lithological units, researchers could better align their geological observations with geophysical signatures, facilitating a clearer understanding of the region's geological history and processes.

Following this, geophysical surveys, including airborne gamma-ray spectrometry and magnetometry, were conducted alongside structural analysis (Step

2). These surveys generated detailed geophysical maps that were instrumental in identifying lithological and structural contacts. Furthermore, the data provided insights into magnetic bodies' continuity in depth and lateral extension. This analysis was key to unraveling the subsurface structure and identifying areas of potential geological interest.

To deepen the understanding of the region, correlations were established between mineral occurrences, soil geochemistry, and stream sediment data (Step 3). This integration of datasets allowed researchers to link surface geochemical patterns with subsurface geological features. Such correlations are essential for identifying mineralization zones and understanding their spatial relationships within the geological framework.

Finally, two lithogeophysical profiles were developed to consolidate the findings (Step 4). The first profile integrated data from three radioelements, lithological units, and a magnetic inversion model, offering a comprehensive representation of subsurface characteristics. The second profile focused on connecting the Magnetic Vector Inversion (MVI) model with mineral occurrences and geochemical results, further refining the interpretation of potential exploration targets. These profiles provided a robust basis for geological analysis and exploration strategies.

The materials used for this study were derived from geophysical, geochemical, and lithological investigations conducted by the Brazilian Geological Service (CPRM) and are freely accessible.

For the processing and interpretation of aeromagnetic and gamma-ray spectrometry data, the database from the Rio Grande do Sul Shield Project (scale 1:250,000) by the Geological Survey of Brazil CPRM was utilized. The acquisition parameters for the aerogeophysical survey included flight lines oriented in an N–S direction, with a 500 m spacing and an average flight altitude of 100 m (CPRM, 2010).

The geochemical data comprised 48 soil sampling points and 47 stream sediment samples, collected as part of the Geochemical Survey Project of Rio Grande do Sul conducted in 1976 and updated in 2021 by CPRM.

The raw geophysical data was processed by CPRM (2010), which includes the removal of the IGRF and corrections in the gamma-ray spectrometric data. The geophysical maps were generated using the Oasis Montaj software (version 2024.1). The VOXI extension was used to create 3D models of magnetic data employing the vectorial magnetization model type Magnetization Vector Inversion (MVI).

For the MVI inversion, cell sizes in X, Y, and Z of 240, 245, and 35, respectively, were considered. The input data considered was the magnetic field reduced to the IGRF; no constraints or weights were added for any type of parameter to avoid bias in the final result. Likewise, magnetization values of groups of rocks were not considered since no previous petrophysical studies were carried out. Additional processing included creating Analytic Signal (AS) and first vertical derivative (1DVz) filters, along with a ternary RGB map derived from gamma-ray spectrometric data. Structural lineaments were manually interpreted from the First Vertical Derivative maps, resulting in a rosette diagram illustrating the lineament trends. QGIS software (version 3.34.9-Prizren) was employed to integrate and interpret geophysical and geological data.

#### 4.2.4.1 Geophysical Data Processing for Copper Occurrence: Theoretical Insights, Evolution, and Effectiveness

Filters such as the analytical signal and the first vertical derivative are essential for enhancing magnetometric data in copper occurrence research. The analytical signal, introduced by Nabighian (1972), combines the gradients of the magnetic field in all three spatial directions, creating a signal independent of the magnetization direction. This property is particularly valuable for identifying subsurface structures and delineating magnetic body edges. Later works, such as MacLeod *et al.*, (1993) and Debeglia and Corpel (1997), expanded on its application, demonstrating its utility for semi-automatically interpreting 2D sources, especially in low magnetic latitudes or areas with complex remanent magnetization. Meanwhile, the first vertical derivative enhances high-frequency components of the data, improving the resolution of shallow magnetic sources (BLAKELY, 1995). Together, these filters enable geoscientists to analyze geological structures associated with copper mineralization more effectively, particularly when integrated with lithological and geochemical datasets (REYNOLDS, 2011).

The processing of magnetometric data requires careful consideration of spatial and temporal variations, anomaly separation, and interpretation techniques to ensure high-resolution results. Early researchers such as Peters (1949) and Nettleton (1954) developed simple methods for anomaly separation, including graphical smoothing and analytical grid systems. Dean (1958) and Clement (1973) later introduced processing schemes in the frequency domain to refine residual separation techniques. Hinze *et*

*al.*, (2013) emphasized the importance of isolating and enhancing anomalies while addressing directional attributes, gradients, and correlations with geological or geophysical variations. These advancements have laid the foundation for modern data interpretation in magnetometry.

The analytical signal (AS), as described by Nabighian (1972, 1974, 1984), has been widely used to locate and determine the depth of magnetic anomaly sources. Applications include interpreting dyke bodies (ATCHUTA RAO *et al.*, 1981) and addressing non-directed remanent magnetization in areas with complex geophysical characteristics (MACLEOD *et al.*, 1993). Hilbert transform pairs, discussed by Debeglia and Corpel (1997), further refined the application of AS in large datasets, making it an indispensable tool in mineral exploration.

Magnetic vector inversion (MVI) techniques have evolved significantly over recent decades. Oldenburg and Pratt (2007) discuss significant advancements in geophysical data inversion, which are essential for mineral exploration. The inversion methods are categorized into three types: Type I (discrete body), Type II (pure property), and Type III (lithologic). Equation (1) represents the misfit function in the inversion process, focusing on minimizing the difference between observed and predicted data.

$$\Phi_d = \sum_{i=1}^N \left( \frac{d_i^{obs} - d_i^{pred}}{\sigma_i} \right)^2 \quad (1)$$

where  $d_i^{pred}$  is predicted data,  $d_i^{obs}$  is observed data, and  $N$  is the number of data. Equation (2) describes the model's objective function, incorporating smoothness and proximity to a reference model.

$$(m) = \alpha_s \int_{\Omega} W_s (m - m_{ref})^2 dv + \alpha_x \int_{\Omega} W_x \left[ \frac{d(m - m_{ref})}{dx} \right]^2 dv + \alpha_y \int_{\Omega} W_y \left[ \frac{d(m - m_{ref})}{dy} \right]^2 dv + \alpha_z \int_{\Omega} W_z \left[ \frac{d(m - m_{ref})}{dz} \right]^2 dv \quad (2)$$

where  $m_{ref}$  is a reference model, the  $\alpha$  coefficients control the relative importance of smoothness in the various directions compared with closeness to a background, and the  $W_s$  are weighting functions.

The use of depth weighting (Equation (3)) is mentioned as a technique to overcome the inherent limitations of potential field data, which lack depth resolution.

$$w(z) = 1/(z + z_0)^{\nu/2} \quad (3)$$

where  $z_0$  is a constant that depends upon flight height and cell size, and  $\nu = 3$  for magnetic data. Since the fields decay as  $1/r^2$ , the exponent would be  $\nu = 2$  for gravity data.

According to Oldenburg and Pratt (2007), integrating geological models and continuously improving computational techniques is paramount. They highlighted potential methods as economical, high-resolution approaches for investigating subsurface structures.

Issues related to magnetic susceptibility inversions, including the influence of remanent magnetization, were discussed by Shearer and Li (2004) and Li *et al.* (2010), who proposed solutions for improving inversion accuracy.

Shearer and Li (2004) address challenges in interpreting magnetic data due to unknown remanent magnetization directions. The authors propose an inversion algorithm that minimizes dependence on magnetization direction by utilizing total gradient data. Equation (4) defines the total gradient  $g$  as the square root of the sum of squares of the partial derivatives of the anomalous magnetic field.

$$\begin{aligned} g &= \|\nabla B\| \\ &= \sqrt{(\partial B / \partial x)^2 + (\partial B / \partial y)^2 + (\partial B / \partial z)^2} \end{aligned} \quad (4)$$

where  $B$  is a given component of the anomalous field, such as the total field anomaly or the vertical anomaly.

The inversion problem is formulated using Tikhonov regularization (Equation (5)), which combines a data misfit term  $\Phi_d$  and a model objective function  $\Phi_m$ , controlled by a regularization parameter  $\beta$ .

$$\Phi = \Phi_d + \beta \Phi_m \quad (5)$$

The methodology incorporates a positivity constraint through a logarithmic barrier method (Equation (6)), ensuring non-negative magnetization values.

$$\Phi = \Phi_d + \beta \Phi_m - 2\lambda \sum_j \ln \kappa_j \quad (6)$$

The algorithm employs a Gauss-Newton approach for iterative minimization (Equation (7)), efficiently calculating the sensitivity matrix necessary for updating the model parameters.

$$\begin{aligned} & (J^T W_d^T W_d J + \beta W_z^T W_z + \lambda X^{-2}) \Delta \vec{\kappa} \\ &= -J^T W_d^T W_d \delta \vec{d}^n - \beta W_m^T W_m \delta \vec{\kappa}^n - \lambda X^{-1} \vec{e} \quad (7) \end{aligned}$$

This approach allows for effective 3D inversion of magnetic data, offering practical applications in fields like petroleum exploration, kimberlite imaging, and crustal studies.

More recently, Ellis *et al.* (2012) introduced Magnetization Vector Inversion (MVI), which incorporates induced and remanent magnetization without prior knowledge of remanent magnetization properties. This innovation has been tested in mineral exploration and demonstrated greater accuracy in interpreting magnetic field data. This technique improves the interpretation of magnetic field data by incorporating both remanent and induced magnetization without prior knowledge of the remanent magnetization's direction or strength. The study highlights that traditional voxel based inversion methods often assume only induced magnetization, leading to potentially misleading interpretations due to the significant presence of remanent magnetization in crustal rocks and mineralized zones.

Key equations include the magnetic field calculation from a volume magnetization (Equation (8)) and the objective function for inversion with Tikhonov regularization (Equation (5)).

$$B(r) = \mu_0 \int_V \frac{M(r') (r-r')}{|r-r'|^3} dV' \quad (8)$$

Through examples with synthetic and real data, including a case study of the Cu-Au Osborne deposit, the authors demonstrate the efficacy of MVI. The results show that incorporating remanent magnetization significantly improves the accuracy of magnetic data interpretation. The study concludes that ignoring remanent

magnetization can lead to misleading interpretations, highlighting the need for comprehensive approaches like MVI in magnetic field data inversion.

#### 4.2.5 Results and Discussions

The results and discussions were divided into the following topics: (i) Separation of lithological units into groups; (ii) Processing of aeromagnetometric and aerogamaespectrometric data; (iii) Integration of geophysical data and information on mineral occurrences, soil geochemistry, and stream sediment; and (iv) Generation of lithogeophysical profiles.

##### 4.2.5.1 Separation of Lithological Units into Groups

The lithological units were compartmentalized into five major representative rock groups with similar petrographic characteristics and formation ages. This step aims to better interpret the geological context with the geophysical signatures (Figure 3).



FIGURE 3 - (a) Map of lithological units, (b) map of group separation. Adapted from CPRM (2021).

The five groups were compartmentalized with similar lithologies described by CPRM (2021) (Figure 3):

**Ultramafic Rocks:** rocks that have undergone intense regional metamorphism, such as metamaflies, metagabbros, serpentinites, and magnesian schists with ages of ~850–630 Ma. The units known as Bossoroca, Arroio Lageadinho, Arroio Cambaizinho, Passo do Ivo, and Palma have been integrated with rocks belonging to the Cerro

Mantiqueiras Formation, composed of metamafites, serpentinites, metagabbros, and magnesian schists, with ages also ranging from ~850–630Ma.

Mafic/Intermediate Rocks: represented by gabbros, tonalites, trondhjemites, diorites, amphibolites, and granodiorites with ages ranging from ~1000–730Ma. The units that compose this large group are the Vila Nova do Sul Suite, Lagoa da Meia Lua Suite, and Passinho Suite.

Plutonic Igneous Rocks: represented by granitoids such as monzogranites, granodiorites, and syenogranites with ages of ~650–540Ma, referred to as the Ramada Granite, Camaquã Pelado Syenogranite, São Manoel Granite, Santa Rita Monzogranite, Jaguari Granite, and Lavras do Sul Intrusive Suite.

Volcaniclastic Rocks: This group is composed of volcaniclastic igneous rocks, which have eventually undergone regional metamorphism. Representative units include the Ibiajutura Formation, consisting of metasandstones, mica schist, phyllite, and slate, with ages ranging from 1000 to 635 Ma. Also, the Acampamento Velho Formation, mainly composed of rhyolites, tuffs, pyroclastic breccias, and ignimbrites with an age of ~650–540Ma, the Arroio dos Nobres Formation composed of conglomerates, siltstones, and sandstones with an age of ~650–540Ma, the Pontas do Salso Formation with metatuffs and epiclastic metasedimentary rocks with an age of ~850–630Ma, and the Hilário Formation mainly composed of andesites with an age of ~650–540Ma.

Sedimentary Rocks: Comprised of sandstone, siltstone, and conglomerate with ages ranging from ~318–270Ma in rocks belonging to the Guatá Group and from ~650–540Ma in rocks of the Maricá Group.

#### 4.2.5.2 Airborne Gamma-Ray Spectrometry, Airborne Magnetometry, and Structural Analysis

Maps of the three radioelement channels K, eTh, and eU and an RGB Ternary map were generated from the gamma-ray spectrometry data made available by CPRM (2010) (Figure 4a–c). For the interpretation of the maps, the lithological group map will be used (Figure 4d). The study area presents strongly delineated lithological units in the RGB Ternary map (Figure 4e). The granitoids of the plutonic igneous rock group are delineated by the high counts of the elements (whitish colors) and higher counts of

the potassium and thorium elements. It is observed that the ternary map delimits the boundaries of the metamorphosed mafic/ultramafic rocks, which have low total element counts (dark colors).

The Mafic/Intermediate rock group shows K, eU, and eTh variations. These variations can be observed in Figure 4a–c. Rocks with higher potassium element counts are related to plutonic igneous rocks (granodiorites and monzogranites) (Figure 4a).

The sedimentary rock group shows a more significant variation in radioelements, generally exhibiting higher values, although some have a higher potassium percentage. These are associated with siltstones, conglomerates, and sand. Sedimentary rocks in contact with mafic and ultramafic units have a higher concentration of mafic minerals and low silica content, facilitating a signature with low counts of K, eU, and eTh.

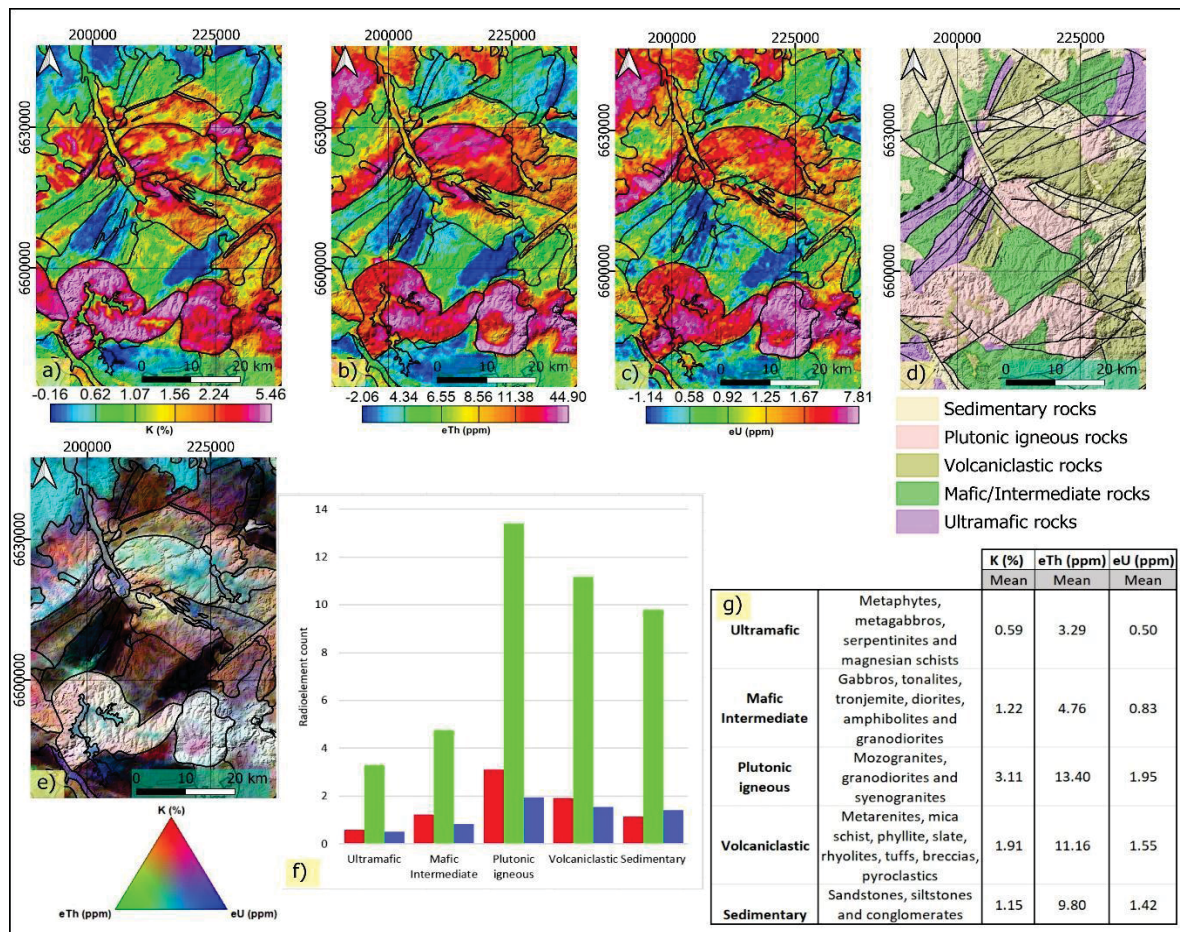


FIGURE 4 - (a) Potassium Channels, (b) Uranium, (c) Thorium, (d) Lithological Group Map, (e) RGB Ternary Map, and (f) Histograms showing the variation of the mean values of eTh, eU, and K concerning the rock groups in the area of interest (the colors represent: K, red; eTh, green; eU, blue), and (g) the table with the average radioelement values for each rock group.

The histograms of radioelement countings and the table with the average radioelement values for each lithotype show significant dispersion and variability (Figure 4f,g). This occurs due to various factors, including flight altitude, thickness of the soil cover, presence of dense vegetation, and variation in mineralogical composition for each lithotype. Despite the considerable variability, patterns can be observed. The group of plutonic igneous rocks has the highest element count in all channels, confirming that the higher the silica content in the rock composition, the higher the radioelement count. In contrast, ultramafic rock groups behave oppositely, showing low radioelement counts.

From the aerial magnetometry database, the Total Magnetic Intensity (TMI) map and Analytic Signal (AS) map were generated (Figure 5a,b). The results show striking contrasts in the magnetic signature in the TMI map with dipolar regions, and circular structures corresponding to the Ramada Granite, Lavras do Sul Granite, and Jaguari Granite are observed. The AS map highlights mafic and ultramafic lithological units and exhibits intense magnetic signatures. Plutonic igneous and sedimentary rock bodies show a weak magnetic signature.

A First Vertical Derivative filter was applied (Figure 5d) to highlight the region's structural framework (Figure 5e). Ultramafic bodies, mafic/intermediate igneous rocks, and volcaniclastic rocks show structural solid control (Figure 5c). The results of structural interpretations and comparisons with measurements made by CPRM (2021) reveal a NE–SW structural trend (Figure 5g). Plutonic igneous lithological units and sedimentary rocks do not show intense structural control (regions identified in Figure 5e in pink color).

Since ultramafic rocks exhibit magnetic contrast compared to other lithologies and have the most significant potential to host mineralization, the Magnetization Vector Inversion (MVI) technique was applied to understand the continuity of subsurface bodies laterally and in-depth and the inclination of lithological bodies (strike and dip) (Figure 5f).

Through the analysis of the MVI inversion results of the aeromagnetometric data along with the structural context described by CPRM (2021), it is observed that ultramafic lithological units have a preferential direction of N45° E and a dip of 50°, which is also observed in depth (Figure 5f).

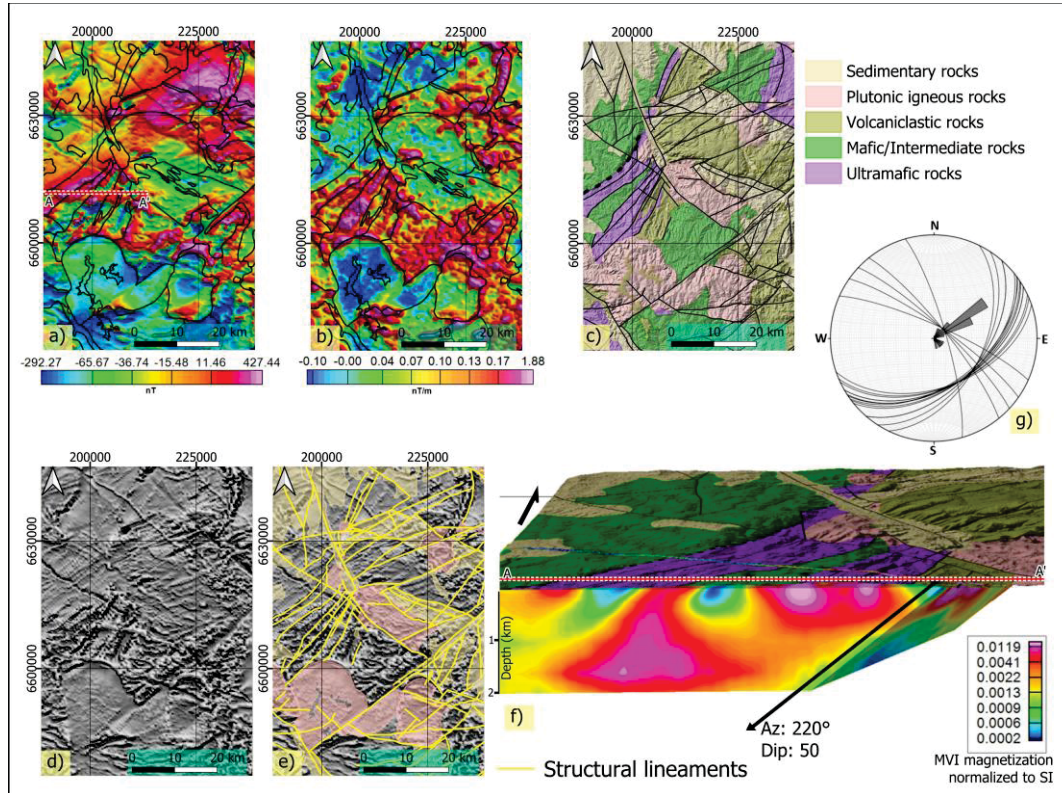


FIGURE 5 - (a) Total Magnetic Anomaly Field Map and indication of the location of the cross-section A–A', (b) the Analytic Signal Map, (c) Lithological Group Map with structural context (CPRM, 2021), (d) First Vertical Derivative Map (1DVz), (e) 1DVz Map lighting structural lineaments and plutonic rocks, (f) Cross Section A–A' of the MVI Inversion Model, and (g) Rosette Diagram

#### 4.2.5.3 Mineral Occurrences, Soil Geochemistry, and Stream Sediment Analysis

Ribeiro (1978) identified potential areas containing mafic-ultramafic bodies, among which four areas were selected for detailed geological study: the Vila Rufino Massif, Mata Grande Massif, Palma Complex, and Cerro Mantiqueira (Figure 6a).

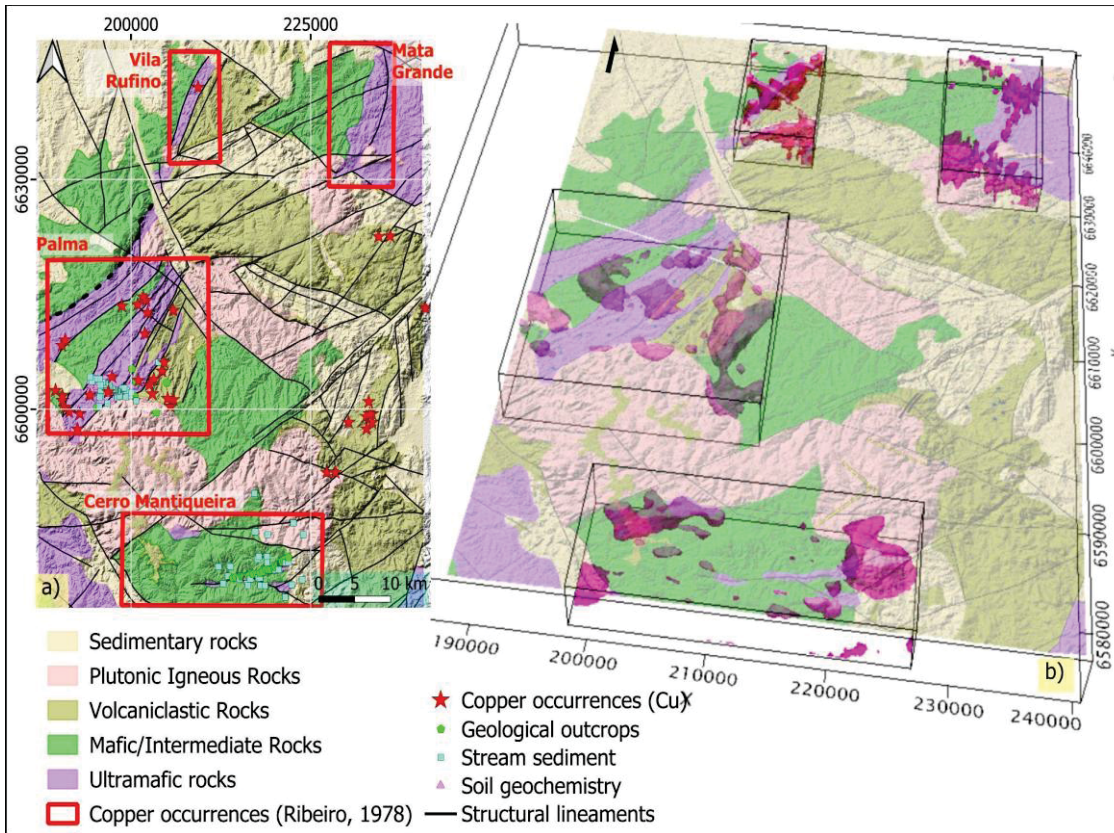


FIGURE 6 - (a) Areas with mineral occurrences hosted in ultramafic bodies. (b) MVI inversion models for the four areas.

The Vila Rufino Massif consists of small bodies of serpentinized dunites in contact with magnesian schists (serpentine-chlorite-talc schists). These are considered products of retro-metamorphism acting on the ultrabasic and basic rocks of the Cerro Mantiqueira Formation. A small occurrence of chrysotile asbestos is known in the southern part of this massif. The entire massif (dunites and schists) measures  $12 \times 5$  km and is in tectonic contact with rocks of the Cambaí subgroup (gneisses and granites) through two parallel faults oriented N20° E.

The Mata Grande Massif consists of an elongated area measuring  $18 \times 2.5$  km with significant occurrences of serpentinized dunite bodies embedded in schistose rocks, trending N20° E, and is responsible for the contact between the Cerro da Mantiqueira Formation and the chlorite schists of the Vacacaí subgroup (to the east) and the gneisses of the Cambaí subgroup (to the west). Occurrences of chrysotile asbestos are recorded at the southern end of the body, and there is knowledge of pyrrhotite, rare and finely disseminated in serpentinites, and talc-chlorite-tremolite schists (Bocci and Ribeiro 1963).

The Palma complex consists of three main occurrences: Passo do Ivo, Jazida da Palma, and Cerro Verde, containing records of disseminated sulfidation and geochemical results from stream sediment and soil samples.

The Cerro Mantiqueira occurrence consists of an elongated body measuring  $5.6 \times 0.4$  km, composed of a silicate magnesian sequence (chlorites, talc-chlorite schists, hornblende-tremolite, actinolite schists, tremolites) and, concordant with it, a carbonate magnesian sequence (limestones with gibertite, dolomites with olivine, and limestones with ankerite). Within these sequences, oriented N70° E, ultrabasic cores appear (Iherzolites, harzburgites, dunites, and serpentinites). Homogeneous basic and acid migmatites of the Cambaí subgroup enclose all these lithological sequences.

To understand the continuity of ultramafic bodies and improve the resolution of inversions, inversion models (MVI) were generated for each area related to the ultramafic bodies described by Ribeiro (1978) (Figure 6b). It can be observed that all of them correlate satisfactorily with lithological and structural information. The bodies that stood out due to their excellent continuity in depth and extent are located in the region known as Palma. Various mineral occurrence records and geochemical studies are also found in this locality. Based on these premises, the Palma region will be detailed in terms of geophysics and detailed information about the mineral paragenesis present in registered occurrences in the region.

#### 4.2.5.4 Palma Region—Occurrences and Geochemistry Information

The information that will be described below is very important for understanding in more detail the cupriferous occurrences in the Palma Region. As previously described, minerals have different magnetic signatures. To understand the contrasts in physical properties, it is important to describe the details of the lithotypes. In addition, historical measurements of stream and rock sediment were detailed, which will be used as integration and validation tools for geophysical data.

Figure 7 details and presents occurrences and geochemical information for this specific area. According to Ribeiro (1978), the Passo do Ivo massif contains disseminated sulfides, such as pyrite, and, in smaller proportions, chalcopyrite and pyrrhotite. CPRM (2021) states that the occurrences are related to metamorphic remobilization and hydrothermalism.

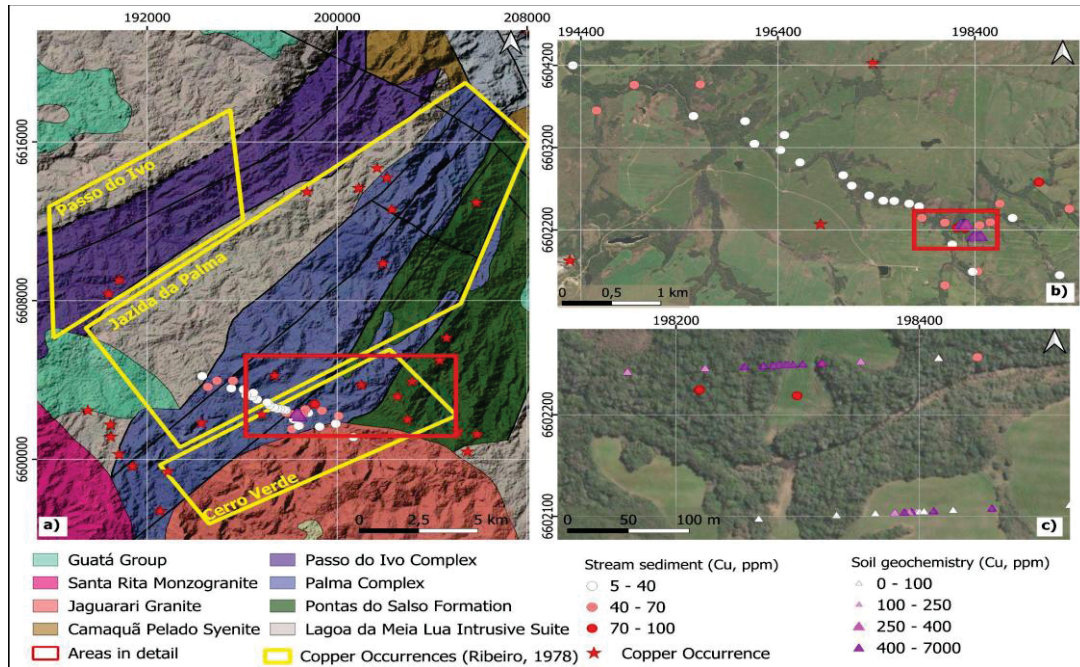


FIGURE 7 - (a) Lithological map with records of Cu occurrences, stream sediment, and soil geochemistry, (b) detailed location of stream sediment samples, and (c) detailed profiles of the two soil sampling points; adapted from CPRM (2021) and Ribeiro (1978).

Jazida da Palma occurs in the Palma Complex and has a gabbro apophysis introduced into marbled limestones. According to Almeida (1970), in Jazida da Palma, there is an intrusion of an epidotized porphyritic gabbro dyke, with a thickness ranging from 10 to 15 m, which emits numerous apophyses. These apophyses intrude along the finishing planes of the limestones and are folded together with them. The lithology of these apophyses is currently formed by a schist to serpentine, chlorite, and biotite and can be classified as a metabasite.

The intrusion developed contact metamorphism, reaching around 2 m in thickness. In the surrounding limestones, there is a mineral paragenesis based on diopside, tremolite, grossular, sphene, and epidote, in addition to sulfide metallic minerals. These are found in basic rocks and limestones but are always confined to the contact zone. Pyrite is the most abundant sulfide, accompanied by chalcopyrite, pyrrhotite-pentlandite, and gold (ALMEIDA 1970).

Studies conducted by the Departamento Nacional de Pesquisa Mineral (DNPM) indicated a mineral paragenesis concerning sulfides: pyrite, chalcopyrite, arsenopyrite, sphalerite, pyrrhotite, and magnetite. Pyrite is the most abundant sulfide, followed by chalcopyrite; the others are rare.

Ribeiro (1978) argues that Jazida da Palma has two favorable conditions for copper, which are possibly genetically related:

- (1) Copper, with nickel and cobalt, linked to ultrabasic masses.
- (2) Copper in deposits originating from the contact metasomatism of these bodies on the limestones of the sedimentary sequence.

The occurrence known as Cerro Verde is located in the western region of the Jaguari Granite and in contact with the host rock, mainly the Palma Complex (RIBEIRO 1978). Quartz lenses with a direction of N45° E were described in this occurrence and were associated with migmatites. The mineralization is found in scattered pockets in the quartz lenses (VILWOCK and JOST 1967). The ore mineralogy consists of magnetite, molybdenite, chalcopyrite, bornite, pyrite, and gold (primary ore), and chalcocite, covellite, cuprite, malachite, and azurite (supergene) have also been identified. All these minerals are associated with quartz, fluorite, calcite, and epidote.

CPRM (2021) indicates 28 occurrences of copper in the area of interest, which measures 22 × 22 km. In the Passo do Ivo metamorphic complex, two occurrences are described. Most occurrences are near the contact between the Jaguari Granite, the Palma Complex, and the Pontas do Salso Formation. Disseminated concentrations of minerals such as chalcopyrite, pyrite, pyrrhotite, and hematite associated with veins at the contact of the Granite with the Pontas do Salso Formation have been described. At the contact of the granite with the Palma Complex, there are records of copper mining activities as the primary substance and gold and molybdenum as secondary substances. CPRM (2021) shows a porphyry Cu-Mo deposit with disseminated mineralizations in metamorphic rock and plutonic igneous rocks such as Monzogranite. The occurrence has mineralogical associations with gold, bornite, chalcopyrite, pyrite, molybdenite, magnetite, fluorite, calcite, and epidote. Other unexploited occurrences have been described in the region, some with mineralogical associations with chalcopyrite, pyrrhotite, and pyrite, possibly associated with faulting in the N45° E direction.

For the study area, 48 soil sampling points and 47 stream sediment samples were used, and 31 elements were analyzed by emission optical spectroscopy. This study is part of the Projeto Levantamento Geoquímico do Rio Grande do Sul (Geochemical Survey Project of Rio Grande do Sul) carried out in 1976 and revised in 2021 by CPRM.

The soil sampling was acquired in the residual soil, considering only horizon A. The collection is mainly concentrated in two profiles with a length of 260 m and a spacing between profiles of 150 m. The results show a variation of Cu from 0 to 7000 ppm, with continuous measurements within a range of 400 to 7000 ppm. Other collections were acquired randomly throughout the area and did not present significant results, ranging from 5 to 40 ppm (Figure 7c).

The stream sediment was collected in a drainage with an NW–SE direction, and the Cu results showed a variation from 5 to 100 ppm. Higher concentrations of Cu occur near the soil sampling profiles, in areas corresponding to the contact between the Jaguari Granite and the Palma Complex (Figure 7b).

#### 4.2.5.5 Data Integration Litho-Geophysical Profiles Analysis

Two profiles were generated based on the previously presented information (Figure 8). Profile A–A" is 22 km long and cuts through all lithological groups, while profile B–B" is 2.5 km long and focuses on the zone where geochemical information is available (Figure 8).

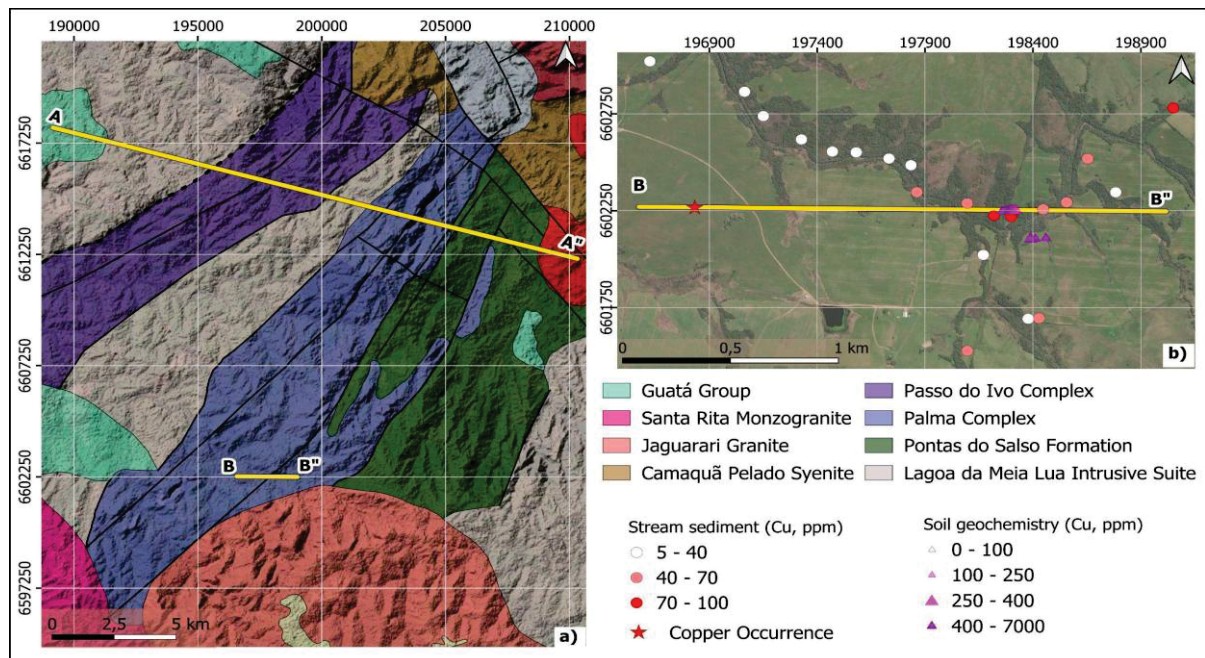


FIGURE 8 - (a) Location map of litho-geophysical profiles and (b) detail of the location of Profile B–B" with information on stream sediment and soil samples.

For the analysis of Profile A–A" (Figure 9), the following elements were used:

- (i) MVI inversion model that presents the signal intensity variation based on the contrast of MVI magnetization normalized to magnetic susceptibility (SI), which means that the generated anomalies can be directly related to the magnetic susceptibility of materials;
- (ii) A graph with the three radioelements (K, eTh, and eU) and the terrain elevation showing signal intensity, varying from low to high intensity.

In the first 3 km of the profile (Figure 9c), it is observed that the radioelements signature is intermediate, and the MVI inversion presents weak anomalies, which is typical of sedimentary rocks such as sandstones and siltstones. From 3 to 7 km of extension, intermediate mafic rocks represented by tonalite, diorite, and granodiorite of the Lagoa da Meia Lua Formation show a significant increase in radioelements, marking the lithological change, and the MVI inversion has an intermediate signature. The meta ultramafic rocks of the Passo do Ivo Formation, represented by magnesian schists and amphibolites, are strongly delineated in the magnetic signature of the MVI model, with a thickness of approximately 3.5 km, showing a low count of radioelements demarcating the lithological change.

Two circular and continuous low anomalies are observed in the direction of the mapped structures as a sinistral shear zone and a sinistral strike-slip fault or shear zone. The magnetometry method and detected anomalies are characterized by identifying structures and mainly demarcating those with regional character. These structures and a lens of the Lagoa Meia Lua Formation appear to delimit the Passo do Ivo Formation. In depth, it is observed that the Passo do Ivo Formation has a continuity that exceeds 150 m in depth with a dip of 50 and azimuth of 220°.

The Palma Complex occurs over approximately 11.5 km along the profile, delineated by a magnetic high with a thickness of 4 km, which agrees with surface geology. The Palma Complex shows substantial indications of copper occurrences, as described in the literature by Ribeiro (1978) and CPRM (2021). The MVI inversion shows subsurface continuity controlled by well-defined structural lineaments in previous geological mappings. The correlation of all this evidence of information indicates a high potential for copper occurrences associated with strong MVI anomalies. The magnetic anomaly is observed to be more intense at depth; it may be that this mineralized ultramafic body is increasing in depth and under strong structural control.

Following the profile, after the Palma Complex, the Pontas do Salso Formation occurs over approximately 17 km along the profile, represented by epiclastic metasedimentary rocks and metavolcanic tuffs. A low magnetic and low radioelement signature is observed, followed by a high magnetic marking (similar to another previous section) of the presence of magnesian schists of the Palma Complex.

At approximately 20.5 km along the profile, a significant increase in the signal intensity of the three radioelements combined with low magnetics near the surface is observed. Thus, it is interpreted that this response is related to the São Manoel Monzogranites and Granodiorites. However, it is suggested that the Palma Complex may also be present at greater depth due to strong magnetic anomalies. This region is also considered to have a high potential for copper occurrences. The contact between the ultramafic rock and plutonic igneous rocks may be favorable for sulfide presence. The lens of the Palma Complex has a greater extent than represented on the surface, extending to approximately 2 km in depth (Figure 9b).

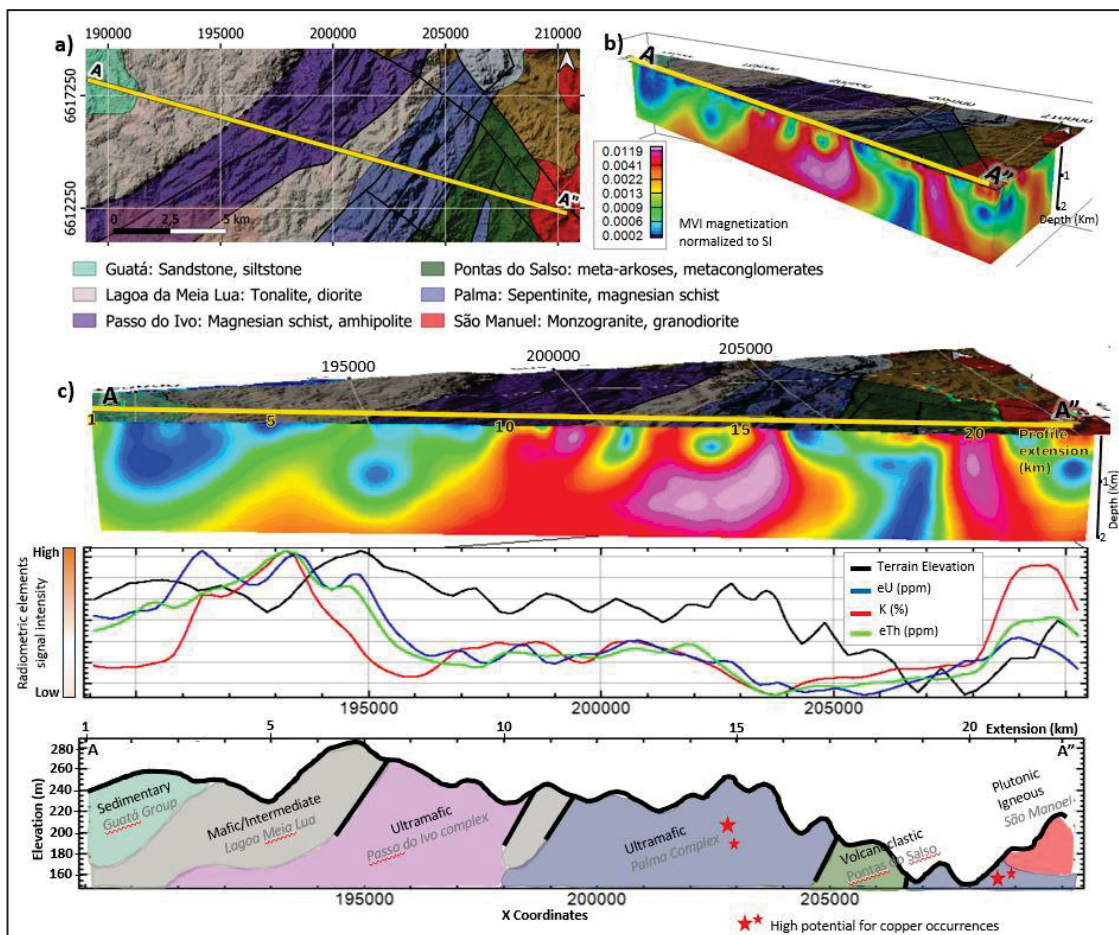


FIGURE 9 - (a) Lithogeophysical Profile A–A”, (b) view of the MVI-generated inversion model. (c) A mosaic presenting the MVI-generated inversion model, graph with radioelement (K, eTh, eU) variations, and interpreted lithogeophysical profile.

The B–B” profile aims to show the relationship between soil and stream sediment geochemical results with MVI data inversion, which may be related to the continuity of host bodies and/or directly related to mineralization (Figure 10). It can be observed that in the section parallel to the mineralized structures with azimuth 225°, parallel to the fracture related to mineralizations, the body shows continuity in depth. The profile cut with a northward direction shows a tendency for continuity towards N45°E.

The MVI inversion model presents more than one magnetic body, and several mineral occurrences have been identified at the surface. Therefore, the study area may have several mineralized bodies that continue in extension and laterally. The structural control of the preferential direction N45° E somehow controls all. Most of those showing more excellent continuity are located near the contact zone between the Jaguarari Granite, the Palma Complex, and the Pontas do Salso Formation.

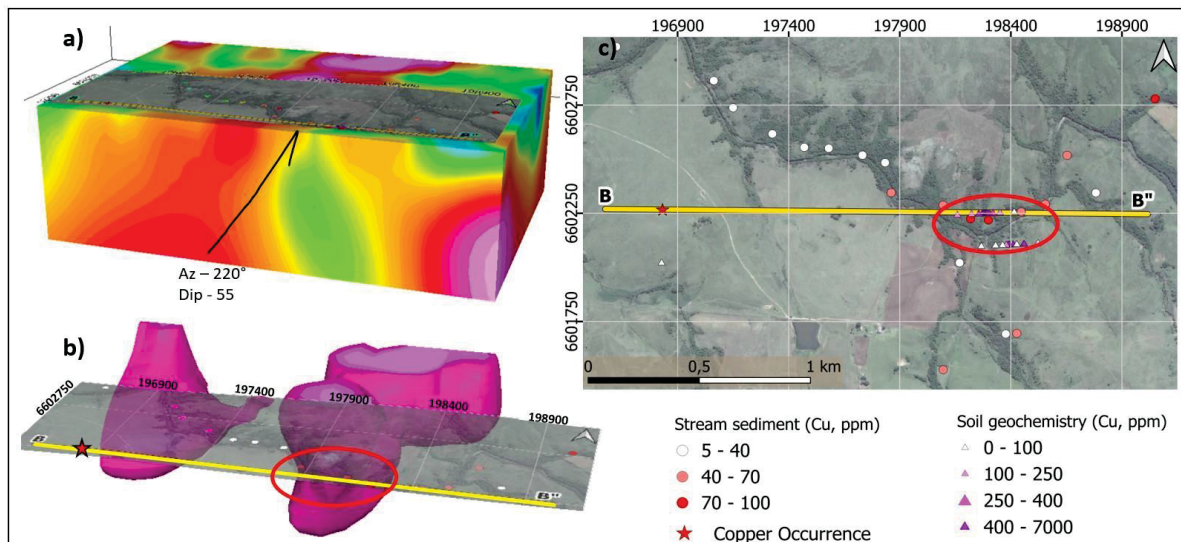


FIGURE 10 - (a) MVI Model of Profile B–B”, (b) separation of selected MVI higher anomalies, and (c) map of Profile B–B” location.

#### 4.2.6 Concluding Remarks

Based on the proposal of this study, the results were satisfactory because, using the suggested workflow, it was possible to delimit potential areas with pre-existing geological mapping data, results from geochemical analyses, structural context, and

products from the processing of airborne geophysical data from magnetometry and gamma spectrometry to understand the behavior of copper signatures in mafic-ultramafic bodies associated with copper occurrences in the Southern Rio Grande Shield. This geoscientific data processing and interpretation routine aims to advance and develop new research in the mineral exploration field in Brazil's southern portion and contribute to discoveries of metallic minerals with economic potential.

Processing aeromagnetic data using the first vertical derivative enhancement filter of the total anomalous magnetic field made it possible to relate the main structural lineaments. An MVI inversion model highlighted the continuities of the bodies in extension and depth.

The maps of the radioelements and ternary showed lithological contacts, and a table showing variations of the values generated from the interpolated airborne data was also presented. These can be used as parameters for future studies in the area and similar lithologies.

The profiles generated for litho-geophysical interpretation (Profile A–A with a length of 22 km) evidenced a detailed correlation of the radioelements delineating lithological contacts; the MVI inversion enriched the discussion on the continuity of ultramafic bodies such as the Palma Complex and on the structural framework delimiting regional structures in the preferred N45E direction. Cross-referencing historical data with new processing suggested areas with high potential for copper occurrences. Profile B–B” achieved satisfactory results in verifying anomalies generated from the MVI inversion. These significantly correlate with historical results from sediment and soil geochemical analyses.

#### 4.3 ARTIGO 2 - *Geophysical Insights into Copper Deposits at Mina Seival, Caçapava do Sul, Brazil: 3D Magnetic Inversions and Euler Deconvolution*

##### **ABSTRACT**

Copper deposits are critical resources for various industrial applications, making their exploration a key focus in economic geology. Geophysical methods, particularly aeromagnetic surveys, have become invaluable in delineating subsurface structures and understanding mineralization patterns. While previous studies have emphasized the role of structures and hydrothermal alteration in controlling copper mineralization within the Hilário Formation, there remains a limited understanding of the three-dimensional geometry and connectivity of these structures at depth. Therefore, this study investigates the geophysical signature of copper mineralization in rocks from the Hilário Formation, located in the Lavras do Sul and Caçapava do Sul regions of Rio Grande do Sul, Brazil. The focus is on understanding the subsurface distribution and geometry of mineralized bodies, utilizing 3D inversion of aeromagnetic data. The integration of geophysical techniques with structural context allows for a detailed analysis of magnetic anomalies associated with inactive mines in the region. Advanced filters, including Tilt Derivative, amplitude of the Analytic Signal (AS), and Euler Deconvolution, were applied to enhance the identification of key structural features controlling mineralization. Previous studies have highlighted the importance of NW-trending faults as primary controls on copper mineralization, favoring hydrothermal alteration, and the results of this study confirm the presence of NW-trending faults intersecting NE structures, suggesting that the intersection of these structural features may host more robust mineralized bodies. Thus, this study provides valuable insights into the use of integrated geophysical methods for mineral exploration and the understanding of subsurface geology in copper-rich regions. Moreover, the integration of these advanced geophysical techniques with detailed structural frameworks has not been extensively applied in this region.

##### 4.3.1 Introduction and Objectives

The region of Lavras do Sul and Caçapava do Sul, in the state of Rio Grande do Sul, holds significant historical and geological importance, particularly regarding mineral exploration. The Seival Mine, one of the main copper producers in southern

Brazil in the early 20th century (LIMA, 2009; SALDANHA et al., 2011), ceased its operations due to the economic depletion of high-grade oxidized copper ore. Since then, understanding the remaining subsurface mineralizations has become a challenge, highlighting the relevance of geophysical and geological studies for mineral prospecting.

The copper mineralization at the Seival Mine is associated with the volcanogenic rocks of the Hilário Formation, Lavras do Sul granitoids, and magmatic dikes. It mainly occurs in fractures and faults with predominant SE-NW and NE-SW orientations, which are possibly related to magmatic processes involving andesitic to trachyandesitic dikes (LOPES et al., 2018). Structural studies integrated with geophysical data enabled the reconstruction of the paleostress tensor responsible for the formation of these faults and fractures, favoring the circulation of hydrothermal fluids and ore deposition (LOPES et al., 2018).

The application of geophysical filtering techniques has been essential for identifying anomalies and mapping structures related to copper exploration in various deposit types. Anderson et al. (2023) investigated porphyry copper systems in the Silverton caldera, Colorado, using magnetic data and magnetic susceptibility measurements to characterize structural variations and hydrothermal alterations. Their study highlighted that magnetite destruction within alteration assemblages, especially in quartz-sericite-pyrite zones, results in low magnetic anomalies, whereas propylitic assemblages exhibit high magnetic susceptibilities and produce moderate to high anomalies. Euler Deconvolution was applied to estimate depths and identify magnetic sources associated with mineralization, indicating depths generally less than 500 m. Natural weathering of the porphyry copper system can affect the physical properties of the rocks, and these processes must be considered when interpreting geophysical data.

Santos et al. (2022) employed magnetic susceptibility measurements and 3D magnetic data inversion to characterize the Furnas IOCG deposit in the Carajás Mineral Province. The results indicated that hydrothermal alteration zones rich in magnetite exhibit high magnetic susceptibility, directly associated with copper and gold mineralization. The 3D modeling revealed the distribution of these magnetic signatures, facilitating ore body delineation. However, challenges such as magnetic remanence and self-demagnetization underscore the need for integration with geological and petrophysical data to enhance interpretive accuracy.

Sandrin and Elming (2007) analyzed the physical properties of drill core rocks and geophysical data from the mineralized area of Tjårrojåkka in northern Sweden to define a geophysical signature for IOCG deposits. Their study demonstrated that copper mineralization is associated with high magnetic susceptibility and gravity anomalies, with a predominance of magnetite and Ti-magnetite. Airborne geophysical data showed a high K/eTh ratio, indicating potassium enrichment correlated with copper mineralization. The study emphasizes that the presence of magnetite can create ambiguities in geophysical data interpretation, highlighting the importance of integrating geophysical and petrophysical analyses.

Mostafaei and Kianpour (2022) proposed an approach for exploring Michigan-type stratabound copper deposits, highlighting the significance of structural zones in mineralization. In the Dochileh copper deposit in Iran, a ground magnetic survey revealed linear trends, one of which was associated with a 2.5 km long fault. Areas of low magnetic intensity coincided with previously identified mineralized zones. Four drill holes targeting these anomalies confirmed the presence of native copper, malachite, and cuprite, demonstrating the effectiveness of magnetometry as an exploratory tool.

The integration of geophysical and geological data is essential for accurately interpreting mineralized structures, enabling a more detailed understanding of the structural and lithological controls on mineralization. Euler Deconvolution is notable for estimating depth and identifying magnetic sources, assisting in the characterization of ore bodies. Additionally, careful assessment of the geophysical signature of both host and surrounding rocks is important, as mineralization may be associated with either high or low magnetic responses, as evidenced by Mostafaei and Kianpour (2022). Thus, combining different geophysical and geological methods reduces uncertainties and improves target delineation, enhancing the efficiency of mineral deposit characterization.

In this study, an investigation is proposed to analyze the geophysical signatures of rocks from the Hilário Formation in the Camaquã Basin, associated with copper mineralization, with a focus on the analysis of aeromagnetic data. Based on 3D inversions of magnetometric data, it was possible to conduct a detailed analysis of the magnetic signatures of inactive mines in the region, providing deeper insights into the geometry and distribution of the mineralized bodies. Euler Deconvolution enabled the identification of the main geological structures and their relationship with tectonic faults, which, according to Lopes (2011, 2013), Lopes et al. (2018), and Fontana et al. (2017),

are key controls for copper mineralization, especially NW-trending faults that promote hydrothermal alteration and the concentration of minerals.

In this study, the integrated application of filtering, enhancement techniques, and methods for interpreting magnetometric data improved the discrimination of geological units, refined the identification of structural features, and characterized mineralized bodies within the study area. While conventional filters aided in identifying surface features, the combination of Euler Deconvolution with magnetic data inversion provided a more robust interpretation directly linked to the local geology. As a result, it was possible to recognize magnetic and structural signatures associated with the main mines and mineral occurrences, to understand the continuity of the bodies at depth and laterally, and to reveal preferential structural patterns trending NE and NW. The analyses also allowed the delimitation of potential mineralized zones, indicating favorable structural corridors, superficial hydrothermal alterations, and deeper regions associated with mineral systems.

This approach makes a significant contribution to advancing the understanding of the local geology and proposes new paths and approaches for mineral prospecting and the study of subsurface copper deposits. Moreover, the application of various enhancement techniques to aeromagnetic data reinforces the importance of integrating geophysical methods to accurately characterize geological structures and mineralized bodies, providing new insights for future mineral exploration campaigns in the region.

#### 4.3.2 Study Area and Regional Geological Setting

The study area is located between the municipalities of Lavras do Sul and Caçapava do Sul, in the state of Rio Grande do Sul, Brazil. Access is provided via the ERS-357 highway (FIGURE 1a).

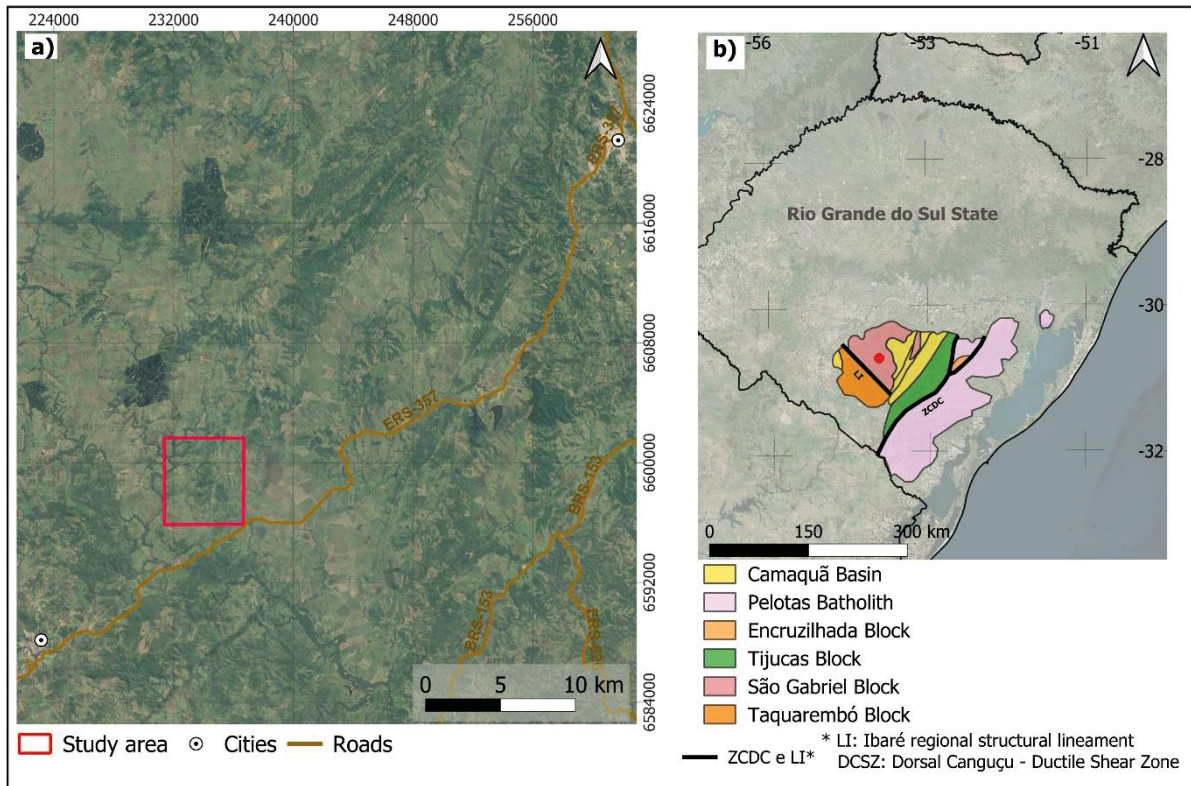


FIGURE 1 - a) Location of the study area near the municipality of Caçapava do Sul. b) Location within the state of Rio Grande do Sul and in the regional geological context. (Modified from HARTMANN et al., 2007; Google, 2025).

Regionally, the area is in the southern portion of the Mantiqueira Province (HASUI et al., 1975; ALMEIDA et al., 1981), known as the Southern Rio Grande Shield (Escudo Sul-Rio-Grandense – ESRG). The ESRG is composed of units from the Dom Feliciano Belt, established during the Neoproterozoic, mainly represented by the São Gabriel and Tijucas Blocks, as well as the Pelotas Batholith. It also includes Paleoproterozoic units such as the Taquarembó Block and part of the Tijucas Block (HARTMANN et al., 2007) (FIGURE 1b).

The São Gabriel Block is described as accretionary prism formed by petrotectonic associations typical of passive margin, back-arc, and juvenile magmatic arc environments, including ophiolites, volcano-sedimentary sequences, and calc-alkaline plutonic bodies with ages dated from 930 to 680 Ma (HARTMANN et al., 2007; PHILIPP et al., 2018). The accretion of the block occurred in episodes during the Neoproterozoic, with magmatism associated with the subduction of the Charrua Ocean, followed by the intrusion of late-orogenic granites and the development of shear zones that influenced regional structuring (PHILIPP et al., 2018; SAALMANN et al., 2011).

Additionally, the area hosts sedimentary and volcanogenic units formed in elongated tectonic basins during the late Neoproterozoic to early Paleozoic. These successions, grouped within the Camaquã Supergroup, overlie the Precambrian basement and are composed of thick layers of conglomerates, sandstones, pelites, and volcanogenic rocks of alkaline affinity. The Supergroup is subdivided into three sub-basins — Western, Central, and Eastern Camaquã — and five main units, organized from base to top: (i) Maricá Group, (ii) Bom Jardim Group, (iii) Acampamento Velho Formation, (iv) Santa Bárbara Group, and (v) Guaritas Group (JANIKIAN et al., 2003; PELOSI and FRAGOSO-CESAR, 2003; RIBEIRO and FANTINEL, 1978; FAMBRINI, 2003; ROBERTSON, 1966; JANIKIAN, 2004).

The Neoproterozoic granitoids of Lavras do Sul, associated with the Hilário Formation, are part of a post-collisional volcano-plutonic center of shoshonitic affinity, linked to tectonic and magmatic events of the Dom Feliciano Belt, with ages ranging from 604 to 590 Ma (LIMA and NARDI, 1998; SILVA et al., 2005; GASTAL et al., 2015). These bodies are directly related to transtensional structures, lamprophyric dikes, and gold mineralization, connecting magmatic evolution to the structural dynamics of the Camaquã Basin (RAPOSO and GASTAL, 2009).

#### 4.3.2.1 Local Geological, Structural Context and Hydrothermal Alteration of the Seival Mine Region

In the early 20th century, the Seival Mine played a significant role in copper production in southern Brazil. Currently, the deposit is considered economically exhausted due to the high content of oxidized copper. The region contains records of several mines that were exploited in the past and are now inactive, as well as mineral occurrences known as Quero-Quero, Lagoa do Jacaré, and Vila do Torrão (RIBEIRO, 1978) (FIGURE 2).

Details regarding the inactive mines are provided by Reischel (1978) and Lopes (2013) as follows:

- i) Barita Mine: The largest of the mines, composed of a lenticular body with NE orientation. It contains chalcocite associated with fault zones, with estimated reserves of approximately 64,000 tons and a copper grade of 1.7% Cu;
- ii) João Dahne Mine: A small body, also NE-trending, but with low copper grades;

iii) Morcego Mine: Characterized by secondary minerals such as malachite and disseminated sulfides (chalcocite), with NS and NE orientations, located near fracture zones in andesite;

iv) Meio and Geral Mines: Exhibit irregular concentrations of malachite, tectonically controlled by a fracture pattern in andesitic tuff, with NE–SW orientations and a steep SW dip;

v) Cruzeta Mine: Characterized by the presence of chalcocite in veins along fractures in porphyritic andesite, with NW–SE orientations and subvertical dip;

vi) Alcides Mine: Composed of disseminated sulfides (chalcocite) in volcanic breccias, with barite as the gangue mineral.

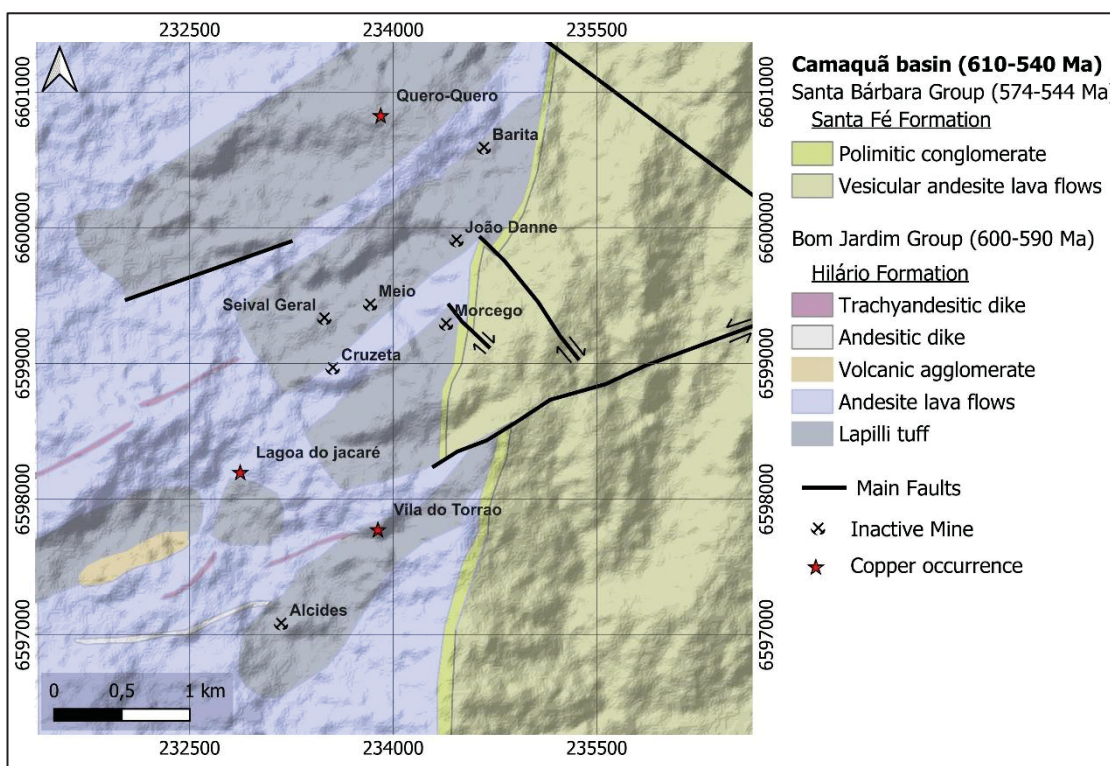


FIGURE 2 – Location of inactive mines in the study area and local geological context (Modified from Lopes et al., 2018; Ribeiro, 1978).

The mineralization in inactive mines is associated with faults and fractures containing copper sulfides such as chalcopyrite, bornite, chalcocite, and covellite (FONTANA et al., 2017). These occurrences are hosted in volcanic rocks of the Hilário Formation, which include tuffs, volcanic breccias, and andesitic lava flows (REISCHL, 1978; LOPES et al., 2014).

Different types of hydrothermal alteration have been identified, including propylitic (250–350 °C) and intermediate argillic (160–230 °C) (BONGIOLO et al., 2008). Interaction with meteoric waters resulted in the precipitation of barite, calcite, and quartz (150–80 °C) (FONTANA et al., 2017).

The basement of the region is composed of rocks from the São Gabriel Block, which consists of a tectonic intercalation of mafic to ultramafic rocks from the Cerro Mantiqueira Ophiolite, tonalitic to dioritic gneisses of the Imbicuí Complex (890–850 Ma) (PHILIPP et al., 2016a), metagranites of the Cambaí Complex (740–700 Ma) (LEITE et al., 1998; HARTMANN et al., 2011), and low-grade metavolcanosedimentary rocks of the Marmeiro Complex. These units represent E–W-trending belts formed during the Passinho and São Gabriel orogenies (890–850 and 760–680 Ma) (CHEMALE, 2000; HARTMANN et al., 2007; SAALMANN et al., 2010; PHILIPP et al., 2018) and were subjected to low- to medium-grade orogenic metamorphism under low-pressure conditions. The relationships among these units reflect deformation and collisional metamorphism processes associated with regional compression, with  $\sigma_1$  oriented NW–SE (CHEMALE, 2000; SAALMANN et al., 2010; PHILIPP et al., 2018).

The mine's structural framework is characterized by a system of strike-slip and normal faults affecting the volcanogenic rocks of the Hilário Formation (LOPES et al., 2018). The main measured trends of these faults are in NE–SW and NW–SE directions, with subvertical dips and, additionally, E–W strike-slip faults were described. Structural analysis indicates that lineations are associated with the strike-slip faults and exhibit sub-horizontal orientations, displaying both dextral and sinistral kinematics. Only a minor portion of the slickenlines exhibits a subvertical orientation, associated with normal faults (Lopes et al., 2018).

The mineralized fractures and faults present NE–SW and NNE–SSW directions, with vertical to subvertical attitudes. Two generations of slickenlines were identified, resembling those observed on fault planes. These slickenlines contain deformed calcite and aligned hematite, indicating distinct structural events. The subvertical slickenlines overprint the sub-horizontal ones, suggesting an initial strike-slip displacement followed by a later normal movement—both characterized by NE–SW directions. These structural features point to a complex tectonic evolution involving strike-slip and extensional regimes at different stages of the geological history of the Seival Mine (Lopes et al., 2018).

Mineralization at the Seival Mine is associated with faults and fractures formed under a maximum compressive stress regime oriented NW–SE. These structures are linked to the evolution of the Caçapava do Sul Shear Zone and the Cabritos–Perau, Segredo, and Palma–Jacques faults. These structures facilitated the circulation of hydrothermal fluids and the subsequent deposition of copper and silver, likely between 600 and 580 Ma (GASTAL et al., 2006; JANIKIAN et al., 2008; ALMEIDA et al., 2012).

The mineralized fractures were formed by local extensional regimes (joints and fractures) that filled the rocks with euhedral and drusy quartz (FONTANA et al., 2017), suggesting a porphyry-epithermal or IOCG-type deposit model (DILLES and EINAUDI, 1992; SILLITOE, 2003, 2010). At the Seival Mine, the presence of copper and silver in whole-rock analyses of monzonitic and andesitic dikes indicates a genetic link between magmatism and mineralization (LOPES, 2013; LOPES et al., 2014; FONTANA et al., 2017).

Considering the contexts presented, Lopes et al. (2014) identified three distinct episodes of hydrothermal alteration:

First phase: Represented by smectite, associated with residual magmatic processes, and occurring in both fibrous and crystalline forms;

Second phase: Characterized by a mineral assembled of chlorite, epidote, carbonate, sulfide, barite, quartz, and hematite. This alteration is pervasive and developed under higher-temperature conditions, with veins composed of carbonate, chlorite, and quartz;

Third phase: Associated with dikes and marked by propylitization and sericitization of feldspars.

According to Lopes (2011), the inactive mines exhibit a preferential NE alignment, while NW-trending faults exert a greater influence on hydrothermal alteration, as illustrated at the Barita Mine (FIGURE 3a). The closer a rock is to a fault zone, the more intense the hydrothermal alteration and, consequently, the greater the mineralization potential. This author also described six drill holes carried out by CBC in 1978, with investigation depths up to 80 meters. The core from borehole SV-11 revealed breccias crosscut by calcite veins and the presence of an Andesite dike. Figure 3b illustrates the core description, showing a gradual increase in carbonate veining toward the surface.

These findings highlight the importance of geological structures and post-collisional magmatism in controlling mineralization and in the formation of the studied deposits, reinforcing the relevance of integrating structural, lithological, and hydrothermal studies.

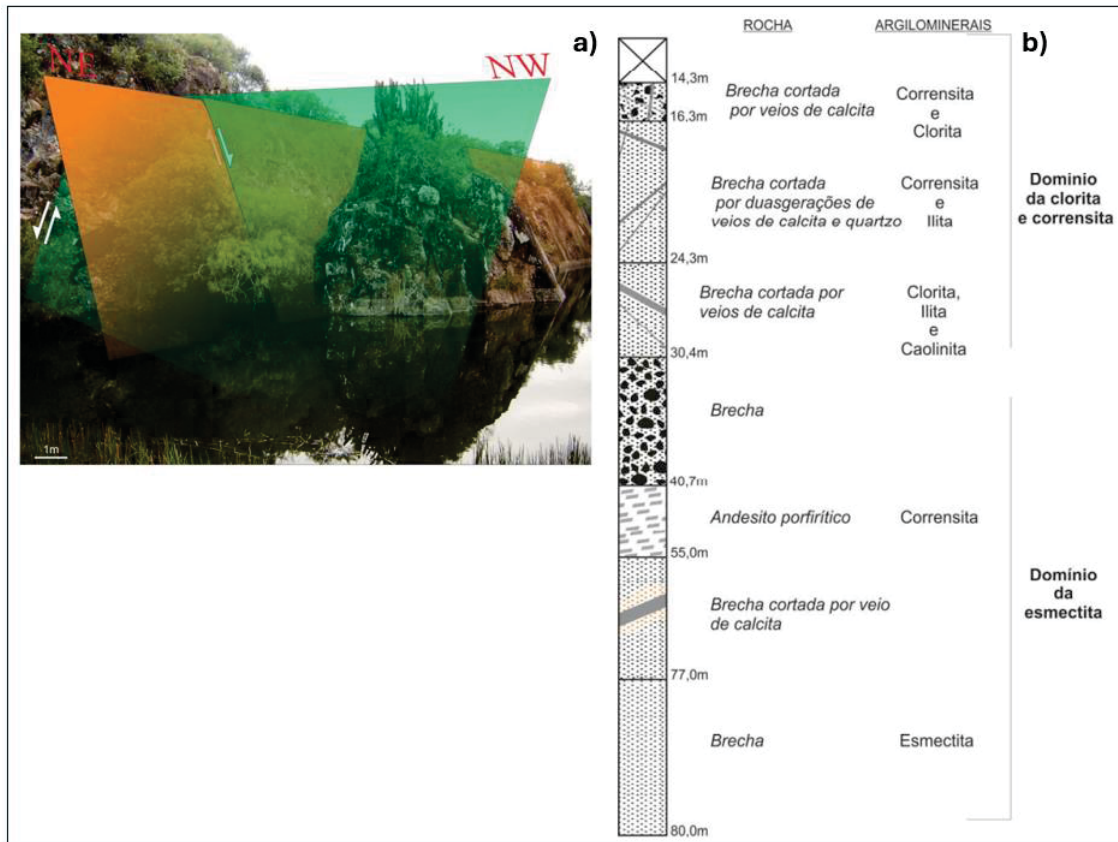


FIGURE 3 - (a) Scheme illustration showing the intersection of NE-NW oriented fault planes at the Barita Mine; (b) Diagram depicting the drill hole and associated clay mineral domains identified through XRD analysis (Modified from Lopes, 2011).

#### 4.3.3 Materials and Methods

The study was structured in three main stages, aiming for an integrated and systematic approach to geophysical and geological analysis (FIGURE 4).

The first stage involved qualitative analysis through geophysical maps, including Total Magnetic Intensity (TMI), Analytical Signal Amplitude (ASA), and Tilt Derivative, as well as the gamma-ray spectrometric map in a ternary RGB color scale. These data were integrated with detailed geological mapping information and previous studies on the main directions of structural lineaments associated with mineralizations. This stage aimed to identify initial patterns and define preliminary targets for investigation.

In the second stage, analyses were deepened through the application of filters, focusing on enhancing structural features. Among the methods used, Euler Deconvolution stood out, allowing the estimation of depths and continuity of anomalous sources. Additionally, to understand the subsurface continuities of the main sources causing the anomalies, magnetometric data inversion was employed. This approach enabled the refinement of geological structure characterization and reduced uncertainties in data interpretation.

In the third and final stage, specific profiles were selected for detailed and integrated analysis, considering the lithological and structural context. Euler Deconvolution and the results from magnetic data inversion were used to validate and refine interpretative models. As a final product, potential areas were delineated for more detailed and in-depth studies, providing a basis for subsequent stages of mineral exploration.

This adopted approach and respective stages allowed for a progressive and detailed analysis, promoting the integration of different methods and data to maximize effectiveness in the identification of prospective targets. The sequential application of geophysical and geological techniques enabled the reduction of uncertainties and the improvement of interpretative models, ensuring greater reliability in defining areas with mineral potential. Thus, the results obtained serve as a robust foundation for the continuity of investigations, contributing to the strategic guidance of future exploration stages.

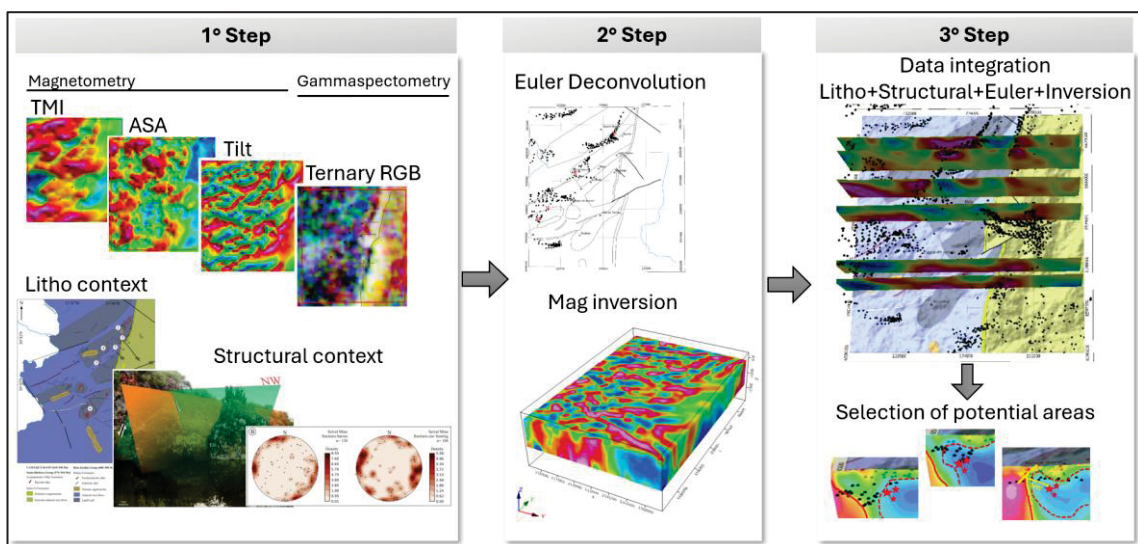


FIGURE 4 - Flowchart illustrating the adopted approach and the development stages defined for this study.

The aerogeophysical database used for the development of this study consists of aeromagnetic and gamma-ray spectrometric data acquired during the Primavera Project, conducted in 2010. Data acquisition and processing were carried out by LASA Prospecções S.A. The data belong to the Applied Geophysics Laboratory at the Federal University of Pampa and were provided for the execution of this study. The project coverage area is in the southernmost region of Brazil, encompassing the municipalities of Caçapava do Sul and Lavras do Sul, with a total coverage of approximately 12,681 km<sup>2</sup>.

The technical parameters employed in the survey are described as follows:

- Flight line direction: N14W.
- Flight line spacing: 200 meters.
- Average flight altitude: 100 meters.

Complementary to the geophysical data, a database was compiled to support a comprehensive analysis of the geological and structural context, as well as information regarding mineral occurrences in the area. These data were collected from scientific articles, theses, and dissertations, providing evidence and a robust foundation for data interpretation and integration with the methodologies employed.

#### 4.3.3.1 The Importance of Rock Physical Properties in Analysis and Interpretation

Studies by Clark (1997), Dentith and Mudge (2014), and Hinze et al. (2013) emphasize the importance of understanding the variations and contrasts in physical properties among different lithotypes, highlighting the influence of factors such as porosity, permeability, and structural control. Clark (1997) underscores the relevance of extracting geological information to enhance the interpretation of magnetic survey data. The author highlights the necessity of magnetic petrophysical studies to better understand the geological processes that influence the formation, modification, and destruction of magnetic minerals in rocks, thereby aiding in the analysis and interpretation of magnetic signatures across various geological settings.

More recently, studies such as that by Anderson et al. (2023) investigated the physical properties of a porphyry copper deposit based on 673 magnetic susceptibility measurements across different lithotypes. The results indicate a wide variation in

magnetic susceptibility, influenced by factors such as weathering, hydrothermal alteration, supergene processes, texture, and the arrangement of minerals.

FIGURE 5a presents a conceptual model of a supergene profile (Sillitoe, 2005; Anderson et al., 2023), illustrating that near-surface oxidation can lead to the reprecipitation of sulfides near the water table, a reduction in magnetite content, and an increase in clay fraction, directly impacting the geophysical response. The study demonstrated that as the intensity of hydrothermal alteration increases toward the top and peripheral zones of the stockworks, a transition occurs between different alteration assemblages: (i) propylitic, (ii) quartz-sericite-pyrite, (iii) quartz-alunite-pyrophyllite, (iv) argillic, and (v) silica. This process results in a progressive reduction in magnetic susceptibility values, suggesting that hydrothermal alteration gradually reduced the magnetite content in the rock.

However, some exceptions were identified, associated with high magnetite concentrations in certain lithotypes. Additionally, the authors report a variation in magnetic response with depth, indicating a general increase in magnetization at greater depths. Rocks affected by potassic alteration, as well as unaltered plutonic basement rocks, exhibit the highest magnetization values (FIGURE 5b).

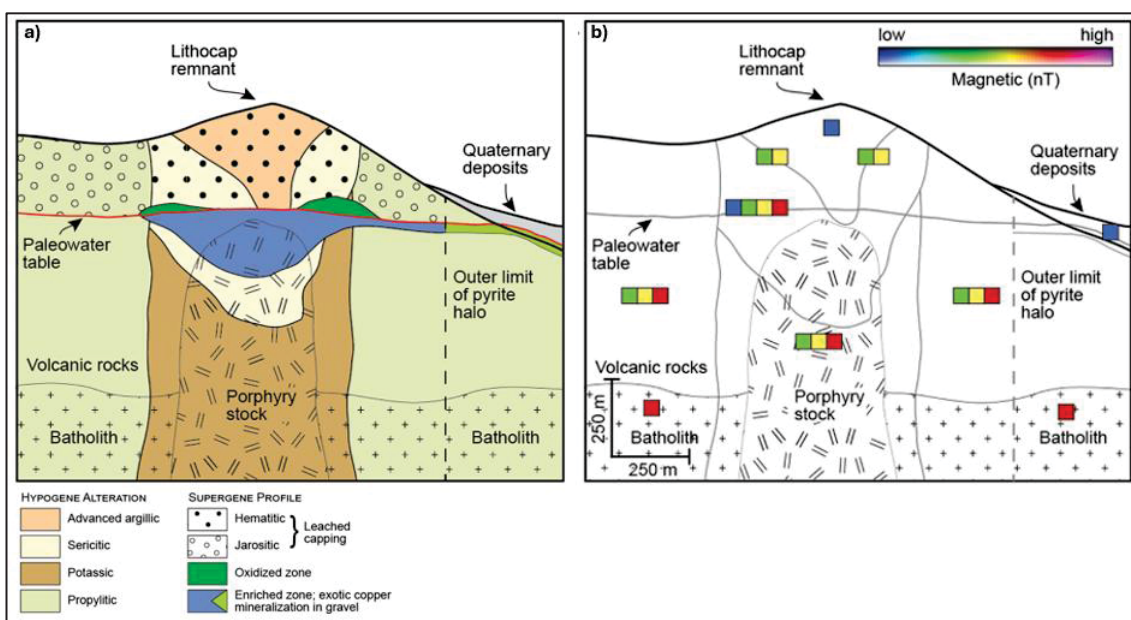


FIGURE 5 - (a) Conceptual model of a supergene profile in a porphyry copper deposit; (b) expected magnetic signature considering different lithologies and hydrothermal alterations (Modified from Sillitoe, 2005; Anderson et al., 2023).

Based on the studies presented, the fundamental importance of understanding the geological aspects of the study area prior to geophysical data processing is

emphasized. Identifying the sources responsible for contrasts in physical properties relies on the analysis of the host and adjacent rocks, types of hydrothermal alteration, mineralogical textures, and evidence of supergene processes. This foundation knowledge is essential for accurate data interpretation and for achieving more precise results.

#### 4.3.3.2 The Use of Filters and Enhancement Techniques in Magnetometric and Gamma-Ray Spectrometric Data for Mineral Exploration

Various radioactive isotopes are known, originating from both natural and artificial sources, although most exhibit low emission intensity. The main sources of gamma radiation at the Earth's surface result from the natural decay of potassium-40 ( $^{40}\text{K}$ ), as well as elements belonging to the uranium-238 ( $^{238}\text{U}$ ) and thorium-232 ( $^{232}\text{Th}$ ) series, which are widely distributed in the composition of most rocks (COX, 1979; TELFORD et al., 1990; DICKIN, 1995; FAURE, 1997).

The application of gamma-ray spectrometry has become an essential tool for geological mapping and mineral exploration. As effective examples, Cotis et al. (2013) identified new exploration targets through the radiometric signature of known sources. Fornazzari Neto and Ferreira (2003), Carrino et al. (2007), and Alhumimidi et al. (2021) employed this technique for mineral prospecting purposes, while Ribeiro and Mantovani (2012) used it to delineate geological contacts. Additionally, Biondi et al. (2001) applied gamma-ray spectrometry to characterize areas affected by hydrothermal alteration.

The interpretation of radiometric data can be conducted through different approaches, such as the development of ratio maps for the elements (K, eTh, and eU) and the generation of Total Count maps — which represent the sum of all counts recorded within the energy window between 0.41 and 2.81 MeV. Moreover, ternary maps can be produced, in which the colors red, green, and blue are assigned, respectively, to the concentrations of potassium (%), thorium (ppm), and uranium (ppm), providing an integrated visualization of the distribution of radioelements (RIBEIRO et al., 2013).

The use of filters and enhancement techniques in magnetometric data is an essential tool for characterizing areas with potential for mineralization, offering an effective approach for geophysical subsurface investigation. The application of filters such as the Analytic Signal Amplitude (ASA), Tilt Derivative, and the Euler

Deconvolution technique has emerged as a key strategy to improve data resolution and reliability, allowing for more accurate analysis of geophysical anomalies. These techniques facilitate the identification of relevant geological structures, such as faults and lithological contacts, which often have high mineral potential, in addition to contributing to the definition of the geometry and extent of mineralized bodies at depth (DENTITH and MUDGE, 2014; HINZE et al., 2013).

The Analytic Signal Amplitude (ASA) is a widely used technique for magnetic data analysis, being particularly effective in detecting anomalies associated with geological structures. Its main advantage lies in its ability to provide a clear image of the spatial distribution of anomalous sources, regardless of the orientation of the magnetic or gravity field vector (NABIGHIAN, 1972).

The concept of the analytic signal applied to magnetic anomalies was initially developed based on the properties of the Hilbert transform (NABIGHIAN, 1972; ATCHUTA RAO et al., 1981; NELSON, 1988; PEDERSEN, 1989; BLAKELY, 1995). ASA is defined as the square root of the sum of the squares of the vertical and orthogonal horizontal derivatives of the magnetic field, with these derivatives being even functions of the Hilbert transform for two-dimensional magnetic sources (DEBEGLIA and CORPEL, 1997).

Pioneering studies (NABIGHIAN, 1972, 1974, 1984; ATCHUTA RAO et al., 1981) demonstrated the effectiveness of ASA in identifying structures such as dikes. Subsequently, Roest et al. (1992) refined this approach for the interpretation of aeromagnetic maps, while MacLeod et al. (1993), Hsu et al. (1996, 1998), and Debeglia and Corpel (1997) expanded its applications, consolidating its use in applied geophysics.

Salem et al. (2008) presented a methodology for interpreting magnetic data using tilt angle derivatives. This method provides a linear equation similar to the 3D Euler deconvolution, allowing automatic estimates of the position and depth of magnetic sources without requiring prior information about their geometry. Unlike Euler deconvolution, which requires a structural index, this approach simplifies interpretation by using second derivatives of the magnetic anomaly and reduces noise effects through upward continuation techniques.

Tested with theoretical simulations and real data, the method showed good correlation with previous studies, demonstrating its efficiency in locating magnetic sources. Salem et al. (2008) highlight the importance of incorporating petrophysical

concepts in the interpretation of magnetic surveys and propose advances in 3D modeling and visualization to enhance the analysis of large datasets. Despite its advantages, the method may present challenges in areas with multiple closely spaced magnetic sources, requiring adjustments in the analysis scale.

#### 4.3.3.3 Euler Deconvolution

Euler Deconvolution is a widely used technique in the interpretation of potential field geophysical data, such as magnetometry and gravimetry, allowing for the localization and depth estimation of anomalous sources. Its classical formulation was introduced by Thompson (1982) and later refined by several authors, including Reid et al. (1990), Barbosa et al. (1999, 2000), and Mushayandebvu et al. (2001).

The fundamental equation of Euler deconvolution for a potential field anomaly  $T(x, y, z)$  generated by a three-dimensional point source is (Equation 1):

$$(x - x_0) \frac{\partial T}{\partial x} + (y - y_0) \frac{\partial T}{\partial y} + (z - z_0) \frac{\partial T}{\partial z} = N(T - B) \quad (1)$$

Where:

- $(x_0, y_0, z_0)$  are the coordinates of the source,
- $N$  is the structural index, related to the geometry of the source (e.g.,  $N = 0$  para geological contacts,  $N = 1$  for dikes,  $N = 2$  for cylinders,  $N = 3$  for spheres) (REID et al., 1990),
- $B$  is the regional background.

The system of equations generated for multiple observations is solved using the least squares method to estimate the unknown parameters (THOMPSON, 1982).

Euler Deconvolution emerged in response to the growing need for automated methods to interpret the large volumes of aeromagnetic data collected since the 1950s by institutions such as the U.S. Geological Survey (USGS) and the Canadian Geological Survey (BARBOSA and SILVA, 2005). In the 1970s, methods such as Werner Deconvolution (HARTMAN et al., 1971), the Naudy Method (1971), and CompuDepth (O'BRIEN, 1972) were developed. However, the Euler Deconvolution, proposed in the 1980s, became the predominant technique (THOMPSON, 1982). In the 1990s, improvements were made to reduce the dispersion of solutions (BARBOSA

et al., 1999; FAIRHEAD et al., 1994) and to enhance the estimation of the structural index (SALEM and RAVAT, 2003).

Among the methodological advances, one of the main challenges of Euler Deconvolution has been the reduction of the solution cloud. To address this, methods were developed to retain only those solutions associated with high signal-to-noise ratios, thereby minimizing the dispersion of results (FAIRHEAD et al., 1994; BARBOSA et al., 1999; MIKHAILOV et al., 2003). Another significant issue was the determination of the structural index ( $N$ ), which was initially defined empirically. The estimation of this parameter was improved through methods based on the correlation between the observed anomaly and the estimated base level (BARBOSA et al., 1999), as well as through the application of the analytic signal for this purpose (SALEM and RAVAT, 2003). Euler Deconvolution was also extended to enable its application in ground surveys with a reduced number of observations – an approach previously unfeasible due to the dispersion of solutions and the requirement for large data volumes (BARBOSA et al., 2000).

Another key improvement was the estimation of additional parameters beyond the source location. Techniques such as extended Euler Deconvolution were developed to determine the dip and susceptibility contrast of geological contacts (MUSHAYANDEBVU et al., 2001). Generalizations of the method were also proposed to handle multiple sources within a single data window, enabling the interpretation of more complex geological environments (HANSEN and SUCIU, 2002).

Euler Deconvolution continues to evolve, with ongoing efforts focused on integration with geophysical inversion algorithms for the reconstruction of 3D geological models (GUILLEN et al., 2004). Additionally, the incorporation of machine learning techniques for improved solution classification and enhanced robustness against noise are active areas of research aimed at making the technique even more efficient and reliable.

According to Sequent (2024), the processing of Euler Deconvolution data follows a series of steps that enable the automated interpretation of potential geophysical data. Initially, raw data are imported into the software using compatible formats, followed by the application of filters to correct regional trends and remove noise that could compromise the accuracy of the analysis.

The configuration of Euler Deconvolution requires the definition of several parameters. One of the key parameters is the Structural Index ( $N$ ), which defines the

relationship between the geometry of the source and the rate of change of the potential field. The Structural Index is a dimensionless value, and to ensure reliable results, it must be selected appropriately. An incorrect choice can lead to scattered or erroneous solutions. Each geological source is associated with a characteristic structural index.

According to Sequent (2024), one of the main limitations of the traditional Euler Deconvolution approach is its sensitivity to noise in the data. Since the method relies on the differentiation of the potential field, small variations or measurement errors can generate scattered solutions that are difficult to interpret. This may result in the formation of a “cloud” of solutions that do not accurately reflect the true position of anomalous sources.

Additionally, the method can be affected by interference from multiple nearby sources. If more than one geological structure influences the data within the same calculation window, the resulting solutions may become ambiguous and imprecise. This occurs because Euler’s equation assumes the presence of a single dominant source in the analyzed region, which is not always the case in complex geological environments (SEQUENT, 2024).

To mitigate these limitations, several strategies have been suggested. One involves applying filters to the data prior to deconvolution, reducing noise and improving the signal-to-noise ratio. Additionally, it is recommended to dynamically adjust the size of the calculation window to minimize interference from nearby sources and obtain more stable solutions. Another approach involves combining Euler Deconvolution with the analytic signal method, which helps validate the choice of the Structural Index by analyzing the symmetry and intensity of the anomalous signal. Statistical methods can also be employed to remove inconsistent solutions and identify the most reliable estimates (SEQUENT, 2024).

These improvements make Euler Deconvolution more robust and suitable for different geological scenarios, enabling more accurate interpretation of potential field data.

In this study, Oasis Montaj software, version 2024.1, was used for data processing. The data did not exhibit significant noise in the Total Magnetic Intensity (TMI), eliminating the need for filtering corrections. Based on tests conducted using the analytic signal method, this approach and product were selected as input data for the application of Euler Deconvolution. The parameters used included a Structural Index of  $N = 2$ , as the bodies tend to exhibit more cylindrical geometries. Several tests

were performed to determine the optimal depth tolerance percentage, with the best fit achieved at 11%, and the window size was set to 15 grid cells.

#### 4.3.3.4 Magnetic data inversion

Another widely used tool in mineral exploration is magnetic data inversion. Magnetization Vector Inversion (MVI) is an advanced geophysical technique employed to interpret magnetic data, particularly in contexts where remanent magnetization or magnetic anisotropy are present. By treating magnetization as a three-dimensional vector, this method enables a more detailed understanding of the subsurface by effectively integrating both induced and remanent magnetization data.

The evolution of MVI research reflects the progressive development of modeling and interpretation techniques for magnetometric data. Baranov (1957) was a pioneer in exploring the effects of remanent magnetization on magnetic anomalies, paving the way for more sophisticated approaches. Later, Blakely (1995) consolidated the mathematical foundations of potential theory applications, which served as the basis for more advanced formulations. Li and Oldenburg (1996) made significant contributions by addressing non-uniqueness problems in magnetic inversion and introducing robust regularization methods, while Zhdanov (2002) expanded these ideas by developing a comprehensive theory of geophysical inversion.

The advancement in vector techniques was led by Tarantola (2005), who provided a unifying framework for inverse problems, emphasizing the importance of a priori constraints and probabilistic methods, thereby consolidating both theoretical and practical progress in geophysical inversions. Subsequently, Lelièvre and Oldenburg (2009) integrated geological data to build more accurate three-dimensional models, which were later refined by Ellis, MacLeod, and Oldenburg (2012) with a specific approach for total magnetization, including both induced and remanent components. These studies demonstrate how MVI inversion has evolved to meet the increasing demands of mineral exploration and geological mapping in complex environments.

For the present study, total magnetic field data reduced to the IGRF was used, with a magnetic field intensity of 22,727.00 nT, an inclination of -37.2°, and a declination of -13.6°. A cell size of 50 x 50 x 25 meters was adopted in X, Y, and Z directions, respectively, with grid dimensions of 154 x 220 x 37 cells (X, Y, and Z). Additionally, parameters related to the maximum investigation depth were adjusted, limiting the depth to approximately 1 km. No additional constraints were applied.

#### 4.3.4 Results and Discussion

The results will be presented in two parts. The first part addresses the qualitative analysis of 2D airborne geophysical maps, while the second part presents a semi-quantitative evaluation, including data inversions and the application of geophysical data enhancement techniques.

As a basis for interpreting the geophysical signatures, relevant geological information compiled from the literature was initially considered.

The mineralizations are associated with the Bom Jardim Group, occurring along faults and fractures that contain copper sulfides such as chalcopyrite, bornite, chalcocite, and covellite (FONTANA et al., 2017). The volcanic rocks of the Hilário Formation include tuffs, volcanic agglomerates, and andesitic flows (REISCHL, 1978; LOPES, 2013; LOPES et al., 2014), all affected by hydrothermal alteration. Additionally, andesitic dikes show a strong relationship with mineralization.

According to Lopes et al. (2018), mineralization at the Seival Mine predominantly occurs in a disseminated manner, associated with stockwork-type structures characterized by irregular and subvertical geometries, influenced by the high permeability of lapillitic tuffs. Occurrences of malachite have also been reported in cavities and within the matrix of volcanic agglomerates. Additionally, hydrothermal veins were identified in lapillitic tuffs, containing disseminated chalcocite in cavities filled with chlorite and hematite, which were later crosscut by calcite veins.

Lopes et al. (2014) classified hydrothermal alteration at the Seival Mine into three distinct phases, detailing mineral assemblages composed of chlorite, epidote, carbonate, sulfides, barite, quartz, and hematite, occurring pervasively, mainly within carbonate, chlorite, and quartz veins. Propylitic alteration and sericitization processes were also described, strongly associated with dikes.

Based on the analysis of the study area, basement rocks and mineralized zones with well-preserved stockwork structures at greater depths are expected to exhibit geophysical signatures characterized by more pronounced magnetization. In contrast, areas affected by hydrothermal alteration and supergene processes, particularly near the surface, tend to display reduced magnetization. In these zones, mineralization may occur in both veinlets and disseminated forms.

The structural context, as well as the presence of dikes and veinlets, represents a relevant indicator for sulfide precipitation, especially when these structures exhibit a

preferred NE-SW orientation. These zones may generate contrasting patterns in the magnetic response, marking transitions between regions of low and high magnetization.

#### 4.3.4.1 Analysis of 2D Maps – Airborne Geophysical Maps

Initially, total magnetic field (TMI), Analytical Signal Amplitude (ASA), Tilt Derivative, and RGB ternary maps (Gamma spectrometry) were analyzed (FIGURE 6).

The total magnetic field map (TMI) (FIGURE 6a) reveals two prominent dipolar regions: one located near the Barite Mine and another to the southwest of the Lagoa do Jacaré occurrence. A stronger magnetic signature is observed southwest of the Quero-Quero occurrence, as well as near the Cruzeta, Meio, and Morcego mines.

The regional analysis of the ASA map (FIGURE 6b) shows that the Barite, Seival Geral, and Alcides mines are associated with areas of low magnetic intensity, suggesting a relationship between these mineralizations and zones of lower magnetic susceptibility. The Vila do Torrão and Lagoa do Jacaré occurrences are also related to low-intensity contexts. However, the other occurrences and mines are located in contrasting zones, indicating the presence of structural control. Another important point for discussion is the presence of some more robust anomalies with higher magnetic intensity, such as the one located southwest of the Quero-Quero occurrence.

The Tilt Derivative filter highlights the magnetic field, evidencing a marked intensity break in the magnetic signal between andesitic rocks/lapilli tuffs and conglomerates (FIGURE 6c). The Seival, Meio, João Danne, and Barita mines appear to be aligned along the continuation of the same structure with a preferential NE-SW orientation. The Quero-Quero, Lagoa do Jacaré, and Vila do Torrão occurrences seem to be associated with a second structural direction oriented NW-SE.

The ternary map, constructed from the concentrations of K, U, and Th, delineates the main lithological contacts in the subsurface (FIGURE 6d). It is observed that the conglomerates of the Santa Fé Formation show enrichment in potassium, while the andesitic lava flows and lapilli tuffs of the Hilário Formation are enriched in uranium and thorium channels. These patterns of gamma-spectrometric signature provide important information for lithological characterization and the differentiation of geological units in the study area.

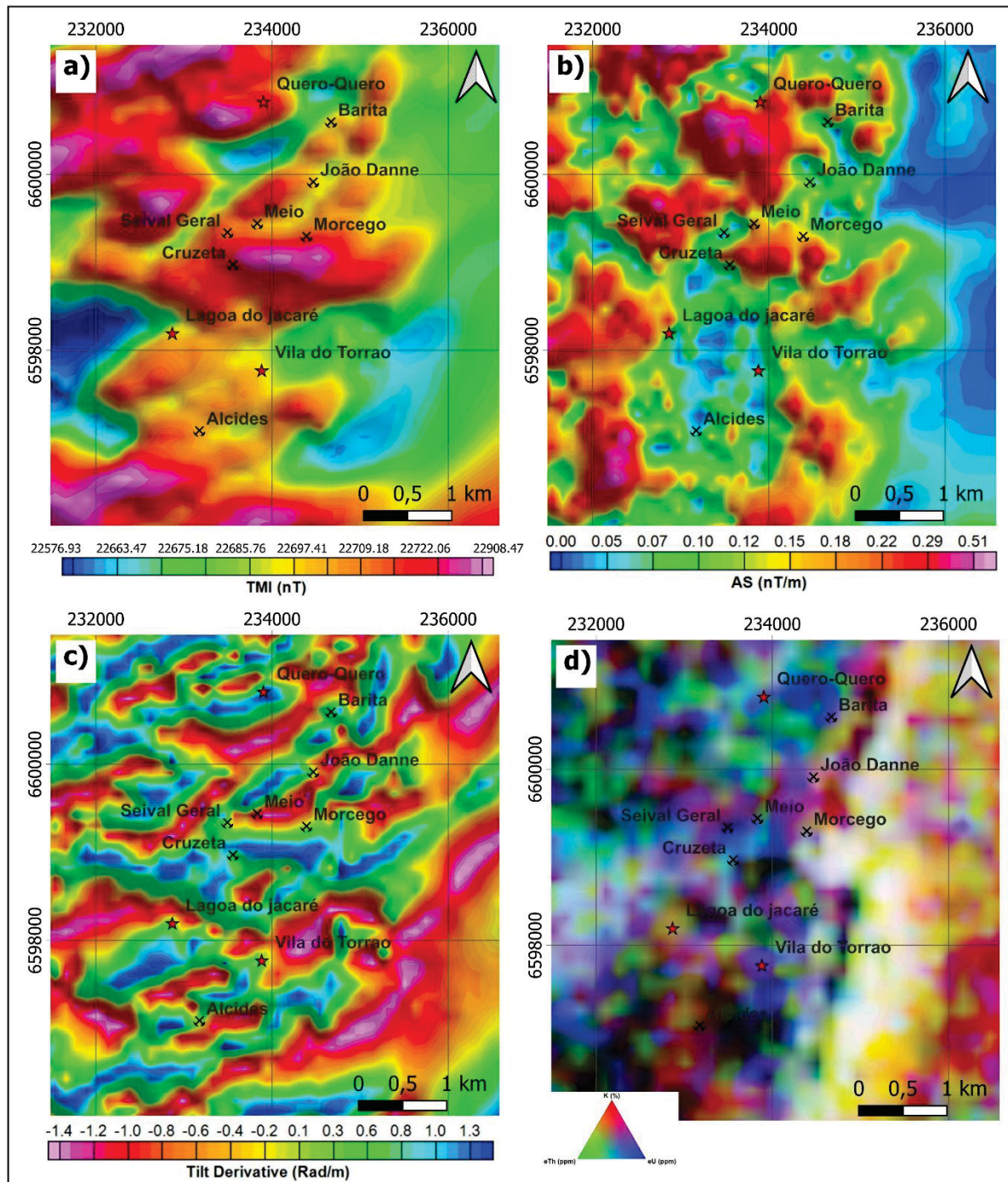


FIGURE 6 - Maps displaying aerogeophysical anomaly values for the study area. a) Total Magnetic Intensity - TMI, b) Analytic Signal Amplitude - ASA, c) Tilt derivative, and d) RGB ternary gamma-ray spectrometry map.

#### 4.3.4.2 Semiquantitative Analysis – Euler Deconvolution, Integrations, and MVI Models

To define the orientation of discontinuities associated with local structures, the Euler Deconvolution technique was employed. The parameters used for data processing were discussed previously (see Section 4.3.3.3). Figure 7 presents the

results of the Euler Deconvolution integrated with lithological, structural, and geomorphological information.

The results revealed two main structural trends related to the copper occurrences. The first, more pronounced trend extends between the Barita Mine and the Quero-Quero occurrence, showing a predominant NE–SW orientation with subordinate NW–SE directions. The estimated depths of the structures detected by this method display a continuous variation of approximately 220 meters. The Digital Elevation Model (DEM) also shows a relief break aligned with the orientation of these detected structures.

The second trend is located at the Seival Geral Mine, where a dominant NE–SW structural orientation is also evident, accompanied by secondary NW–SE features. The depth continuity of these sources is less uniform, with an estimated thickness variation of about 145 meters.

Euler Deconvolution delineated continuous structures near lithological contacts, such as east of the Barita Mine, where a continuous structural feature is observed along the contact between vesicular andesitic lava flows and polymictic conglomerates.

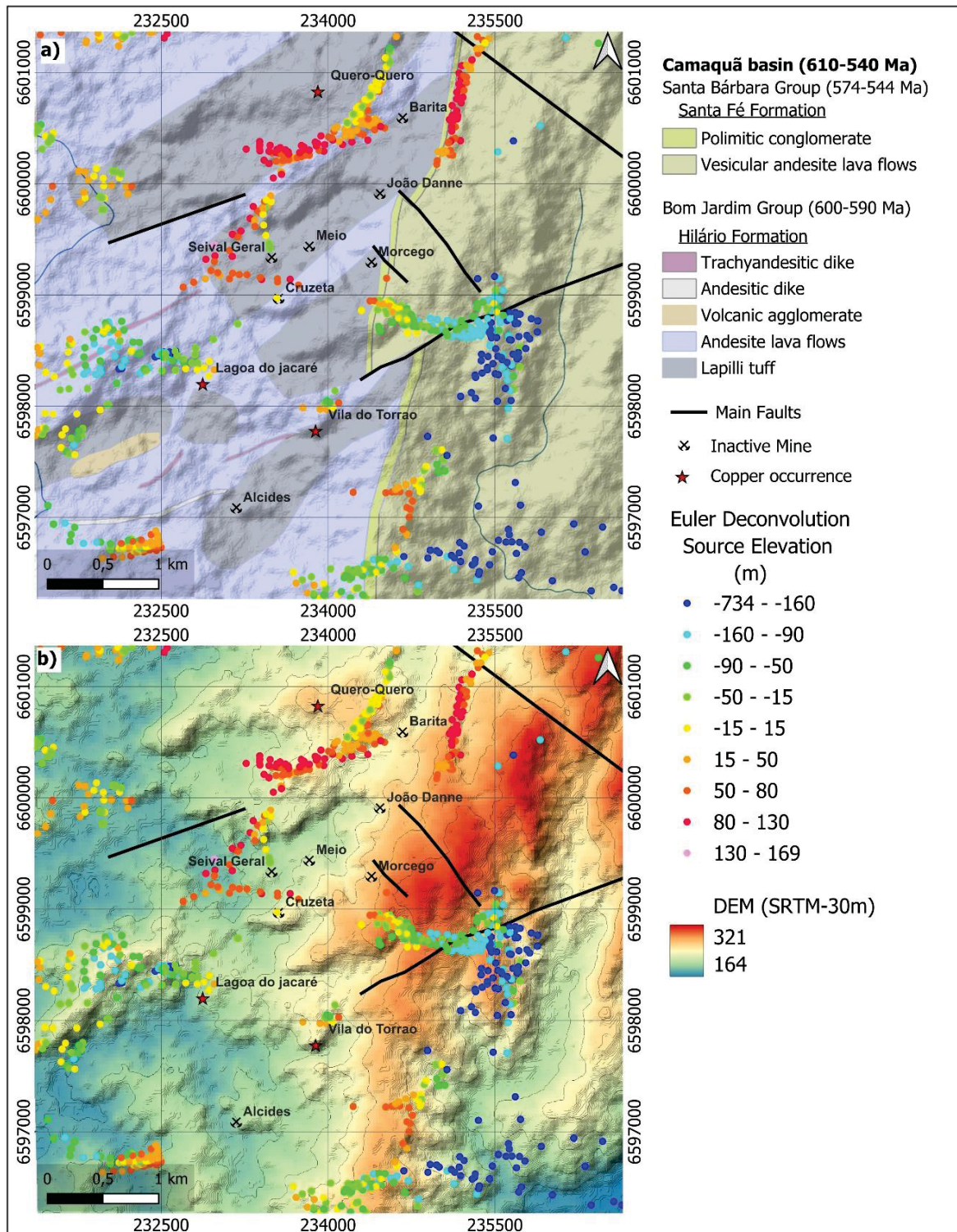


FIGURE 7- (a) Euler Deconvolution map generated using a Structural Index of 2, overlaid with the lithological context; (b) same results overlaid with the digital elevation model (Adapted from Lopes et al., 2018).

To understand the depth and lateral continuities of the main mines and occurrences in the region in relation to magnetic susceptibility contrasts, a magnetic data inversion was performed using the MVI (Magnetization Vector Inversion) method.

The parameters used and technical specifications were previously discussed (see Section 4.3.3.4).

FIGURE 8a shows the MVI model. For the inversion, a broader area was considered to minimize edge effects and reduce possible noise. The study area is highlighted by the yellow rectangle in the same figure.

Vertical profiles were generated within the area of interest, positioned to intersect the main lithologies and structures perpendicularly. Six profiles were selected as best represent the area and the continuity of structures and geometries at depth. The optimal placement of these profiles, also considering the Euler Deconvolution results, was oriented in the W–E direction (FIGURE 8b).

The lithogeophysical profiles cover a total length of 6 km and reach depths of up to 1 km. The geological map, including copper occurrences and inactive mines, was superimposed on the model, together with the Euler Deconvolution results represented by black dots (FIGURE 8c).

For the interpretation of the magnetic signature results, the terms “low magnetic intensity” will refer to regions with MVI contrasts around 0.0001 (represented in blue), and “high magnetic intensity” will refer to contrasts greater than 0.001.

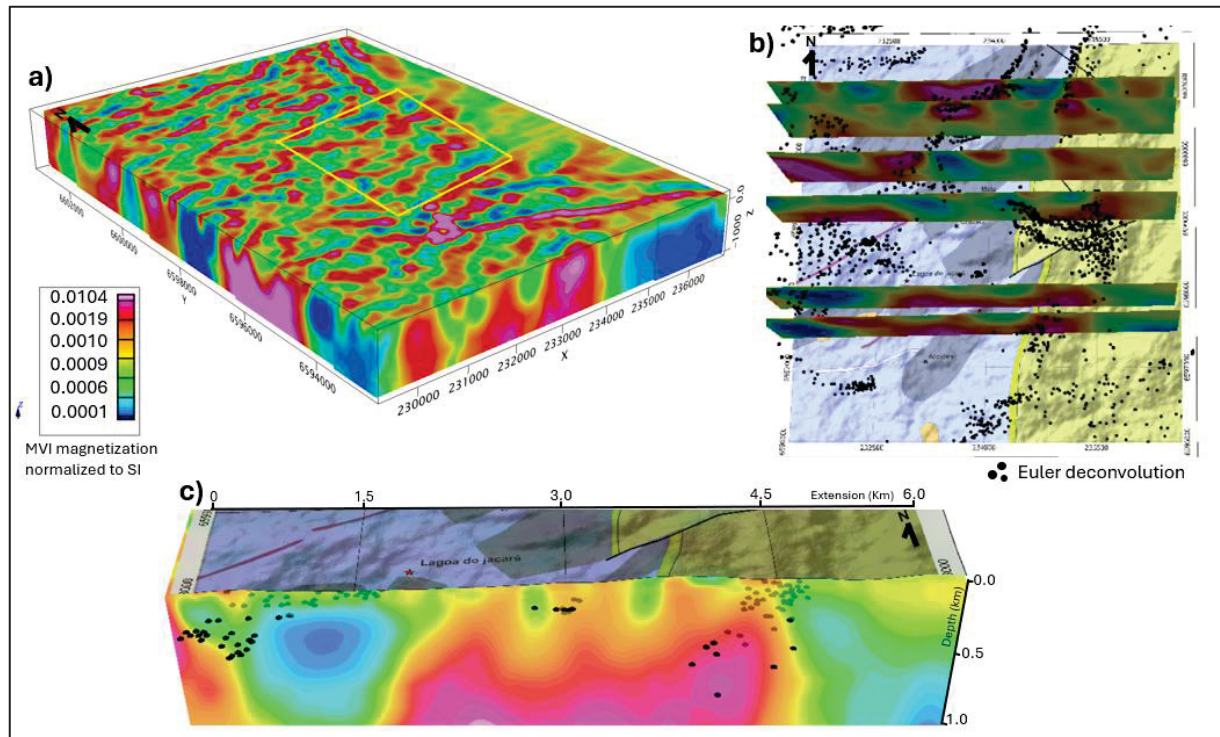


FIGURE 8 – MVI models and generated sections for the study area. a) MVI inversion model; the yellow polygon outlines the study area. b) Selected vertical profiles from the MVI model. c) Geophysical profile overlaid with the geological map and Euler Deconvolution results.

In FIGURE 9, the six profiles, labeled A–A', B–B', C–C', D–D', E–E', and F–F', are shown. These were defined to analyze the results of the integration between the Euler Deconvolution technique, magnetic inversions, and existing geological information.

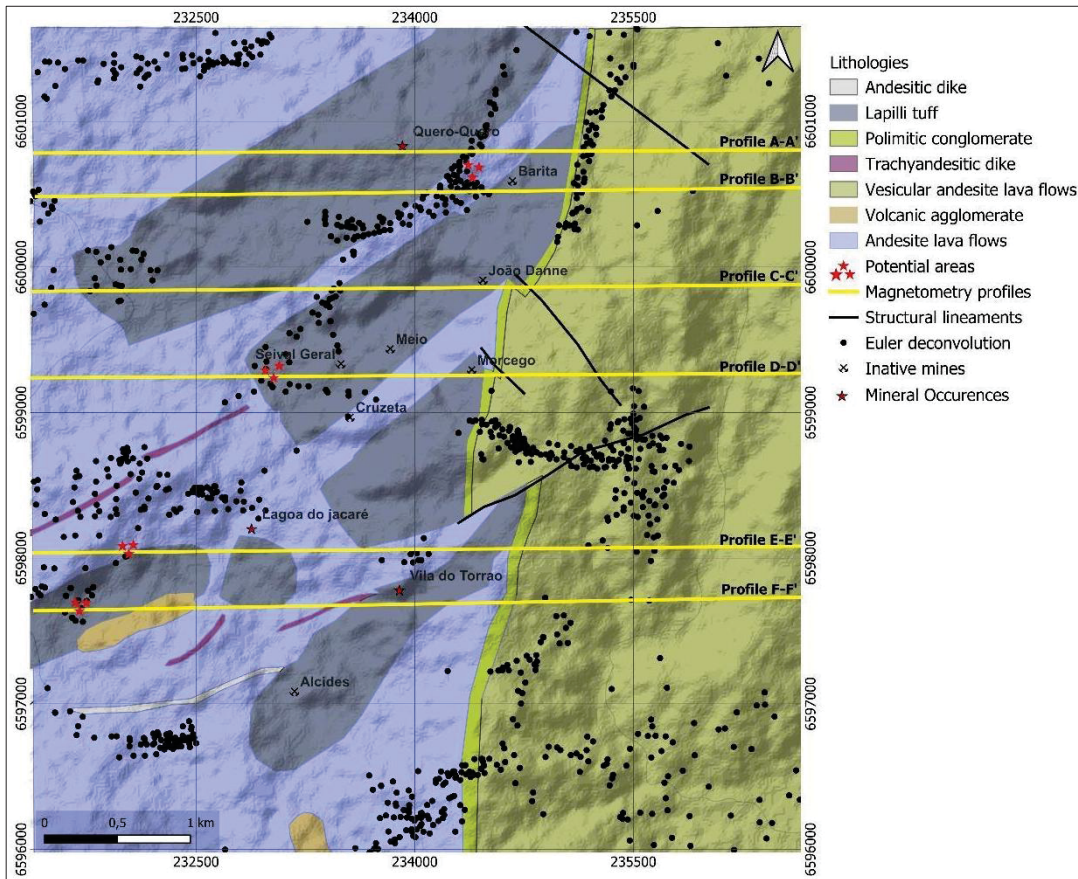


FIGURE 9 - Lithological map of the study area, defined profiles, and Euler Deconvolution results (Modified from Lopes et al., 2018).

The lithogeophysical cross-sections along the defined profiles are presented below. In profile A–A' (FIGURE 10a), a magnetic low is identified, associated with the Quero-Quero occurrence, extending to approximately 500 meters in depth and 600 meters in length. Below 500 meters, a more intense magnetic signature is observed, which, according to the literature, may be related to the basement or to mineralized zones with stockwork-type structures (characterized by increased magnetic intensity).

Another continuous magnetic low is evident to the east of the Quero-Quero occurrence, with about 700 meters in length and reaching 900 meters in depth, corresponding to the Barita Mine. The Euler Deconvolution technique highlights robust structures, especially on the western wall of the body.

In profile B–B' (FIGURE 10b), two magnetic lows are observed: one related to the continuation of the Quero-Quero occurrence and another, more pronounced, representing the Barita Mine. The latter reaches about 1 km in depth and extends to 700 meters. The Euler Deconvolution indicates a continuous NE-trending structure on the eastern wall, correlated with the lithological contact between lapilli tuffs and polymictic conglomerates. On the western wall, intersections of robust NE and NW-trending structures are identified. These intersections corroborate the observations by Lopes (2011), who described similar structures in the Barita Mine, associated with hydrothermal alteration and intense mineralization.

Profile C–C' (FIGURE 10c) highlights lapilli tuffs interbedded with lenses of andesitic lava flows. The lithological boundaries are clearly defined by the magnetic signature, with a lens of andesitic lava showing an intermediate magnetic response (blue line in FIGURE 10c). Near the João Danne Mine, a magnetic low is identified at approximately 1.3 km depth and about 600 meters in length, suggesting a mineralized zone under the influence of hydrothermal alteration.

The low magnetic signal intensity may result from hydrothermal alteration or disseminated mineralization zones. The Euler Deconvolution indicates an intersection of NE and NW-trending structures near the western wall of the magnetic body. To the west of profile C–C', a high-intensity magnetic anomaly is observed, extending about 1.2 km in length and reaching 1 km in depth. This body is located southwest of the magnetic high associated with the Quero-Quero occurrence in profile B–B', suggesting continuity of the body in that direction. No previous occurrences have been identified near this anomaly, and the body does not outcrop. Additionally, a continuity of structures, albeit of lower intensity, is indicated by the Euler Deconvolution results.

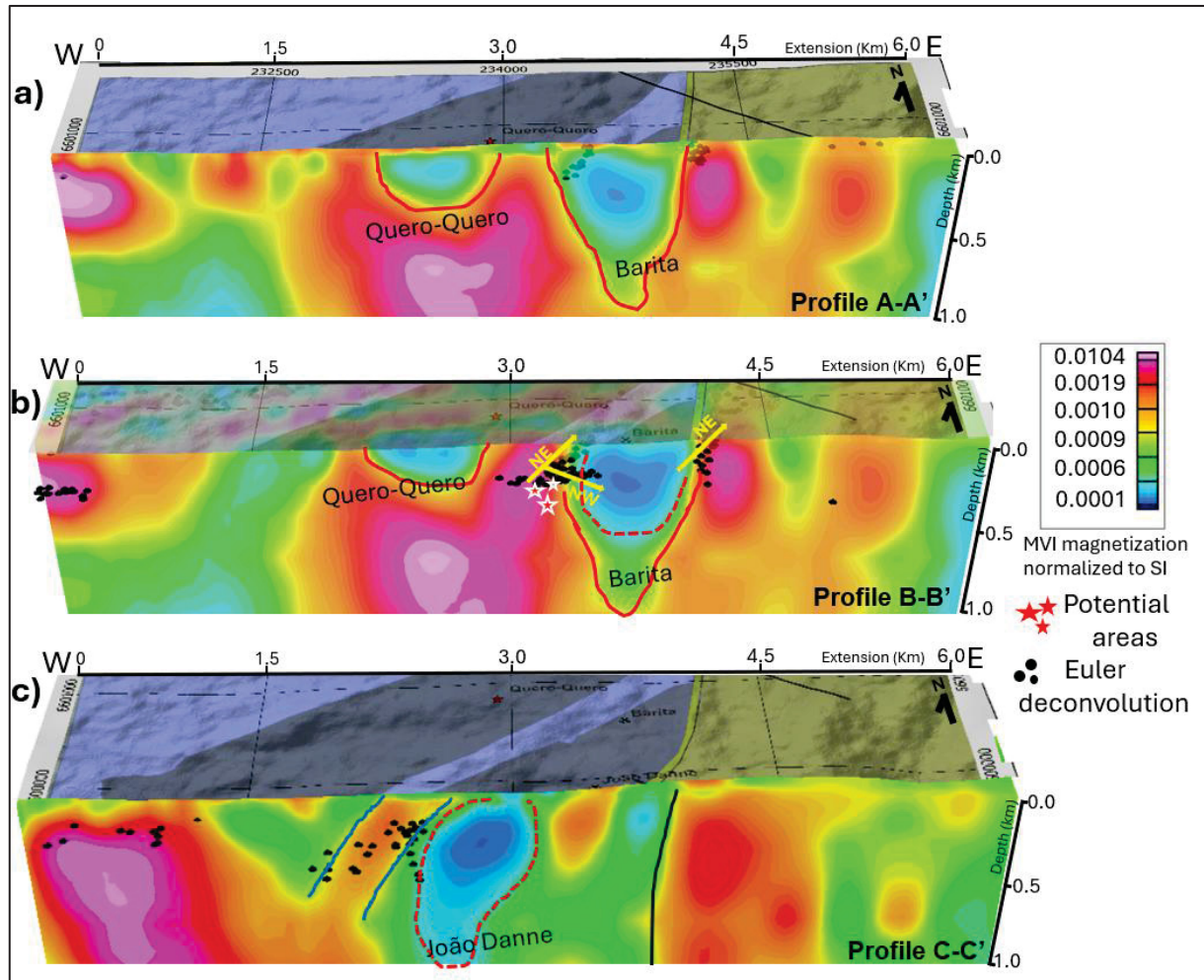


FIGURE 10 - Lithogeophysical profiles A-A' (a), B-B' (b), C-C' (c) with magnetic inversion and Euler deconvolution, overlaid by the local geology map.

The D-D' profile (FIGURE 11a) encompasses the Seival Geral, Meio, and Morcego mines, which are located in close proximity and are characterized by a consistently low-intensity magnetic signature. The magnetic body extends approximately 2.3 km in length and reaches a depth of about 1.4 km. In the central region, a more pronounced magnetic low stands out, with an estimated depth of 750 meters and a length of 1.5 km.

The magnetic low region may also be associated with mineralized zones related to hydrothermal alteration and disseminated mineralization. Using the Euler technique, an intersection of NE- and NW-trending structures was identified on the western flank of the magnetic body, consistent with the pattern previously observed at the Barita Mine. Over a stretch of approximately 1.5 km, a zone of high magnetic intensity is observed, with a transition zone toward the magnetic lows, structurally controlled as indicated by the Euler Deconvolution. This area represents a target of interest for

further investigation, as trachyandesites dikes trending SW–NE have been described near the profile (as shown in the geological map of profile E–E', FIGURE 11b). These dikes may be strongly associated with mineralization. The most prospective area is located at the intersection of structural trends and the transition zone between magnetic highs and lows (highlighted as a potential area in FIGURE 11a).

In profile E–E' (FIGURE 11b), located near the Lagoa do Jacaré occurrence, it is observed that the low-intensity magnetic body increases in volume at depth toward the SW. This body extends to approximately 800 meters depth and has a lateral extent of about 650 meters. The Euler Deconvolution technique identified the presence of structures with a preferential NE trend. Continuous high magnetic anomalies are observed at greater depths; these may represent basement lithotypes, as they do not show significant structural features delineated by the Euler Deconvolution and the body extends into the conglomerates of the Santa Fé Formation.

Profile F–F' (FIGURE 11c) highlights two low-intensity magnetic anomalies. The first, with higher amplitude, corresponds to the continuity of the Lagoa do Jacaré occurrence. The Euler Deconvolution delineated NE-trending structures at a depth of approximately 1.2 km and extending for about 1 km. Near the Vila do Torrão occurrence, a weak low-intensity magnetic anomaly was identified; however, no significant structure was delineated by the Euler Deconvolution in this sector. The high-intensity magnetic anomalies follow the same pattern observed in Profile E–E', and are likely related to the basement.

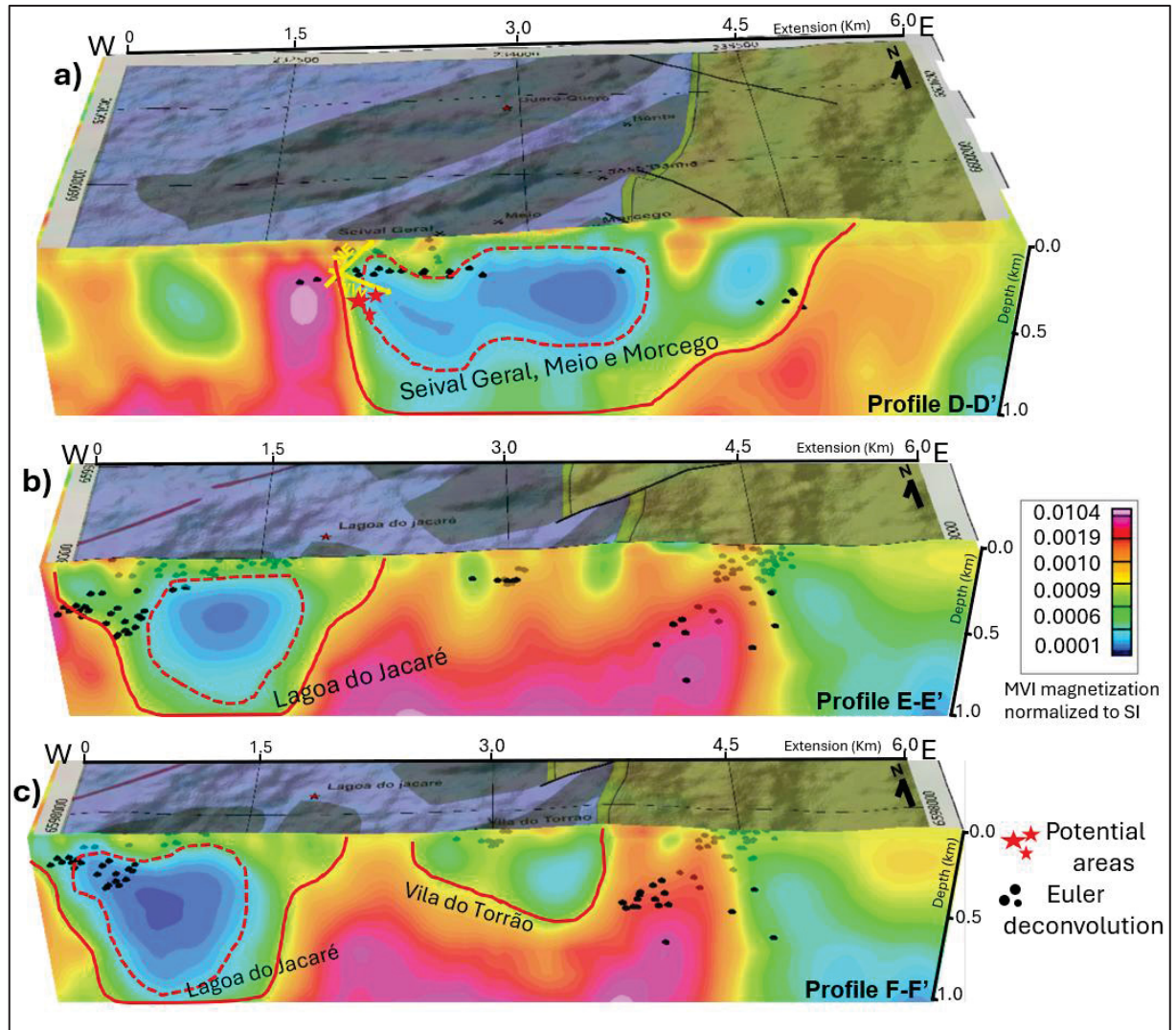


FIGURE 11 - Lithogeophysical profiles D–D' (a), E–E' (b), and F–F' (c) with magnetic inversion and Euler deconvolution, overlaid on the local geological map.

The integrated analysis of the six lithogeophysical profiles enabled the identification of significant patterns in the magnetic signature of the study area, highlighting two main behaviors:

i) Continuity of low-intensity magnetic signatures:

Low-intensity magnetic signatures predominantly occur near the surface and exhibit well-defined structural control, with a preferential SW–NE orientation, as evidenced by Euler Deconvolution. These bodies are robust both laterally and in depth and appear interconnected in the subsurface. Furthermore, the presence of hydrothermal alteration and disseminated mineralization—observed in currently

inactive mines—reinforces the significance of these zones as potential targets for mineral exploration.

#### ii) Continuity of high-intensity magnetic signatures:

High-intensity magnetic zones are generally located adjacent to low-intensity areas, which may indicate a mineralogical transition zone within a context involving regions with altered physical properties (due to hydrothermal alteration) and more preserved zones. These anomalies exhibit structural control, also evidenced by Euler Deconvolution, and do not outcrop at the surface, suggesting a possible association with mineralized zones containing preserved stockwork-type structures. A continuity of these signatures is observed along profiles A–A', B–B', and C–C', also showing a preferential SW–NE orientation. Additionally, the anomalous highs identified in profiles E–E' and F–F' were interpreted as corresponding to the basement.

Based on these results, future exploratory investigations should focus on three main aspects: (i) the zone of low magnetic intensity associated with hydrothermal alteration; (ii) structural control, with emphasis on delineating the preferential orientations of the structures; and (iii) the high-intensity magnetic zone, aiming to characterize the lithotypes associated with the identified magnetic bodies. It is noteworthy that the analyzed lithogeophysical profiles indicate areas that combine these characteristics, which are considered priority targets for further investigation. These elements are essential for enhancing the geological understanding of the area and for defining strategic targets in mineral exploration programs.

#### 4.3.5 Conclusions

In this study, the application of filters and enhancement techniques to magnetic data played a fundamental role in the interpretation and definition of discontinuities associated with structural geology, as well as in the characterization of mineralized bodies in the study area. These approaches allowed for improved distinction between different geological units, revealed structural features, and refined the identification of prospective targets, significantly contributing to the reduction of uncertainties and the construction of a more precise and reliable geological model.

Although conventional filters, such as the tilt derivative and the Analytic Signal Amplitude (ASA), were useful for identifying some superficial features, they did not add

significant information for a more in-depth analysis. In contrast, the application of Euler Deconvolution combined with magnetic data inversion demonstrated more robust results directly associated with known geological structures and lithological contacts.

These techniques enabled a more precise identification and characterization of magnetic and structural signatures associated with the main mines and mineral occurrences in the region, such as the Barite Mine, Quero-Quero Occurrence, Seival Geral Mine, and Lagoa do Jacaré occurrence. The detailed analysis made it possible to correlate magnetic signatures with the underlying geological structures, providing a deeper understanding of the distribution of mineralized bodies.

Furthermore, it was possible to understand the continuities of the magnetic bodies in the subsurface, both in depth and laterally. This information is important for mapping and modeling mineral deposits, allowing estimates of their dimensions and the identification of connections between different mineralized areas.

Another relevant point was the evidence of preferential structural patterns, mainly in the NE and NW directions. These directions were recognized as important controllers of mineralization in the region, suggesting that structural systems play a significant role in controlling the location and extent of mineral deposits.

Finally, the analyses allowed the delimitation of potential mineralization areas, gathering essential characteristics for understanding the mineral system. Zones with favorable structural context, evidenced by the Euler Deconvolution results, were considered associated with the presence of magnetic lows near the surface, indicating hydrothermal alteration, disseminated mineralization, and distal portions of the mineral system. Additionally, a transition to magnetic highs at greater depths was observed, suggesting a high likelihood of corresponding to a proximal zone, better preserved in the mineralized system, which may be related to a higher concentration of sulfides in structures such as stockwork types.

The results reinforce the relevance of integrating advanced geophysical techniques, such as Euler Deconvolution and data inversion, with prior geological information. This approach not only improves data interpretation but also provides a solid basis for future mineral exploration campaigns, highlighting priority targets for detailed investigation.

## 5 CONSIDERAÇÕES FINAIS

Os resultados obtidos ao longo deste trabalho, desde a seleção das áreas potenciais até o detalhamento das assinaturas geofísicas, culminaram na elaboração de dois artigos científicos. Esses artigos demonstram a relevância de uma análise minuciosa de estudos prévios e da integração de dados geológicos e geofísicos preexistentes. A utilização de informações públicas, previamente publicadas, permitiu estabelecer uma sistemática eficiente para análise integrada, contribuindo significativamente para a assertividade na seleção de áreas promissoras para futuras pesquisas minerais e, consequentemente, para a redução de custos na prospecção mineral.

O primeiro artigo teve como foco a caracterização das assinaturas geofísicas em áreas com ocorrências cupríferas hospedadas em rochas ultramáficas no ESRG. A abordagem incluiu a análise de dados gamaespectrométricos, mapas de primeira derivada vertical e inversões de dados aeromagnetométricos, todos integrados a dados pré-existentes de ocorrências minerais, geoquímica de solos e sedimentos de corrente.

Já o segundo artigo concentrou-se na caracterização das assinaturas geofísicas de ocorrências cupríferas associadas a rochas vulcânicas da mesma região. Neste estudo, foram utilizados mapas geofísicos como amplitude do sinal analítico, *tilt derivative* e mapas ternários RGB (gamaespectrometria), além de técnicas avançadas, como Deconvolução de Euler e inversões magnetométricas, com o objetivo de compreender a continuidade das estruturas e dos corpos mineralizados em subsuperfície.

De forma inédita, este trabalho apresenta a caracterização das assinaturas geofísicas dos principais litotipos do ESRG associados a mineralizações cupríferas com maior potencial. Até então, os estudos na região focavam prioritariamente na caracterização estrutural, hidrotermal ou mineralógica, sem aprofundar a análise integrada com foco em prospecção mineral.

Em ambos os artigos, foram produzidas interpretações litogeofísicas que propõem uma sistemática para orientar trabalhos de prospecção, baseando-se na leitura de mapas geofísicos correlacionados com o conhecimento geológico prévio dos sistemas minerais. Essa abordagem demonstrou que em extensas províncias mineralógicas, o primeiro passo fundamental para o sucesso de uma pesquisa mineral está na

identificação das áreas com maior probabilidade de concentrar mineralizações significativas.

A geofísica, portanto, é essencial nesse processo, desde que interpretada com o devido critério, considerando que as anomalias detectadas refletem contrastes físicos e não necessariamente mineralizações. É fundamental compreender quais propriedades estão em contraste e como esses dados se relacionam com o contexto geológico local.

Diante dos resultados alcançados, ressalta-se a importância de continuar investindo na aplicação de técnicas de inversão geofísica e na integração de dados multidisciplinares para aprimorar a caracterização de sistemas mineralizados. Futuras pesquisas devem incorporar análises geoquímicas mais detalhadas e investigações geológicas complementares em campo para validar as áreas-alvo e aprofundar o entendimento dos mecanismos de formação dos corpos mineralizados.

Assim, este trabalho não apenas contribui para o avanço do conhecimento geológico da região estudada, como também estabelece uma base metodológica sólida para orientar futuras iniciativas de exploração mineral.

## REFERÊNCIAS

- AITKEN, A. R.; OCCHIPINTI, S. A.; LINDSAY, M. D.; TRENCH, A. **A role for data richness mapping in exploration decision making.** *Ore Geology Reviews*, v. 99, p. 398–410, 2018.
- ALHUMIMIDI, M. S.; ABOUD, E.; ALQAHTANI, F.; AL-BATTAHIEN, A.; SAUD, R.; ALQAHTANI, H. H.; ALJUHANI, N.; ALYOUSIF, M. M.; ALYOUSEF, K. A. **Gamma-ray spectrometric survey for mineral exploration at Baljurashi area, Saudi Arabia.** *Journal of Radiation Research and Applied Sciences*, v. 14, p. 82–90, 2021.
- ALMEIDA, D. del P. M. de; ZERFASS, H.; BASEI, M. A. S.; PETRY, K.; GOMES, C. H. **The Acampamento Velho Formation, a lower Cambrian bimodal volcanic package: geochemical and stratigraphic studies from the Cerro do Bugio, Perau and Serra de Santa Bárbara (Caçapava do Sul, Rio Grande do Sul, RS, Brazil).** *Gondwana Research*, Amsterdam, v. 5, n. 3, p. 721-733, 2002. DOI: [http://doi.org/10.1016/S1342-937X\(05\)70640-7](http://doi.org/10.1016/S1342-937X(05)70640-7).
- ALMEIDA, D. P. M.; CHEMALE JR., F.; MACHADO, A. **Late to post-orogenic Brasiliano-Pan-African volcano-sedimentary basins in the Dom Feliciano Belt, southernmost Brazil.** In: AL-JUBOURY, A. I. (Ed.). *Petrology – New Perspectives and Applications*. 2012. p. 73–135. DOI: 10.5772/25189.
- ALMEIDA, F.F.M. **Diferenciação tectônica da Plataforma Brasileira.** In: SBG, Congresso Brasileiro de Geologia, 23, Salvador. BA. *Anais...* v.I, p. 29-46. 1969.
- ALMEIDA, F. F. M.; HASUI, Y.; BRITO NEVES, B. B.; FUCK, R. A. **Brazilian structural provinces: An introduction.** *Earth Science Reviews*, v. 17, p. 1–29, 1981.
- ALMEIDA, F. F. M. de; HASUI, Y.; BRITO-NEVES, B. B. de; FUCK, R. A. **Províncias estruturais brasileiras.** In: SIMPÓSIO DA GEOLOGIA DO NORDESTE, 8., 1977, Campina Grande, PB. *Atas [...]*. Campina Grande, PB: SBG, 1977. p. 363-391.
- ALMEIDA, I. **Geologia da jazida de mármore de Palma, município de São Gabriel, Rio Grande do Sul.** In: CONGRESSO BRASILEIRO DE GEOLOGIA, 1970. *Anais...* 1970. p. 138. Disponível em: [https://www.sbg.org.br/anais\\_digitalizados/1970-BRASILIA/CBG1970.pdf](https://www.sbg.org.br/anais_digitalizados/1970-BRASILIA/CBG1970.pdf). Acesso em: 15 fev. 2024.
- ANDERSON, E. D.; YAGER, D. B.; DESZCZ-PAN, M.; HOOGENBOOM, B. E.; RODRIGUEZ, B. D.; SMITH, B. D. **Geophysical data provide three-dimensional insights into porphyry copper systems in the Silverton caldera, Colorado, USA.** *Ore Geology Reviews*, v. 152, 2023. DOI: <https://doi.org/10.1016/j.oregeorev.2022.105223>.
- ASF DAAC - ALASKA SATELLITE FACILITY DISTRIBUTED ACTIVE ARCHIVE CENTER. **ALOS\_PALSAR\_Radiometric\_Terrain\_Corrected\_high\_res;** Inclui material © JAXA/METI 2011. 2019. Disponível em: <https://www.asf.alaska.edu>. Acesso em: 11 mar. 2019. DOI: 10.5067/Z97HFCNKR6VA.

ATCHUTA RAO, D.; RAM BABU, H. V.; SANKER NARAYAN, P. V. **Interpretation of magnetic anomalies due to dikes: The complex gradient method.** *Geophysics*, v. 46, p. 1572–1578, 1981. DOI: <https://doi.org/10.1190/1.1441164>

ATTWOOD, J. **Especialistas alertam para possível crise de cobre que frearia a economia global.** *Blog Bloomberg Linea Brasil*, 2022. Disponível em: <https://www.bloomberglinea.com.br/2022/09/25/especialistas-alertam-para-possivel-crise-de-cobre-que-frearia-a-economia-global/>. Acesso em: 19 set. 2023.

BAARS, F. J.; MATOS, G. M.; ABRAM, M. B. **Metalogenia Quantitativa do Brasil: Base do Conhecimento, Métodos e Exemplos.** In: **Geologia, Tectônica e Recursos Minerais do Brasil: Texto, Mapas & SIG.** Brasília: CPRM, 2003. p. 449-499.

BABINSKI, M.; CHEMALE, F.; HARTMANN, L. A.; VAN SCHMUS, W. R.; DA SILVA, L. C. **Juvenile accretion at 750–700 Ma in southern Brazil.** *Geology*, v. 24, p. 439–442, 1996.

BADI, W. R. S. **Mineralização de chumbo e zinco em arenitos do Distrito de Camaquã, RS.** 1983. 154 f. Dissertação (Mestrado em Geociências) – Universidade Federal do Rio Grande do Sul, Porto Alegre, 1983.

BADI, W. S. R.; GONZALEZ, A. P. **Jazida de metais básicos de Santa Maria, Caçapava do Sul, RGS.** In: DEPARTAMENTO NACIONAL DE PRODUÇÃO MINERAL (Ed.). *Principais depósitos minerais do Brasil*. v. 3: Metais básicos não ferrosos e Al. Brasília, 1988. p. 157-170.

BARANOV, V. **A new method for interpretation of aeromagnetic maps: pseudo-gravimetric anomalies.** *Geophysics*, v. 22, n. 2, p. 359–383, 1957. Disponível em: <https://pubs.geoscienceworld.org/seg/geophysics/article/22/2/359/67330/A-new-method-for-interpretation-of-aeromagnetic>. Acesso em: 5 jan. 2025.

BARBOSA, V. C. F.; MEDEIROS, W. E.; SILVA, J. B. C. **Making Euler deconvolution applicable to small ground magnetic surveys.** *Journal of Applied Geophysics*, v. 43, p. 55–68, 2000. DOI: [https://doi.org/10.1016/S0926-9851\(99\)00047-6](https://doi.org/10.1016/S0926-9851(99)00047-6).

BARBOSA, V. C. F.; MEDEIROS, W. E.; SILVA, J. B. C. **Stability analysis and improvement of structural index estimation in Euler deconvolution.** *Geophysics*, v. 64, p. 48–60, 1999. DOI: <https://doi.org/10.1190/1.1444529>.

BARBOSA, V. C. F.; SILVA, J. B. C. **Deconvolução de Euler: passado, presente e futuro – um tutorial.** *Revista Brasileira de Geofísica*, v. 23, n. 3, p. 243-250, 2005. DOI: <https://doi.org/10.1590/S0102-261X2005000300004>.

BICCA, M. M.; CHEMALE JÚNIOR, F.; JELINEK, A. R.; OLIVEIRA, C. H. E. de; GUADAGNIN, F.; ARMSTRONG, R. **Tectonic evolution and provenance of Santa Bárbara Group, Camaquã Mines region, Rio Grande do Sul, Brazil.** *Journal of South American Earth Sciences*, Amsterdam, v. 48, p. 173-192, 2013. DOI: <http://doi.org/10.1016/j.jsames.2013.09.006>.

BIONDI, J. C.; BARTOSZECK, M. K.; VANZELA, A. G. **Análise da favorabilidade para depósitos de caulim na bacia de Campo Alegre (SC).** *Revista Brasileira de Geociências*, v. 31, n. 1, p. 59-66, 2001. Disponível em: <https://ppegeo.igc.usp.br/portal/wp-content/uploads/tainacan-items/15906/43813/10445-12452-1-SM.pdf>. Acesso em: 11 abr. 2023.

BLAKELY, R. J. **Potential Theory in Gravity and Magnetic Applications.** Cambridge: Cambridge University Press, 1995. Disponível em: <https://doi.org/10.1017/CBO9780511549816>. Acesso em: 08 set. 2024.

BOCCI, P.; RIBEIRO, M. J. **Mapeamento Preliminar Geológico da Área n.5 da Quadrícula Arroio São Sepé.** Dissertação (Mestrado) – Universidade Federal do Rio Grande do Sul, Porto Alegre, 1963.

BONGIOLI, E. M.; PATRIER-MAS, P.; MEXIAS, A. S.; BEAUFORT, D.; FORMOSO, M. L. L. **Spatial and temporal evolution of hydrothermal alteration at Lavras do Sul, Brazil: evidence from dioctahedral clay minerals.** *Clays and Clay Minerals*, v. 56, p. 222–243, 2008. DOI: 10.1346/CCMN.2008.0560207.

BORBA, A. W.; MIZUSAKI, A. M. P. **Santa Bárbara Formation (Caçapava do Sul, southern Brazil): depositional sequences and evolution of an Early Paleozoic postcollisional basin.** *Journal of South American Earth Sciences*, Amsterdam, v. 16, p. 365-380, 2003. DOI: [https://doi.org/10.1016/S0895-9811\(03\)00102-0](https://doi.org/10.1016/S0895-9811(03)00102-0)

BREUSTEDT, B.; HÖCK, V.; WIEDENBECK, M. **Geophysical and geochemical exploration for copper in the Central African Copperbelt.** *Economic Geology*, v. 106, p. 693–716, 2011.

CAMOZZATO, E.; TONILO, J. A.; LAUX, J. H. **Metalogênese do Cinturão Dom Feliciano e Fragmentos Paleocontinentais associados (RS/SC).** In: SILVA, M. G. et al. **Metalogênese das províncias tectônicas brasileiras.** 2014. p. 517-556.

CARRINO, T. A.; SOUZA FILHO, C. R. de; LEITE, E. P. **Avaliação do uso de dados aerogeofísicos para mapeamento geológico e prospecção mineral em terrenos intemperizados: o exemplo de Serra Leste, província mineral de Carajás.** *Revista Brasileira de Geofísica*, v. 25, n. 3, p. 307-320, 2007. DOI: <https://doi.org/10.1590/S0102-261X2007000300007>.

CHEMALE JR., F. **Evolução geológica do Escudo Sul-Rio-Grandense.** In: HOLZ, M.; DE ROS, L. F. (Eds.). **Geologia do Rio Grande do Sul.** 2000. p. 13–52.

CLARK, D. A. **Magnetic Petrophysics and Magnetic Petrology; Aids to Geological Interpretation of Magnetic Surveys.** AGSO *Journal of Australian Geology and Geophysics*, v. 17, p. 83-103, 1997. Disponível em: <https://www.scirp.org/reference/ReferencesPapers?ReferenceID=2144451>. Acesso em: 03 ago. 2024.

CLEMENT, W. G. **Basic principles of two-dimensional digital filtering.** *Geophysics*, v. 21, p. 125–145, 1973.

COMPANHIA BRASILEIRA DE COBRE - CBC. **Relatório de reavaliação na área do decreto nº. 70.926 (DNPM 7566/64), Cerro dos Martins, município de Caçapava do Sul.** Porto Alegre, 1978. 2 v.

COSTA, I. S. L. **Desafios e oportunidades da geofísica na descoberta de recursos minerais no Brasil.** *Boletim SBGf*, v. 130, p. 22–24, 2024. Disponível em: [https://sbgf.org.br/boletim/reader/boletim\\_130/](https://sbgf.org.br/boletim/reader/boletim_130/). Acesso em: 16 abr. 2024.

COTIS, D. S.; MANTOVANI, M. S. M.; RIBEIRO, V. B.; SANTOS, R. P. Z. **Geophysical characterization of magnetic anomaly Jauru River (Mato Grosso, Brazil).** In: INTERNATIONAL CONGRESS OF THE BRAZILIAN GEOPHYSICAL SOCIETY, 13., 2013, Rio de Janeiro. *Anais [...]*. Rio de Janeiro: SBGf, 2013. Disponível em: [https://sbgf.org.br/mysbgf/eventos/expanded\\_abstracts/13th\\_CISBGf/Geophysical%20Characterization%20of%20Magnetic%20Anomaly%20Rio%20Jauru%20\(Mato%20Grosso,%20Brazil\).pdf](https://sbgf.org.br/mysbgf/eventos/expanded_abstracts/13th_CISBGf/Geophysical%20Characterization%20of%20Magnetic%20Anomaly%20Rio%20Jauru%20(Mato%20Grosso,%20Brazil).pdf). Acesso em: 11 abr. 2023.

COX, K. G.; BELL, J. D.; PANKHURST, R. J. **The interpretation of igneous rocks.** Londres: George Allen & Unwin, 1979. 450 p. DOI: <http://dx.doi.org/10.1007/978-94-017-3373-1>.

CPRM – COMPANHIA DE PESQUISA DE RECURSOS MINERAIS. **Mapa e arquivos vetoriais de associações tectônicas e recursos minerais Escudo Sul-Rio-Grandense.** Escala 1:500.000, 2021. Disponível em: <https://geosgb.sgb.gov.br/downloads/>. Acesso em: 20 fev. 2024.

CPRM – COMPANHIA DE PESQUISA DE RECURSOS MINERAIS. **Projeto Aerogeofísico Escudo do Rio Grande do Sul – Dados em XYZ e Relatório Final do Levantamento e Processamento dos Dados Magnetométricos e Gamaespectrométricos.** 2010. Disponível em: <https://geosgb.sgb.gov.br/downloads/>. Acesso em: 24 fev. 2024.

DAVIES, R. S.; DAVIES, M. J.; GROVES, D.; DAVIDS, K.; BRYMER, E.; TRENCH, A.; SYKES, J. P.; DENTITH, M. **Learning and Expertise in Mineral Exploration Decision-Making: An Ecological Dynamics Perspective.** *International Journal of Environmental Research and Public Health*, v. 18, p. 9752, 2021. DOI: <https://doi.org/10.3390/ijerph18189752>.

DAVIES, R. S.; GROVES, D. I.; TRENCH, A.; DENTITH, M. **Towards producing mineral resource-potential maps within a mineral systems framework, with emphasis on Australian orogenic gold systems.** *Ore Geology Reviews*, v. 94, p. 326–350, 2020.

DEAN, W. C. **Frequency analysis for gravity and magnetic interpretation.** *Geophysics*, v. 23, p. 97–127, 1958.

DEBEGLIA, N.; CORPEL, J. **Automatic 3-D interpretation of potential field data using analytic signal derivatives.** *Geophysics*, v. 6, p. 87–96, 1997. DOI: <https://doi.org/10.1190/1.1444149>

- DENTITH, M. C.; MUDGE, S. **Geophysics for the Mineral Exploration Geoscientist**. Cambridge: Cambridge University Press, 2014. 454 p. ISBN-10: 0521809517, ISBN-13: 978-0521809511.
- DICKIN, A. D. **Radiogenic isotope geology**. Cambridge: Cambridge University Press, 1995. 490 p.
- DICKSON, B. L.; SCOTT, K. M. **Interpretation of aerial gamma-ray surveys – Adding the geochemical factors**. *AGSO Journal of Australian Geology & Geophysics*, v. 17, p. 187–200, 1997.
- DILLES, J. H.; EINAUDI, M. T. **Wall-rock alteration and hydrothermal flow paths about the Ann Mason porphyry copper deposit, Nevada; a 6-km vertical reconstruction**. *Economic Geology Bulletin*, v. 87, p. 1963–2001, 1992. DOI: <https://doi.org/10.2113/gsecongeo.87.8.1963>.
- DJOMO, H. D.; SEZINE, E. D.; YANDJIMAIN, J. **Integration of airborne magnetic and geological data for mineral prospectivity mapping in the Ambam-Amvom rainforest area, Archean Ntem Complex, southern Cameroon**. *Scientific African*, v. 24, e02157, 2024.
- DRIEMEYER, D. **Estudo da zonação vertical da alteração hidrotermal e mineralizações associadas na área do Depósito Santa Maria-Minas do Camaquã, RS**. 2018.
- ELLIS, R. G.; WET, B.; MCLEOD, I. N. **Inversion of Magnetic Data from Remanent and Induced Sources**. *ASEG Extended Abstracts*, v. 2012, p. 1–4, 2012.
- FAIRHEAD, J. D.; BENNETT, K. J.; GORDON, D. R. H.; HUANG, D. **Euler: Beyond the “Black Box”**. In: *PROCEEDINGS OF THE 64TH ANNUAL INTERNATIONAL MEETING, SOCIETY OF EXPLORATION GEOPHYSICISTS*, 1994. *Proceedings...* 1994. p. 422-424. DOI: <https://doi.org/10.1190/1.1932113>.
- FAMBRINI, G.L. **O Grupo Santa Bárbara (Neoproterozoico III) da Bacia do Camaquã, Rio Grande do Sul**. 2003. 293 f. Tese de Doutorado, Instituto de Geociências, Universidade de São Paulo. 2003.
- FAMBRINI, G.L.; FRAGOSO-CESAR, A.R.S. **Análise estratigráfica do grupo Santa Bárbara (Ediacarano) na Sub-bacia Camaquã Oriental, RS**. *Revista Brasileira de Geociências*, v. 36 (4). p.663-678. 2006.
- FAURE, G. **Principles and applications of geochemistry**. Nova Iorque: Prentice Hall, 1997. 589 p.
- FERREIRA, F. J. F.; FRUCHTING, A.; GUIMARÃES, G. B.; ALVES, L. S.; MARTIN, V. M. O.; ULRICH, H. H. G. J. **Levantamentos gamaespectrométricos em granitos diferenciados. II: O exemplo do Granito Joaquim Murtinho, Complexo Granítico Cunhaporanga, Paraná**. *Revista do Instituto de Geociências—USP*, v. 9, p. 55–72, 2009.

**FONTANA, E. Hidrotermalismo e mineralizações das rochas vulcânicas da Mina do Seival: evolução geoquímica e isotópica ( $\delta^{34}\text{S}$ ,  $\delta^{18}\text{O}$  e  $\delta^{13}\text{C}$ ) dos fluidos e sua correlação com outros depósitos de minérios epitermais da Bacia do Camaquã – Rio Grande do Sul – Brasil.** 2016.

**FONTANA, E.; MEXIAS, A. S.; RENAC, C.; NARDI, L. V. S.; LOPES, R. W.; GOMES, M. E. B.; BARATS, A.** *Hydrothermal alteration of volcanic rocks in Seival Mine Cu-mineralization – Camaquã Basin – Brazil (Part I): Chloritization process and geochemical dispersion in alteration halos.* *Journal of Geochemical Exploration*, v. 177, p. 45–60, 2017. DOI: <https://doi.org/10.1016/j.gexplo.2017.02.004>.

**FORD, K.; KEATING, P.; THOMAS, M. D.** *Overview of geophysical signatures associated with Canadian ore deposits.* In: GEOLOGICAL ASSOCIATION OF CANADA, MINERAL DEPOSITS DIVISION, SPECIAL PUBLICATION, 2007, St. John's, NL, Canada. *Proceedings...* 2007. p. 939–970. Disponível em: <https://ostrnrcan-dostnrcan.canada.ca/handle/1845/181490>. Acesso em: 16 abr. 2024.

**FORNAZZARI NETO, L.; FERREIRA, F. J. F.** *Gamaespectrometria integrada a dados exploratórios multifonte em ambiente SIG aplicada à prospecção de ouro na folha Botuverá, SC.* *Revista Brasileira de Geociências*, v. 33, n. 2 (Suplemento), p. 197-208, 2003. Disponível em: <https://geologia.ufpr.br/wp-content/uploads/2017/08/gamaespectometria7.pdf>. Acesso em: 20 abr. 2024.

**GARCIA, M. A. M.** *Petrologia do Complexo Palma, Rio Grande do Sul.* 1980. 133 f. Dissertação (Mestrado) – Curso de Pós-Graduação em Geociências, Universidade Federal do Rio Grande do Sul, Porto Alegre, 1980.

**GASTAL, M. C.; FERREIRA, F. J. F.; CUNHA, J. U.; ESMERIS, C.; KOESTER, E.; RAPOSO, M. I. B.; ROSSETTI, M. M. M.** *Alojamento do granito Lavras e a mineralização aurífera durante evolução de centro vulcão-plutônico pós-colisional, oeste do Escudo Sul-riograndense: dados geofísicos e estruturais.* *Brazilian Journal of Geology*, v. 45, n. 2, p. 217-241, jun. 2015. DOI: 10.1590/23174889201500020004.

**GASTAL, M. C.; LAFON, J. M.; FERREIRA, F. J. F.; MAGRO, F. U. S.; REMUS, M. V. D.; SOMMER, C. A.** *Reinterpretação do Complexo Intrusivo Lavras do Sul – RS, de acordo com os sistemas vulcão-plutônicos de subsidência. Parte I: geologia, geofísica e geocronologia ( $207\text{Pb}/206\text{Pb}$  e  $206\text{Pb}/238\text{U}$ ).* *Revista Brasileira de Geologia*, v. 36, p. 109–124, 2006. DOI: 10.25249/0375-7536.2006361109124.

**GOOGLE. Google Satellite.** Disponível em: <https://www.google.com/maps>. Acesso em: 08 janeiro. 2025.

**GUILLEN, A.; COURRIOUX, G.; CALCAGNO, P.; FITZGERALD, D.; LEES, T.; HANSEN, R. O.; SUCIU, L.** *Multiple-source Euler deconvolution.* *Geophysics*, v. 67, p. 525–535, 2002. DOI: <https://doi.org/10.1190/1.1468613>.

HANSEN, R. O.; SUCIU, L. **Multiple-source Euler deconvolution.** *Geophysics*, v. 67, n. 2, p. 525–535, 2002. Disponível em: <https://doi.org/10.1190/1.1468613>. Acesso em: 6 May. 2025.

HARTMANN, L. A.; CHEMALE, F.; PHILIPP, R. P. **Evolução geotectônica do Rio Grande do Sul no Pré-Cambriano.** In: IANNUZZI, R.; FRANTZ, J. C. (Eds.). **50 Anos de Geologia: Instituto de Geociências.** Paulista: Editora Comunicação e Identidade, 2007. p. 97–123. Disponível em: <http://multimidia.ufrgs.br/conteudo/bibgeo/repositorio/memorial/1998-2007/50anoscontribuicoes/50%20anos%20contribuicoes.pdf>. Acesso em: 12 nov. 2023.

HARTMANN, L. A.; LEITE, J. A. D.; DA SILVA, L. C.; REMUS, M. V. D.; MCNAUGHTON, N. J.; GROVES, D. I.; FLETCHER, I. R.; SANTOS, J. O. S.; VASCONCELLOS, M. A. Z. **Advances in SHRIMP geochronology and their impact on understanding the tectonic and metallogenic evolution of southern Brazil.** *Australian Journal of Earth Sciences*, v. 47, p. 829–844, 2000.

HARTMANN, L.A.; PHILIPP, R.P.; LIU, D.; WANG, L.; SANTOS, J.O.S.; VASCONCELLOS, M.A.Z. Paleoproterozoic magmatic provenance of detrital zircons, Porongos Complex quartzites, southern Brazilian shield. **International Geology Review**, v. 46. p. 127-157. 2004.

HARTMANN, L. A.; PHILIPP, R. P.; SANTOS, J. O. S.; MCNAUGHTON, N. J. **Time frame of 753–680 Ma juvenile accretion during the São Gabriel orogeny, southern Brazil.** *Gondwana Research*, v. 19, p. 84–99, 2011. DOI: <https://doi.org/10.1016/j.gr.2010.05.001>.

HARTMANN, L.; NARDI, L.; FORMOSO, M.; REMUS, M.; DE LIMA, E.; MEXIAS, A. **Magmatism and metallogeny in the crustal evolution of Rio Grande do Sul shield, Brazil.** *Pesquisas*, v. 26, p. 45–63, 1999.

HARTMANN, R. R.; TESKEY, D. J.; FRIEDBERG, J. L. **A system for rapid digital aeromagnetic interpretation.** *Geophysics*, v. 36, p. 891–918, 1971. Disponível em: <https://pubs.geoscienceworld.org/seg/seggeophysics/article-pdf/36/5/891/3155728/891.pdf>. Acesso em: 1 jul. 2025.

HASUI, Y.; CARNEIRO, C. D. R.; COIMBRA, A. M. **The Ribeira Folded Belt.** *Revista Brasileira de Geociências*, v. 5, p. 257-266, 1975.

HEGAB, M. A. E. R.; SALEM, S. M. **Mineral-bearing alteration zones at Gebel Monqul area, North Eastern Desert, Egypt, using remote sensing and gamma-ray spectrometry data.** *Arabian Journal of Geosciences*, v. 14, p. 1869, 2021.

HINZE, W. J.; VON FRESE, R. R. B.; SAAD, A. H. **Gravity and Magnetic Exploration: Principles, Practices, and Applications.** New York: Cambridge University Press, 2013. 512 p. ISBN 978-0-521-87101-3.

HRONSKY, J. M. A.; GROVES, D. I. **Science of targeting: Definition, strategies, targeting and performance measurement.** *Australian Journal of Earth Sciences*, v. 55, p. 3–12, 2008. DOI: <https://doi.org/10.1080/08120090701581356>

HSU, S. K.; SIBUET, J. C.; SHYU, C. T. **High-resolution detection of geologic boundaries from potential anomalies: An enhanced analytic signal technique.** *Geophysics*, v. 61, p. 373-386, 1996. DOI: [10.1190/1.1443966](https://doi.org/10.1190/1.1443966).

HSU, S. K.; COPPENS, D.; SHYU, C. T. **Depth to magnetic source using the generalized analytic signal.** *Geophysics*, v. 63, p. 1947-1957, 1998. DOI: <https://doi.org/10.1190/1.1444488>

IAEA – INTERNATIONAL ATOMIC ENERGY AGENCY. **Airborne gamma ray spectrometer surveying.** Vienna: IAEA, 1991. (Technical Reports Series, n. 323).

IGLESIAS, C. M. F. **Análise integrada de dados geológicos e estruturais para a prospecção de ouro na região de Torquato Severo (RS).** 2000. 101 f. Dissertação (Mestrado em Engenharia) – Universidade Federal do Rio Grande do Sul, Porto Alegre, 2000. Disponível em: <https://rigeo.sgb.gov.br/handle/doc/212>. Acesso em: 24 abr. 2024.

JANIKIAN L. **Sequências deposicionais e evolução paleoambiental do Grupo Bom Jardim e da Formação Acampamento Velho, Supergrupo Camaquã, Rio Grande do Sul.** 2004. 189 f. Tese de Doutorado, Instituto de Geociências, Universidade Federal do Rio Grande do Sul. Porto Alegre. 2004.

JANIKIAN, L.; ALMEIDA, R. P.; FRAGOSO-CESAR, A. R. S.; FAMBRINI, G. L. **Redefinição do Grupo Bom Jardim (Neoproterozoico III) em sua área-tipo: Litoestratigrafia, evolução paleoambiental e contexto tectônico.** *Revista Brasileira de Geociências*, p. 347-360, 2003.

JANIKIAN, L.; ALMEIDA, R. P.; TRINDADE, R. I. F.; FRAGOSO-CESAR, A. R. S.; D'AGRELLA-FILHO, M. S.; DANTAS, E. L.; TOHVER, E. **The continental record of Ediacaran volcano-sedimentary successions in southern Brazil and their global implications.** *Terra Nova*, v. 20, p. 259–266, 2008. DOI: <https://doi.org/10.1111/j.1365-3121.2008.00814.x>.

KEAREY, P.; BROOKS, M.; HILL, I. **Geofísica de Exploração.** São Paulo: Oficina de Textos, 2009. 438 p. ISBN: 978-85-86238-91-8.

KLEIN, G. **A naturalistic decision making perspective on studying intuitive decision making.** *Journal of Applied Research in Memory and Cognition*, v. 4, p. 164–168, 2015.

KONOPÁSEK, J.; KOSLER, J.; TAJCMAŇOVÁ, L.; ULRICH, S.; KITT, S. L. **Neoproterozoic igneous complex emplaced along major tectonic boundary in the Kaoko Belt (NW Namibia): ion probe and LA ICP-MS dating of magmatic and metamorphic zircons.** *Journal of the Geological Society, London*, v. 165, p. 153–165, 2008.

KRÖNER, S.; KONOPÁSEK, J.; KRÖNER, A.; PASSCHIER, C. W.; POLLER, U.; WINGATE, M. T. D.; HOFFMANN, K. H. **U-Pb and Pb-Pb zircon ages for metamorphic rocks in the Kaoko Belt of Northwestern Namibia: a Palaeo- to**

**Mesoproterozoic basement reworked during the Pan-African orogeny.** South African Journal of Geology, v. 107, p. 455–476, 2004.

LAUX, J. H. **Escudo Sul-Rio-Grandense, estado do Rio Grande do Sul.** Brasília: CPRM. 2021. Escala 1:500.000 Programa Geologia, Mineração e Transformação Mineral: Levantamentos geológicos e de potencial mineral de novas fronteiras. Disponível em: <https://rigeo.sgb.gov.br/jspui/handle/doc/20521>. Acesso em: 05 abril de 2025.

LAUX, J. H. **Geologia e recursos minerais da folha Lagoa da Meia Lua, SH. 21-ZB-VI: estado do Rio Grande do Sul.** CPRM, 2017. 255 p.

LAUX, J. H.; LINDENMAYER, Z. G. **As minas do Camaquã: um século de evolução de hipóteses genéticas.** In: RONCHI, L. H.; LOBATO, A. O. C. (Coord.). *Minas do Camaquã: um estudo multidisciplinar*. São Leopoldo: UNISINOS, 2000. p. 133-164.

LEITE, J. A. D.; HARTMANN, L. A.; FERNANDES, L. A. D.; McNAUGHTON, N. J.; SOLIANI, E. A. JR.; KOESTER, E.; SANTOS, J. O. S.; VASCONCELLOS, M. A. Z. **Zircon U-Pb SHRIMP dating of gneissic basement of the Dom Feliciano Belt, southernmost Brazil.** Journal of South American Earth Sciences, v. 13, p. 739–750, 2000.

LEITE, J. A. D.; HARTMANN, L. A.; MCNAUGHTON, N. J.; CHEMALE JR., F. **SHRIMP U/Pb zircon geochronology of Neoproterozoic juvenile and crustal reworked terranes in southernmost Brazil.** International Geology Review, v. 40, p. 688–705, 1998. DOI: 10.1080/00206819809465232.

LELIÈVRE, P. G.; OLDENBURG, D. W. **A 3D total magnetization inversion applicable when significant, complicated remanence is present.** Geophysics, v. 74, n. 3, p. L21–L30, 2009. DOI: <https://doi.org/10.1190/1.3103249>.

LEÃO-SANTOS, M.; MORAES, R.; LI, Y.; RAPOSO, M. I.; ZUO, B. **Hydrothermal Alteration Zones' Magnetic Susceptibility Footprints and 3D Model of Iron Oxide-Copper-Gold (IOCG) Mineralization, Carajás Mineral Province, Brazil.** Minerals, v. 12, p. 1581, 2022. DOI: <https://doi.org/10.3390/min12121581>.

LI, Y.; OLDENBURG, D. W. **3-D inversion of magnetic data.** Geophysics, v. 61, n. 2, p. 394-408, 1996. DOI: <https://doi.org/10.1190/1.1443968>.

LI, Y.; SHEARER, S. E.; HANEY, M. M.; DANNEMILLER, N. **Comprehensive approaches to 3D inversion of magnetic data affected by remanent magnetization.** Geophysics, v. 75, p. L1–L11, 2010.

LIMA, J. M. **Geologia e Mineração no Rio Grande do Sul: Um estudo histórico sobre a Mina Seival e suas contribuições econômicas.** Porto Alegre: Editora UFRGS, 2009.

LIMA, E. F.; NARDI, L. V. S. **The Lavras do Sul Shoshonitic Association: implications for the origin and evolution of Neoproterozoic shoshonitic**

**magmatism in southernmost Brazil.** *Journal of South American Earth Sciences*, v. 11, n. 1, p. 67–77, jan. 1998. Disponível em: [https://doi.org/10.1016/S0895-9811\(97\)00037-0](https://doi.org/10.1016/S0895-9811(97)00037-0). Acesso em: 16 jun. 2025.

LOPES, R. W. **Alteração hidrotermal e mineralização de cobre na Mina do Seival, Bacia do Camaquã, RS.** 2011. 91 f. Trabalho de Conclusão de Curso (Graduação em Geologia) – Universidade Federal do Rio Grande do Sul, Porto Alegre, 2011.

LOPES, R. W. **Caracterização petrográfica e geoquímica da Mina do Seival, Bacia do Camaquã, RS.** 2013. 75 f. Dissertação (Mestrado em Geociências) – Universidade Federal do Rio Grande do Sul, Porto Alegre, 2013.

LOPES, R. W.; FONTANA, E.; MEXIAS, A. S.; GOMES, M. E. B.; NARDI, L. V. S.; RENAC, C. **Caracterização petrográfica e geoquímica da sequência magmática da Mina do Seival, Formação Hilário (Bacia do Camaquã – Neoproterozoico), Rio Grande do Sul, Brasil.** *Pesquisa em Geociências*, v. 41, p. 51–64, 2014.

LOPES, R. W.; MEXIAS, A. S.; PHILIPP, R. P.; BONGIOLO, E. M.; RENAC, C.; BICA, M. M.; FONTANA, E. **Au-Cu-Ag mineralization controlled by brittle structures in Lavras do Sul Mining District and Seival Mine deposits, Camaquã Basin, southern Brazil.** *Journal of South American Earth Sciences*, v. 88, p. 197–215, 2018. DOI: <https://doi.org/10.1016/j.jsames.2018.08.017>.

MACHADO, N.; KOPPE, J. C.; HARTMANN, L. A. **A late Proterozoic U-Pb age for the Bossoroca Belt, Rio Grande do Sul, Brazil.** *Journal of South American Earth Sciences*, v. 3, p. 87–90, 1990

MACLEOD, I. C.; JONES, K.; DAI, T. F. **3-D analytic signal in the interpretation of total magnetic field data at low magnetic latitudes.** *Exploration Geophysics*, v. 24, p. 679–688, 1993. DOI: <https://doi.org/10.1071/EG993679>

MARCUS, G. **Deep learning: A critical appraisal.** *arXiv*, 2018. Disponível em: <https://arxiv.org/abs/1801.00631>. Acesso em: 16 abr. 2024.

MCCUAIG, T. C.; BERESFORD, S.; HRONSKY, J. **Translating the mineral systems approach into an effective exploration targeting system.** *Ore Geology Reviews*, v. 38, p. 128–138, 2010.

MCCUAIG, T. C.; SHERLOCK, R. L. **Exploration Targeting.** In: EXPLORATION 17: SIXTH DECENNIAL INTERNATIONAL CONFERENCE ON MINERAL EXPLORATION, 2017, Perth, Austrália. *Anais...* Perth, 2017.

MERO, J. L. **Uses of the gamma-ray spectrometer in mineral exploration.** *Geophysics*, v. 25, p. 1054–1076, 1960.

MIKHAILOV, V.; GALDEANO, A.; DIAMENT, M.; GVISHIANI, A.; AGAYAN, S.; BOBOUDINOV, S.; GRAEVA, E.; SAILHAC, P. **Application of artificial intelligence for Euler solutions clustering.** *Geophysics*, v. 68, p. 168–180, 2003. DOI: <https://doi.org/10.1190/1.1543204>.

MOSTAFAEI, K.; KIANPOUR, M. **Application of Magnetometry in Manto-type Copper Deposit Exploration, Case study: Meyami, Iran.** *The Mining-Geology-Petroleum Engineering Bulletin*, p. 1-14, 2022. DOI: 10.17794/rgn.2022.5.1.

MUSHAYANDEBVU, M. F.; VAN DRIEL, P.; REID, A. B.; FAIRHEAD, J. D. **Magnetic source parameters of 2D structures using extended Euler deconvolution.** *Geophysics*, v. 66, p. 814–823, 2001.

NABIGHIAN, M. N. **Additional comments on the analytic signal of two-dimensional magnetic bodies with polygonal cross-section.** *Geophysics*, v. 39, p. 85–92, 1974. DOI: <https://doi.org/10.1190/1.1440416>

NABIGHIAN, M. N. **The analytic signal of two-dimensional magnetic bodies with polygonal cross-section. Its properties and use for automated anomaly interpretation.** *Geophysics*, v. 37, p. 507–517, 1972. DOI: <https://doi.org/10.1190/1.1440276>

NABIGHIAN, M. N. **Toward a three-dimensional automatic interpretation of potential field data via generalized Hilbert transforms—Fundamental relations.** *Geophysics*, v. 49, p. 780–786, 1984. DOI: <https://doi.org/10.1190/1.1441706>

NARDI, L. V. S. **Geochemistry and Petrology of the Lavras Granite Complex, RS, Brazil.** 1984. Tese (Doutorado em Geologia) — Department of Geology, King's College, University of London, London, 268 p.

NARDI, L.V.S.; LIMA, E.F. **A associação shoshonítica de Lavras do Sul, RS.** Revista Brasileira de Geologia. v. 15(2). p. 139-146. 1985.

NAUDY, H. **Automatic determination of depth on aeromagnetic profiles.** *Geophysics*, v. 36, p. 717–722, 1971. DOI: <https://doi.org/10.1190/1.1440207>.

NELSON, J. B. **Comparison of gradient analysis techniques for linear two-dimensional magnetic sources.** *Geophysics*, v. 53, p. 1088-1095, 1988. DOI: [10.1190/1.1442545](https://doi.org/10.1190/1.1442545).

NETTLETON, L. L. **Regionals, residuals, and structures.** *Geophysics*, v. 19, p. 1–22, 1954.

O'BRIEN, D. P. **CompuDepth – A new method for depth-to-basement calculation.** In: 42nd ANNUAL INTERNATIONAL MEETING, SOCIETY OF EXPLORATION GEOPHYSICISTS, 1972, Anaheim, California. *Proceedings...* Anaheim: SEG, 1972.

OGAH, J. A.; ABUBAKAR, F. **Solid mineral potential evaluation using integrated aeromagnetic and aeroradiometric datasets.** *Nature Scientific Reports*, v. 14, p. 1637, 2024.

OLDENBURG, D. W.; PRATT, D. A. **Geophysical Inversion for Mineral Exploration: A Decade of Progress in Theory and Practice.** In: PROCEEDINGS OF THE EXPLORATION 07: FIFTH DECENTNIAL INTERNATIONAL CONFERENCE ON MINERAL EXPLORATION, 2007, Toronto, ON, Canada. *Proceedings...* Toronto, 2007. p. 61–95.

OLIVEIRA, D. S. **Uso da geofísica no atual cenário da exploração mineral—como adicionar valor num contexto desafiador.** *Boletim SBGf*, v. 130, p. 18–21, 2024. Disponível em: [https://sbgf.org.br/boletim/reader/boletim\\_130/](https://sbgf.org.br/boletim/reader/boletim_130/). Acesso em: 16 abr. 2024.

PEDERSEN, L. B. **Relations between horizontal and vertical gradients of potential fields.** *Geophysics*, v. 54, p. 662-663, 1989. DOI: [10.1190/1.1442694](https://doi.org/10.1190/1.1442694).

PELOSI, A.P.M.R.; FRAGOSO-CESAR A.R.S. **Considerações estratigráficas e paleogeográficas do Grupo Maricá (Neoproterozoico III), Rio Grande do Sul.** Revista Brasileira de Geociências. V. 33(2). 2003.

PETERS, L. J. **The direct approach to magnetic interpretation and its practical application.** *Geophysics*, v. 14, p. 290–320, 1949.

PHILIPP, R. P.; PIMENTEL, M. M.; BASEI, M. A. S. **Tectonic evolution of the São Gabriel terrane, Dom Feliciano belt, southern Brazil: the closure of the Charrua Ocean.** In: SIEGESMUND, S.; OYHANTÇABAL, P.; BASEI, M. A. S.; ORIOLO, S. (Eds.). **Geology of the SW Gondwana.** Regional Geology Review. Springer, 2018. p. 243–266. DOI: [https://doi.org/10.1007/978-3-319-68920-3\\_10](https://doi.org/10.1007/978-3-319-68920-3_10).

PHILIPP, R. P.; PIMENTEL, M. M.; CHEMALE JR., F. **Tectonic evolution of the Dom Feliciano belt in southern Brazil: geological relationships and U–Pb geochronology.** *Brazilian Journal of Genetics*, v. 46, p. 83–104, 2016. DOI: <https://doi.org/10.1590/2317-4889201620150016>.

PIRES, C. A. F. **Modelamento e avaliação de dados geofísicos e geoquímicos aplicada na pesquisa de metais básicos e Au no prospecto Volta Grande (complexo intrusivo Lavras do Sul, RS, Brasil).** 2002.

PORCHER, C. A.; LEITES, S. R.; RAMGRAB, G. E.; CAMOZZATO, E. **Passo do Salsinho, Folha SH.22-Y-A-I-4: estado do Rio Grande do Sul.** Brasília: CPRM, 1995. Escala 1:100.000. Programa Levantamentos Geológicos Básicos do Brasil – PLGB. Disponível em: <http://rigeo.cprm.gov.br/jspui/handle/doc/8610>. Acesso em: 25 janeiro 2025.

RAMGRAB, G.; TONIOLO, J. A.; FERREIRA, J. A. F.; MACHADO, J. L. F.; BRANCO, P. M.; SUFFERT, T. **Principais recursos minerais do Rio Grande do Sul.** In: HOLZ, M.; DE ROS, L. F. **Geologia do Rio Grande do Sul.** Porto Alegre: CIGO/UFRGS, 2000. p. 407-445.

RAPOSO, M. I. B.; GASTAL, M. C. **Emplacement setting of the granite pluton of the Lavras do Sul Intrusive Complex (Rio Grande do Sul State), south Brazil: determined by magnetic anisotropies.** *Tectonophysics*, v. 466, p. 18-31, 2009.

REEVES, C. **Aeromagnetic Surveys: Principles, Practice and Interpretation.** Washington, DC: Earth-Works, 2005. 155 p.

REID, A. B.; ALLSOP, J. M.; GRANSER, H.; MILLETT, A. J.; SOMERTON, I. W. **Magnetic interpretation in three dimensions using Euler deconvolution.** *Geophysics*, v. 55, p. 80–91, 1990.  
DOI: <https://doi.org/10.1190/1.1442774>.

REISCHL, J. L. **Mineralizações cupríferas associadas a vulcânicas da Mina Seival, RS.** In: CONGRESSO BRASILEIRO DE GEOLOGIA, 30., 1978, Recife. *Anais...* Recife: SBG, 1978. v. 4, p. 1568-1582.

REMUS, M. V. D. **Metalogênese dos depósitos hidrotermais de metais-base e Au do Ciclo Brasiliano no Bloco São Gabriel, RS.** 1999. 170 f. Tese (Doutorado) – Instituto de Geociências, Universidade Federal do Rio Grande do Sul, Porto Alegre, 1999.

REMUS, M. V. D.; HARTMANN, L. A.; MCNAUGHTON, N. J.; GROVES, D. I.; REISCHL, J. L.; DORNELES, N. T. **The Camaquã Cu (A, Ag) and Santa Maria Pb-Zn (Cu, Ag) Mines of Rio Grande do Sul, Southern Brazil: Is their mineralization syngenetic, diagenetic or magmatic hydrothermal?** In: WORKSHOP: DEPÓSITOS MINERAIS BRASILEIROS DE METAIS-BASE, 1998, Salvador. *Anais [...]*. Salvador: ADIMB, 1998. p. 58-67.

REYNOLDS, J. M. **An Introduction to Applied and Environmental Geophysics.** 2. ed. Chichester: Wiley, 2011.

RIBEIRO, J. M. **Mapa Previsional do Cobre no Escudo Sul-Rio-Grandense.** Nota explicativa. Ministério de Minas e Energia. Departamento Nacional da Produção, 1978. 104 p.

RIBEIRO, M. J. M. **Mapa previsional do cobre no Escudo Sul Rio-Grandense: nota explicativa.** Brasília: DNPM/DFPM, 1978. (*Boletim Geológico*, n. 3, Seção Geologia Econômica, n. 1). 104 p.

RIBEIRO, M.; BOCCHI, P. R.; FIGUEIREDO, F. P. M. **Geologia da quadrícula de Caçapava do Sul, Rio Grande do Sul - Brasil.** *Boletim DNPM*, Rio de Janeiro, n. 127, 1966.

RIBEIRO, M.; FANTINEL, L.M. **Associações petrotectônicas do Escudo Sul-Riograndense: I Tabulação e distribuição das associações petrotectônicas do Escudo do Rio Grande do Sul.** Ihneríngia, Série Geologia, Porto Alegre, 5: 19-54. 1978.

RIBEIRO, V. B.; MANTOVANI, M. S. M. **Contribuição geofísica ao estudo do Batólito Granítico Santa Helena, sudoeste do Cráton Amazônico.** *Geologia USP. Série Científica*, v. 12, n. 2, p. 65-82, 2012. DOI: <https://doi.org/10.5327/Z1519-874X2012000200005>.

RIBEIRO, V. B.; MANTOVANI, M. S. M.; LOURO, V. H. A. **Aerogamaespectrometria e suas aplicações no mapeamento geológico.** *Terrae Didática*, v. 10, n. 1, p. 29-51, 2014. DOI: <https://doi.org/10.20396/td.v10i1.8637386>.

ROEST, W. R.; VERHOEF, J.; PILKINGTON, M. **Magnetic interpretation using the 3-D analytic signal.** *Geophysics*, v. 57, n. 1, p. 116–125, 1992. Disponível em: [https://www.researchgate.net/publication/277551383 Magnetic interpretation using 3-D analytic signal](https://www.researchgate.net/publication/277551383_Magnetic_interpretation_using_3-D_analytic_signal). Acesso em: 5 April. 2025.

ROBERTSON J.F. **Revision of Stratigraphy and nomenclature of rock units in Caçapava-Lavras Region.** *Notas e Estudos, IG-UFRGS*, Porto Alegre, 1(2): 41-54. 1966.

SAALMANN, K.; GERDES, A.; LAHAYE, Y.; HARTMANN, L. A.; REMUS, M. V. D. **A multiple accretion at the eastern margin of the Rio de la Plata craton: the prolonged Brasiliano orogeny in southernmost Brazil.** *International Journal of Earth Sciences*, v. 100, p. 355–378, 2011. DOI: <https://doi.org/10.1007/s00531-010-0564-8>.

SAALMANN, K.; HARTMANN, L. A.; REMUS, M. V. D.; KOESTER, E.; CONCEIÇÃO, R. V. **Sm-Nd isotope geochemistry of metamorphic volcano-sedimentary successions in the São Gabriel Block, southernmost Brazil: evidence for the existence of juvenile Neoproterozoic oceanic crust to the east of the Rio de la Plata craton.** *Precambrian Research*, v. 136, p. 159–175, 2005.

SAALMANN, K.; REMUS, M. V. D.; HARTMANN, L. A. **Geochemistry and crustal evolution of volcano-sedimentary successions and orthogneisses in the São Gabriel Block, southernmost Brazil — relics of Neoproterozoic magmatic arcs.** *Gondwana Research*, v. 8, p. 143–161, 2005.

SAALMANN, K.; REMUS, M. V. D.; HARTMANN, L. A. **Structural evolution and tectonic setting of the Porongos belt, southern Brazil.** *Geological Magazine*, v. 143, p. 59–88, 2006.

SALDANHA, M. G. et al. **A Mina Seival e a mineração de cobre no sul do Brasil: Uma análise geológica e histórica.** *Revista Brasileira de Geociências*, v. 41, n. 2, p. 123-135, 2011.

SALEM, A.; RAVAT, D. **A Combined Analytic Signal and Euler Method (AN-EUL) for Automatic Interpretation of Magnetic Data.** *Geophysics*, v. 68, p. 1952-1961, 2003. DOI: <http://dx.doi.org/10.1190/1.1635049>.

SALEM, A.; WILLIAMS, S.; FAIRHEAD, D.; SMITH, R.; RAVAT, D. **Interpretation of magnetic data using tilt-angle derivatives.** *Geophysics*, v. 73, n. 1, p. 1–10, 2008. DOI: <https://doi.org/10.1190/1.2799992>

SAMPAIO, R. P.; SILVA, J. C.; FERREIRA, M. A. **Aplicação de dados aerogamaespectrométricos para identificação de anomalias radiométricas em áreas de cobre e ferro no estado de Alagoas, Brasil.** *Revista Brasileira de Geofísica*, v. 42, p. 23–35, 2024.

SANDRIN, A.; ELMING, S. **Physical properties of rocks from borehole TJ71305 and geophysical outline of the Tjårrojåkka Cu-prospect, northern Sweden.** *Ore Geology Reviews*, v. 30, p. 56–73, 2007. DOI: 10.1016/j.oregeorev.2006.02.002.

SCHMIDHUBER, J. **Deep learning in neural networks: An overview.** *Neural Networks*, v. 61, p. 85–117, 2015.

SEQUENT. **User guide for Grav/Mag Interpretation Extension.** Oasis Montaj 2023.2. Bentley Subsurface company, 67 p., 2024.

SHEARER, S.; LI, Y. **3D Inversion of magnetic total gradient data in the presence of remanent magnetization.** In: SEG TECHNICAL PROGRAM EXPANDED ABSTRACTS. Tulsa, OK, USA: Society of Exploration Geophysicists, 2004. p. 774–777.

SHIVES, R. B. K.; FORD, K. L.; PETER, J. M. **Mapping and exploration applications of gamma-ray spectrometry in the Bathurst Mining Camp, Northeastern New Brunswick.** In: MASSIVE SULFIDE DEPOSITS OF THE BATHURST MINING CAMP, NEW BRUNSWICK, AND NORTHERN MAINE. Tulsa, OK, USA: Society of Exploration Geophysicists, 2003.

SILLITOE, R. H. **Iron oxide–copper–gold deposits: an Andean view.** *Mineralium Deposita*, v. 38, p. 787–812, 2003. DOI: 10.1007/s00126-003-0379-7.

SILLITOE, R. H. **Porphyry copper systems.** *Economic Geology*, v. 105, p. 3–41, 2010. DOI: <https://doi.org/10.2113/gsecongeo.105.1.3>.

SILLITOE, R. H. **Supergene Oxidized and Enriched Porphyry Copper and Related Deposits.** In: HEDENQUIST, J. W.; THOMPSON, J. F. H.; GOLDFARB, R. J.; RICHARDS, J. P. (Eds.). **One Hundredth Anniversary Volume.** 2005. DOI: <https://doi.org/10.5382/AV100.22>.

SILVA, E. O.; COSTA, S. S.; FEITOZA, L. M. **Caracterização litogeofísica da folha Rio Mucajáí, estado de Roraima.** In: SIMPÓSIO BRASILEIRO DE SENSORIAMENTO REMOTO, 13., 2007. *Anais...* 2007. p. 6183–6190. Disponível em: <http://marte.sid.inpe.br/col/dpi.inpe.br/sbsr@80/2006/11.15.23.57.32/doc/6183-6190.pdf>. Acesso em: 15 abr. 2024.

SILVA, L. C.; McNAUGHTON, N. J.; ARMSTRONG, R.; HARTMANN, L. A.; FLETCHER, I. R. **The Neoproterozoic Mantiqueira Province and its African connections: a zircon-based U-Pb geochronologic subdivision for the Brasiliano/Pan-African systems of orogens.** *Precambrian Research*, v. 136, p. 203–240, 2005.

SOMMER, C. A. **O vulcanismo ácido da porção sul do Platô do Taquarembó, Dom Pedrito-RS.** 1994. 149 f. Dissertação (Mestrado) – Programa de Pós-Graduação em Geociências, Universidade Federal do Rio Grande do Sul, Porto Alegre, 1994.

SOMMER, C. A. **O vulcanismo neoproterozóico do Platô da Ramada, região de Vila Nova do Sul, RS.** 2003. 179 f. Tese (Doutorado) – Programa de Pós-Graduação em Geociências, Universidade Federal do Rio Grande do Sul, Porto Alegre, 2003.

SOMMER, C. A.; LIMA, E. F. de; NARDI, L. V. S.; FIGUEIREDO, A. M. G.; PIEROSAN, R. **Potassic and low- and high-Ti mildly alkaline volcanism in the Neoproterozoic Ramada Plateau, southernmost Brazil.** *Journal of South American Earth Sciences*, Amsterdam, v. 18, p. 237–254, 2005. DOI: <http://doi.org/10.1016/j.jsames.2004.11.003>

SOMMER, C. A.; LIMA, E. F. de; NARDI, L. V. S.; LIZ, J. D.; WAICHEL, B. L. **The evolution of Neoproterozoic magmatism in Southernmost Brazil: shoshonitic, high-K tholeiitic and silica saturated, sodic alkaline volcanism in post-collisional basins.** *Anais da Academia Brasileira de Ciências*, Rio de Janeiro, v. 78, n. 3, p. 573-589, 2006. DOI: <https://doi.org/10.1590/S0001-37652006000300015>

SOUZA, J. L.; FERREIRA, F. J. F. **Anomalias aerogamaespectrométricas (K, eU e eTh) da quadricula de Araras (SP) e suas relações com processos pedogenéticos e fertilizantes fosfatados.** *Revista Brasileira de Geofísica*, v. 23, p. 251–274, 2005.

TARANTOLA, A. **Inverse Problem Theory and Methods for Model Parameter Estimation.** Philadelphia: SIAM, 2005. 342 p.  
DOI: <https://doi.org/10.1137/1.9780898717921>.

TEIXEIRA, G.; GONZALES, M. **Minas do Camaquã, município de Caçapava do Sul, RS.** In: SCHOBENHAUS, C.; COELHO, C. E. S. (Coord.). **Principais depósitos minerais do Brasil: metais básicos não-ferrosos, ouro e alumínio.** Brasília: DNPMCSVRD, 1988. v. 3. p. 34-40.

THOMPSON, D. T. **EULDPH: A new technique for making computer-assisted depth estimates from magnetic data.** *Geophysics*, v. 47, p. 31–37, 1982.  
DOI: <https://doi.org/10.1190/1.1441278>.

TONIOLO, J. A.; GIL, C. A. A.; SANDER, A. **Metagenia das bacias neoproterozóico-eopaleozóicas do Sul do Brasil: Bacia do Camaquã.** Porto Alegre: CPRM, 2007. (Informe de Recursos Minerais. Série Metais: Informes Gerais, 1). Disponível em: <https://rigeo.sgb.gov.br/handle/doc/1744>. Acesso em: 15 abr. 2024.

TONIOLO, J. A.; REMUS, M. V. D.; MACAMBIRA, M. J. B.; MOURA, C. A. V. **Metalogênese do Depósito de Cobre Cerro dos Martins, RS: revisão e geoquímica isotópica de Sr, S, O e C.** *Revista Pesquisas em Geociências*, Porto Alegre, v. 31, n. 2, p. 41-67, 2004.

UWIDUHAYE, J.; NGARUYE, J. C.; SAIBI, H. **Defining potential mineral exploration targets from the interpretation of aeromagnetic data in Western Rwanda.** *Ore Geology Reviews*, v. 128, p. 103927, 2021.  
DOI: <https://doi.org/10.1016/j.oregeorev.2020.103927>.

VEDANA, L. A.; PHILIPP, R. P. Análise petrográfica e proveniência dos metassedimentos do Complexo Pontas do Salso, Terreno São Gabriel, Cinturão Dom Feliciano, RS. Pesquisas em Geociências, v. 43, n. 3, p. 229–248, 2016.

VEDANA, L. A.; PHILIPP, R. P.; BASEI, M. A. S. Tonian to early Cryogenian synorogenic basin of the São Gabriel Terrane, Dom Feliciano Belt, southernmost Brazil. International Journal of Geology, 2017. Disponível em: <http://dx.doi.org/10.1080/00206814.2017.1328709>. Acesso em: 16 jun. 2025.

VILWOCK, J.; JOST, H. Mineralizações de cobre, molibdênio e ouro nas cabeceiras do rio Vacacaí, São Gabriel. In: CONGRESSO BRASILEIRO DE GEOLOGIA, 21., 1967, Curitiba. Anais... Curitiba, 1967. p. 80–102.

WILDNER, W.; LIMA, E. F. de. Vulcanoclásticas Bossoroca e pillow lavas do Arroio Mudador: um evento vulcânico único? In: CONGRESSO BRASILEIRO DE GEOLOGIA, 38., 1994, Balneário Camboriú, SC. Boletim de Resumos Expandidos [...]. Balneário Camboriú, SC: SBG, 1994. v. 3, p. 117-118.

WILFORD, J.; BIERWIRTH, P.; CRAIG, M. Application of gamma-ray spectrometry in soil/regolith mapping and geomorphology. *Journal of Geochemical Exploration*, v. 60, p. 217–226, 1997.

WITHERLY, K.; ALLARD, M. The evolution of the use of geophysics in the search for blind VHMS deposits in the Abitibi greenstone belt, Québec, Canada. In: SEG TECHNICAL PROGRAM EXPANDED ABSTRACTS, 2010. Anais... 2010. p. 1743-1747. DOI: <https://doi.org/10.1190/1.3513179>.

ZHDANOV, M. S. **Geophysical Inverse Theory and Regularization Problems**. 1. ed. Amsterdam: Elsevier Science, 2002. DOI: <https://doi.org/10.1016/C2012-0-03334-0>.